Universidade de Aveiro
Departamento de
Electrónica, Telecomunicações e Informática.
2016

Rómulo José Magalhães Martins Antão

Modelação e Controlo de Sistemas com Incertezas baseados em Lógica Difusa de Tipo-2

Type-2 Fuzzy Logic: Uncertain Systems' Modeling and Control

Rómulo José Magalhães Martins Antão

Modelação e Controlo de Sistemas com Incertezas baseados em Lógica Difusa de Tipo-2

Type-2 Fuzzy Logic: Uncertain Systems' Modeling and Control

Tese apresentada à Universidade de Aveiro para cumprimento dos requisitos necessários à obtenção do grau de Doutor em Engenharia Eletrotécnica, realizada sob a orientação científica do Professor Doutor Rui Manuel Escadas Ramos Martins, professor auxiliar do Departamento de Eletrónica, Telecomunicações e Informática da Universidade de Aveiro, e do Professor Doutor Alexandre Manuel Moutela Nunes da Mota, professor associado do Departamento de Electrónica, Telecomunicações e Informática da Universidade de Aveiro

o júri /the jury

presidente / president

Luís Filipe Pinheiro de Castro
Professor Catedrático da Universidade de Aveiro

vogais / examiners committee

José Alfredo Ribeiro da Silva Matos
Professor Catedrático da Faculdade de Engenharia da Universidade do Porto

José António Tenreiro Machado
Professor Coordenador com Agregação do Instituto Superior de Engenharia do Porto

Luis Miguel Pinho de Almeida
Professor Associado da Faculdade de Engenharia da Universidade do Porto

José Alberto Gouveia Fonseca
Professor Associado da Universidade de Aveiro

Rui Alexandre de Matos Araújo
Professor Auxiliar da Universidade de Coimbra

José António Barros Vieira
Professor Adjunto do Instituto Politécnico de Castelo Branco

Rui Manuel Escadas Ramos Martins (Orientador)
Professor Auxiliar da Universidade de Aveiro

agradecimentos

O culminar desta Tese representa uma importante etapa na minha vida que, para além de me trazer realização pessoal, realçou também a importância que algumas pessoas têm para a minha felicidade e ambição em ser melhor. Deixo por isso a minha palavra de apreço a todos os que me ajudaram durante este percurso, dando os seus melhores conselhos e proporcionando bons momentos de diversão e iluminação.

Dedico esta Tese à minha Família, pelos bons valores que todos me transmitiram e por terem sempre estado um passo atrás de mim apoiando a realização dos meus objectivos.

During the course of this work, Rómulo Antão was supported by the Portuguese government organization Foundation for Science and Technology (FCT), which conceded a PhD grant with reference SFRH/BD/71601/2010.

Palavras-chave Lógica Difusa de Tipo 2, Modelação de Sistemas, Controlo Preditivo baseado em Modelos

Resumo

A última fronteira da Inteligência Artificial será o desenvolvimento de um sistema computacional autónomo capaz de "rivalizar" com a capacidade de aprendizagem e de entendimento humana. Ainda que tal objetivo não tenha sido até hoje atingido, da sua demanda resultam importantes contribuições para o estado-da-arte tecnológico atual. A Lógica Difusa é uma delas que, influenciada pelos princípios fundamentais da lógica proposicional do raciocínio humano, está na base de alguns dos sistemas computacionais "inteligentes" mais usados da atualidade.

A teoria da Lógica Difusa é uma ferramenta fundamental na suplantação de algumas das limitações inerentes à representação de informação incerta em sistemas computacionais. No entanto esta apresenta ainda algumas lacunas, pelo que diversos melhoramentos à teoria original têm sido introduzidos ao longo dos anos, sendo a Lógica Difusa de Tipo-2 uma das mais recentes propostas. Os novos graus de liberdade introduzidos por esta teoria têm-se demonstrado vantajosos, particularmente em aplicações de modelação de sistemas não-lineares complexos. Uma das principais vantagens prende-se com o aumento da robustez dos modelos assim desenvolvidos comparativamente àqueles baseados nos princípios da Lógica Difusa de Tipo-1 sem implicar necessariamente um aumento da sua dimensão. Tal propriedade é particularmente vantajosa considerando que muitas vezes estes modelos são utilizados como suporte ao desenvolvimento de sistemas de controlo que deverão ser capazes de assegurar o comportamento ótimo de um processo em condições de operação variáveis. No entanto, o estado-da-arte da teoria de controlo de sistemas baseada em modelos não tem integrado todos os melhoramentos proporcionados pelo desenvolvimento de modelos baseados nos princípios da Lógica Difusa de Tipo-2.

Por essa razão, a presente tese propõe-se a abordar este tópico desenvolvendo uma metodologia de síntese de Controladores Preditivos baseados em modelos Takagi-Sugeno seguindo os princípios da Lógica Difusa de Tipo-2. De modo a cumprir este objetivo, quatro linhas de investigação serão debatidas neste trabalho.

Resumo (Continuação)

Primeiramente proceder-se-á ao desenvolvimento de uma metodologia de treino de Modelos Difusos de Tipo-2 simplificada, focada em dois paradigmas: manter a clareza dos intervalos de incerteza introduzidos sobre um Modelo Difuso de Tipo-1; assegurar a validade dos diversos modelos localmente lineares que constituem a estrutura Takagi-Sugeno, de modo a torná-los adequados a métodos de síntese de controladores baseados em modelos.

O modelo desenvolvido é tipicamente utilizado para extrapolar o comportamento do sistema numa janela temporal futura. No entanto, quando usados em aproximações de sistemas não lineares, os modelos do tipo Takagi-Sugeno estabelecem um compromisso entre exatidão e complexidade computacional. Assim, é proposta a utilização dos princípios da Lógica Difusa de Tipo-2 para reduzir a influência dos erros de modelação nas estimações obtidas através do ajuste dos intervalos de incerteza dos parâmetros do modelo.

Com base na estrutura Takagi-Sugeno, um método de linearização local de modelos não-lineares será utilizado em cada ponto de funcionamento do sistema de modo a obter os parâmetros necessários para a síntese de um controlador otimizado numa janela temporal futura de acordo com os princípios da teoria de Controlo Preditivo Generalizado - um dos algoritmos de Controlo Preditivo mais utilizado na indústria. A qualidade da resposta do sistema em malha fechada e a sua robustez a perturbações serão então comparadas com implementações do mesmo algoritmo baseadas em métodos de modelação mais simples.

Para concluir, o controlador proposto será implementado num *System-on-Chip* baseado no *core* ARM Cortex-M4. Com o propósito de facilitar a realização de testes de implementação de algoritmos de controlo em sistemas embutidos, será apresentada também uma plataforma baseada numa arquitetura *Processor-In-the-Loop*, que permitirá avaliar a execução do algoritmo proposto em sistemas computacionais com recursos limitados, aferindo a existência de possíveis limitações antes da sua aplicação em cenários reais.

A validade do novo método proposto é avaliada em dois cenários de simulação comummente utilizados em testes de sistemas de controlo não-lineares: no Controlo da Temperatura de uma Cuba de Fermentação e no Controlo do Nível de Líquidos num Sistema de Tanques Acoplados. É demonstrado que o algoritmo de controlo desenvolvido permite uma melhoria da performance dos processos supramencionados, particularmente em casos de mudança rápida dos regimes de funcionamento e na presença de perturbações ao processo não medidas.

Keywords Type-2 Fuzzy Logic, System Modeling, Model Predictive Control

Abstract

The development of an autonomous system capable of matching human knowledge and learning capabilities embedded in a compact yet transparent way has been one of the most sought milestones of Artificial Intelligence since the invention of the first mechanical general purpose computers. Such accomplishment is yet to come but, in its pursuit, important contributions to the state-of-the-art of current technology have been made. Fuzzy Logic is one of such, supporting some of the most used frameworks for embedding human-like knowledge in computational systems.

The theory of Fuzzy Logic overcame some of the difficulties that the inherent uncertainty in information representations poses to the development of computational systems. However, it does present some limitations so, aiming to further extend its capabilities, several improvements over its original formalization have been proposed over the years such as Type-2 Fuzzy Logic - one of its most recent advances. The additional degrees of freedom of Type-2 Fuzzy Logic are showing greater potential to supplant its original counterpart, especially in complex non-linear modeling tasks. One of its main outcomes is its capability of improving the developed model's robustness without necessarily increasing its dimensionality comparatively to a Type-1 Fuzzy Model counterpart. Such feature is particularly advantageous if one considers these model as a support for developing control systems capable of maintaining a process's optimal performance over changing operating conditions. However, state-of-the art model-based control theory does not seem to be taking full advantage of the improvements achieved with the development of Type-2 Fuzzy Logic based models.

Therefore, this thesis proposes to address this problem by developing a Model Predictive Control system supported by Interval Type-2 Takagi-Sugeno Fuzzy Models. To accomplish this goal, four main research directions are covered in this work.

Abstract (Continuation)

Firstly, a simpler method for training a Type-2 Takagi-Sugeno Fuzzy Model focused on two main paradigms is proposed: maintaining a meaningful interpretation of the uncertainty intervals embedded over an estimated Type-1 Fuzzy Model; ensuring the validity of several locally linear models that constitute the Takagi-Sugeno structure in order to make them suitable for model-based control approaches.

Based on the developed model, a multi-step ahead estimation of the process behavior is extrapolated. However, as Takagi-Sugeno Fuzzy Models establish a trade-off between accuracy and computational complexity when used as a non-linear process approximation, it is proposed to apply the principles of Type-2 Fuzzy Logic to reduce the influence of modeling uncertainties on the obtained estimations by adjusting the model parameters' uncertainty intervals.

Supported by the developed Type-2 Takagi-Sugeno Fuzzy Model, a locally linear approximation of each current operation point is used to obtain the optimal control law over a prediction horizon according to the principles of Generalized Predictive Control - one of the most used Model Predictive Control algorithms in Industry. The improvements in terms of closed loop tracking performance and robustness to unmodeled operation conditions are then assessed comparatively to Generalized Predictive Control implementations based on simpler modeling approaches.

Ultimately, the proposed control system is implemented in a general purpose System-on-a-Chip based on a ARM Cortex-M4 core. A Processor-In-the-Loop testing framework, developed to support the implementation of control loops in embedded systems, is used to evaluate the algorithm's turnaround time when executed in such computationally constrained platform, assessing its possible limitations before deployment in real application scenarios.

The applicability of the new methods introduced in this thesis is illustrated in two simulated processes commonly used in non-linear control benchmarking: the Temperature Control of a Fermentation Reactor and the Liquid Level Control of a Coupled Tanks System. It is shown that the developed control system achieves an improved closed loop performance of the above mentioned processes, particularly in the cases of quick changes in the operation regime and in presence of unmeasured external disturbances.

Contents

List of Figures

List of Tables

List of Acronyms

ANFIS	Adaptive Network based Fuzzy Inference System.
ANN	Artificial Neural Network.
ARX	Auto-Regressive with eXogenous inputs.
CARIMA	Controlled Auto-Regressive Incremental Moving Average.
CARMA	Controlled Auto-Regressive Moving Average.
CE	Control Effort.
CTS	Coupled Tanks System.
DMC	Dynamic Matrix Control.
EODS	Enhanced Opposite Direction Searching Algorithm.
FCM	Fuzzy C-Means.
FL	Fuzzy Logic.
FLS	Fuzzy Logic System.
FOU	Footprint of Uncertainty.
FPU	Floating-Point Unit.
FS	Fuzzy Set.
GPC	Generalized Predictive Control.
HIL	Hardware-In-the-Loop.
IT1FS	Interval Type-1 Fuzzy Set.
IT2FLS	Interval Type-2 Fuzzy Logic System.
IT2FS	Interval Type-2 Fuzzy Set.
KM	Karnik-Mendel.
LMF	Lower Membership Function.
MAC	Model Algorithmic Control.

MCU	Micro-Controller Unit.
MF	Membership Function.
MIMO	Multiple-Input Multiple-Output.
MPC	Model Predictive Control.
MSE	Mean Squared Error.
NARX	Non-Linear Auto-Regressive with eXogenous inputs.
NSE	Normalized Squared Error.
PIL	Processor-In-the-Loop.
RBFN	Radial Basis Function Network.
RLS	Recursive Least Squares.
RLSDF	Recursive Least Squares with Directional Forgetting.
SISO	Single-Input Single-Output.
SNR	Signal-to-Noise Ratio.
TR	Type-Reduction.
TS	Takagi-Sugeno.
UMF	Upper Membership Function.

Chapter 1

Introduction

The development of control algorithms flexible enough to correctly manipulate a process close to its best performance metrics without human supervision has been one the most sought goals of control and system modeling theory. The work of Zadeh during the early 60's in the theory of Fuzzy Sets (FSs) and Fuzzy Logic (FL) introduced a fundamental degree of fuzziness in computational systems that overcame the difficulties of obtaining accurate descriptions of models and control systems due to the inherent variability and noisy operation conditions of real world processes. His achievements significantly contributed to the state-of-the-art of current technology in a broad range of applications and even today, on the 50^{th} anniversary of Fuzzy Logic's seminal work [1], continue to bring about new approaches to optimize the way information uncertainty is accounted for in computational systems - Type-2 FL is one of its most recent extensions.

Despite invariably linked with information fuzziness, the original Fuzzy Logic theory does not consider the inherent uncertainty of assigning a single membership function to each FS defined over a numerical domain - each membership function chosen is itself crisp since it is totally defined without considering any variability on its parameters (such as its center, width, endpoints or shape). Type-2 FL theory overcomes this limitation by introducing additional degrees of freedom in a membership function concept so higher levels of uncertainty over the chosen representation are accounted for. Ultimately, a Type-2 FS embeds itself a large number of Type-1 FSs under the same label yielding a blurred Fuzzy Set representation.

Inspired by the simplicity of developing rule based systems, Fuzzy Logic Systems (FLSs) (either based on the Mamdani or Takagi-Sugeno (TS) structures) were naturally improved by introducing the Type-2 Fuzzy Logic formalisms to accommodate higher levels of uncertainties in the system's parameters. This transition is fairly natural since the basic principles of fuzzy logic are independent of the nature of the membership functions, requiring

only little changes in the typical FLS structure. As a elemental part of a FLS, Type-2 FSs provides a better coverage of the crisp domain of interest and ultimately contribute to the reduction of the number of rules required to approximate complex input-output data relationships [2]. While the additional degrees of freedom of Type-2 FSs shown greater potential to supplant conventional information representation methodologies [3, 4], especially in complex scenarios described by non-linear data dependencies, generally their use requires a greater computational effort due to complexity of the required algebras. For that reason, a great amount of research in Type-2 Fuzzy Logic domains has been put towards developing more efficient representations, such as Interval Type-2 Fuzzy Sets [5], in order to overcome this bottleneck and further extend its applicability to real world scenarios. Such approach is already yielding promising results, leading to successful applications in traditional Fuzzy Logic domains such as modeling, control or classification systems.

1.1 Motivation

As far as control systems development is concerned, the state-of-the-art of Type-2 Fuzzy Logic Systems does not seem to be taking full advantage of the most important achievements of model based control algorithms. Literature mainly highlights approaches based on PID structures [6, 7, 8] - whose discrete-time implementations still have deep roots in traditional continuous-time concepts such as step response analysis. One can also find model-based approaches using Direct Inverse models, obtained by means of analytical methods that directly invert Type-2 TS Fuzzy Models [9, 10] or by directly modeling the inverse dynamics of the system [11]. While inverse model controllers are intuitively simple and eventual steady-state errors can be compensated by integrating the inverse model in an Internal Model Control structure [10], such approaches may not work satisfactory when a system's inverse model is not well-damped, or it may not work at all due to the presence of zeros on the right half of the complex s-plane. To some extent, Type-2 Fuzzy Control state-of-the-art is not considering the improvements brought by model-based control design techniques such as Pole-Placement [12] or Model Predictive Control (MPC) [13]. The latter approach has become, in fact, one of the most popular methods in both industrial and academic communities, which efficiently handles a wide range of control problems with large number of design variables such as systems with multiple control inputs and control signal constraints. One of its simplest, yet robust implementations is the Generalized Predictive Control (GPC) algorithm [14].

The process's model is a cornerstone of every MPC implementation and its accuracy ultimately defines the quality of the control system in terms of tracking capabilities and robustness to external disturbances. While most of time linear approximations are enough, in some applications it is of uttermost importance to develop models that take in account the possible non-linearities of the process. Traditionally, MPC implementations are based on linear models but, in order to extend its theory to the control of non-linear processes, the combination of Fuzzy Models with MPC implementations has become increasingly debated in recent years and has been object of important studies regarding its stability and applicability [15, 16, 17]. More particularly, TS Fuzzy models shown advantageous for such purpose by two main reasons:

- Capability of modeling complex non-linear processes using input-output data along with *a priori* knowledge of the system provided by the user. By combining the efficiency of fuzzy reasoning in handling uncertain information and the neural networks learning ability in model's development, TS Fuzzy systems retain an important level of interpretability and adaptability in their structure.

- Its structure follows a two-layered computing scheme which partitions a non-linear system as a contributions of several locally linear models. Such topology avoids the use of extensive non-linear optimization algorithms during its training and allows the design of model based controllers according to linear control theory.

Type-2 Fuzzy Logic is formal extension of its original Type-1 counterpart and sharing many of its applications but, up to the day no literature was found proposing the use of Type-2 TS Fuzzy Models as support for MPC algorithms. Since both topics are currently disjoint fields of expertise, the main goal of this thesis is to propose a systematic methodology to merge both domains and assess the performance improvements achieved over traditional implementations of MPC. Hence, is this work main goal to develop closed loop control algorithm based on Model Predictive Control theory and a Type-2 Fuzzy Models which can be implemented in general purpose embedded system.

1.2 Thesis Contributions

This thesis provides the following contributions to the state-of-the-art of process modeling and control:

- Provide simpler methods for training a Type-2 TS Fuzzy Model. While currently every parameters of a Type-2 TS Fuzzy model is obtained as a single error minimization problem, it is computationally more efficient and tractable to the user to consider two separate problems: the training of a supporting Type-1 TS Fuzzy System and the introduction of a Footprint-of-Uncertainty over the respective parameters. The width of the latter can be empirically adjusted so the approximation capabilities of the model are improved.

- Apply the principles of Type-2 FL to reduce the influence of modeling uncertainties on a locally linear n-step ahead predictor. The development of a multi-step predictor for a non-linear system typically establish a trade-off between accuracy and computational complexity. While a good compromise can be usually achieved using locally linear approximations from a TS Fuzzy Model, in changing operation regimes the predictor's validity may be significantly reduced. Though, its performance can be improved by obtaining a linearized model from a Type-2 TS Fuzzy Model and so the necessary procedures will be proposed.

- Introduce the concepts of Type-2 FL in the development of model based controllers according to the GPC principles. By synthesizing a control law based on linearized Type-2 TS Fuzzy Model, a superior closed loop tracking performance and robustness to unmodeled operation conditions can be achieved when compared to traditional GPC implementations.

- Provide a framework to develop a closed loop controller based on GPC theory and a Type-2 TS Fuzzy Models in embedded platforms. The higher computational requirements of Type-2 FL based systems impose significant constraints over their use in real-time applications. Therefore the algorithm's turnaround time will be evaluated when executed in a ARM Cortex-M4 microcontroller in order to assess its possible applications and limitations.

1.3 Publications

The main contributions of this thesis resulted following published works:

- **Rómulo Antão**, Alexandre Mota, Rui Escadas Martins, Model-Based Control using Interval Type-2 Fuzzy Logic Systems, submitted to the Soft Computing Journal ISSN: 1432-7643, Springer, October (2015)
- **Rómulo Antão**, Alexandre Mota, Rui Escadas Martins, Generalized Predictive Control using Interval Type-2 Fuzzy Models, IEEE International Conference on Fuzzy Systems (Fuzz-IEEE), Istanbul, Turkey, (2015)
- **Rómulo Antão**, Alexandre Mota, Rui Escadas Martins, Adaptive Control of a Buck Converter with an ARM Cortex-M4, 16th International Power Electronics and Motion Control Conference and Exposition (PEMC), Antalya, Turkey, (2014)
- **Rómulo Antão**, Alexandre Mota, Rui Escadas Martins, A Self Tuning Regulator based on the ARM Cortex-M4, 6th Workshop on Adaptive and Reconfigurable Embedded Systems - (APRES), ACM Special Interest Group on Embedded Systems, Volume 11, Number 3, ISSN: 1551-3688, (2014)

1.4 Thesis Outline

The thesis work spans over six chapters, organized as follows:

- *Chapter 2* introduces the fundamental concepts of Fuzzy Logic Systems and their extension to a particular branch of the Type-2 Fuzzy Logic theory based on Interval Type-2 Fuzzy Sets.
- *Chapter 3* focuses on a particular implementation of the fuzzy inference mechanisms, the Takagi-Sugeno Fuzzy Systems, presenting the improvements of its traditional formulation (based on Type-1 Fuzzy Sets) according to the most recent developments on Type-2 Fuzzy Sets' theory. The procedures for system identification based on the proposed structure are outlined.

- *Chapter 4* presents an approach for the development of a n-step ahead prediction model based on the linearization of a Type-2 Takagi-Sugeno Fuzzy Model. The capabilities of such methodology are evaluated using two non-linear processes as benchmark systems.

- *Chapter 5* proposes the use of Interval Type-2 Fuzzy Models for the development of a Model Predictive Controller according to the Generalized Predictive Control theory. Based on the two benchmark scenarios presented in the previous chapter, the performance of the respective closed loop control systems will be evaluated under several unmeasured external disturbances.

- *Chapter 6* presents a Processor-in-the-Loop framework based on a ARM Cortex M4 development board and the MATLAB's Simulink. The proposed system is implemented in order evaluate the feasibility of implementing Type-2 Fuzzy Logic Systems in computationally constrained platforms but also to improve the development and testing stages of complex embedded systems, providing an easier transition between the simulation and real world environments.

- Finally *Chapter 7* presents the concluding remarks of this thesis discussing some possible lines of work for future development.

Chapter 2

Fuzzy Logic Systems

2.1 Introduction

Human mind has always shown a remarkable capability of coordinating a wide variety of physical and mental tasks without using any explicit measurements and computations. Great efforts were made since the early 1950s towards the development of a scientific theory of intelligence and the development of an artificial model of the brain capable to mimic our perception, cognition and behavioral systems [18, 19]. Despite the accomplishments of system's theory and artificial intelligence, which are increasingly present in our daily activities, in practice computational systems still present several limitations that keep them behind human capabilities. The high dimensionality of information structures stored in computational systems resulting from the use of crisp measurements is one of the major burdens that the development of an intelligence framework must overcome. Uncertainty and imprecision on information can at first instance be seen as a downside for a decision process but they are important compression mechanisms that let people take them in a quick way. Without such tools, taking a decision would be a never ending process, requiring every infinitesimal part of information and their respective combinations to be considered. Therefore, the development of intelligent systems has to focus on the human capability of manipulating imprecise, uncertain and sometimes incomplete information.

Already on 1965, Zadeh was challenged by this problem and, on his seminal paper [1], lays the foundation-stone of a methodology known as Fuzzy Logic, where the objects of computation are words and propositions drawn from natural language. While Boolean logic results are restricted to 0 and 1, FL defines for the first time a computational framework to efficiently manipulate intermediate results between the values of absolute true and absolute false. The fuzzy information representation is based on Fuzzy Sets, which are no more than

a simple way to translate a crisp measurement into a degree of belonging in a linguistic label. This means that fuzzy sets can handle some concepts that we commonly deal with in daily life, like "very cold", "cold", "hot", "very hot", without having to know the specific temperature ranges each concept refers to. Therefore, Fuzzy Logic is more like human thinking because of its reliance on degrees of truth and the use of linguistic variables.

Initially, FL theory was not well-received by the peer community in engineering domains due to its unusual vagueness. However, since 1970, it has been widely applied in control applications, establishing successive milestones. Its principles were used to control a laboratory-built steam engine by Mamdani at the University of London in 1974 [20] and the first industrial application was a cement kiln controller built in Denmark in 1979 [21]. Despite born in the USA and theoretically validated in Europe, it was in Japan that FL gained broad notoriety when several Japanese companies pioneered successful practical applications with high impact in the society. One of the most renowned projects was presented in 1987, when Hitachi turned over control of a subway in Sendai, Japan, to a fuzzy system. Fuzzy control techniques were used in all the critical operations of the train's control system, such as accelerating, breaking, and stopping operations [22] but also in planning traffic and predicting customer usage of subway facilities. In 1987, Yamakawa successfully developed a fuzzy controller applied to a inverted pendulum experiment - one of the classic control problems [23]. A few years later, NASA took fuzzy logic beyond our planet aboard the Endeavour space shuttle, transporting a Commercial Refrigerator Incubator Module as an experimental payload, which successfully allowed the control of a test chamber's air temperature according to a pre-programmed profile [24]. Since then, several companies have used fuzzy logic to control hundreds of household appliances, implement decision making systems and improve the performance of many other electronic devices present in our daily life such as air conditioners, video cameras, televisions, washing machines, bus time tables, medical diagnoses or anti-lock braking systems.

Fuzzy Logic Systems are typically developed around two main types of inference mechanisms: the Mamdani [25] and the Takagi-Sugeno [26] ones. Despite the differences between both methods, when non-linear Fuzzy Sets are used to model linguistic labels, FLSs become non-linear structures with universal approximation capabilities [27], a property of major importance when they are used as support for modeling and control techniques. Since both inference mechanisms share a significant amount of methods, this chapter will introduce primarily the basic concepts of FSs theory based on the Mamdani inference.

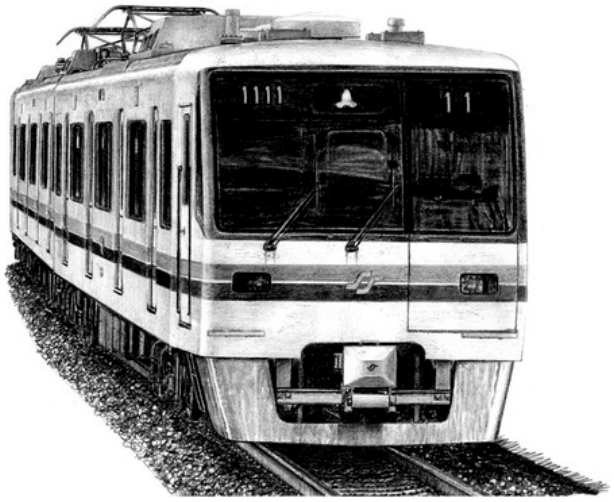

Figure 2.1: Sendai Subway 1000 Series - The first subway coach using a Fuzzy Control system [28].

2.2 Type-1 Fuzzy Sets

With the development of Fuzzy Logic, Type-1 FSs were defined for the first time. Type-1 FSs are a computational formalism that mimics our tendency to group crisp measurements displayed under a numeric scale using the same linguistic term when a more specific distinction is not required for a good understanding. For example, we describe temperatures using a linguistic terms that go from *Very Cold* to *Very Hot*, speed using terms from *Very Slow* to *Very Fast* or the visible colors from *Violet* to *Red*. With these descriptions, we are capable of abstract ourselves from the crispness of numeric scales expressed in $^{\circ}C$, km/h or nm. Each Type-1 FS is syntactically represented by a label F_i characterized by a Membership Function (MF), a two-dimensional function that defines the degree of association of a numeric value under the respective linguistic label using a crisp number between [0-1]. Different shapes of MFs can be considered, namely triangular, trapezoidal or gaussian shaped functions. Figure (2.2) depicts an example of a generic input domain partitioned using gaussian shaped MFs.

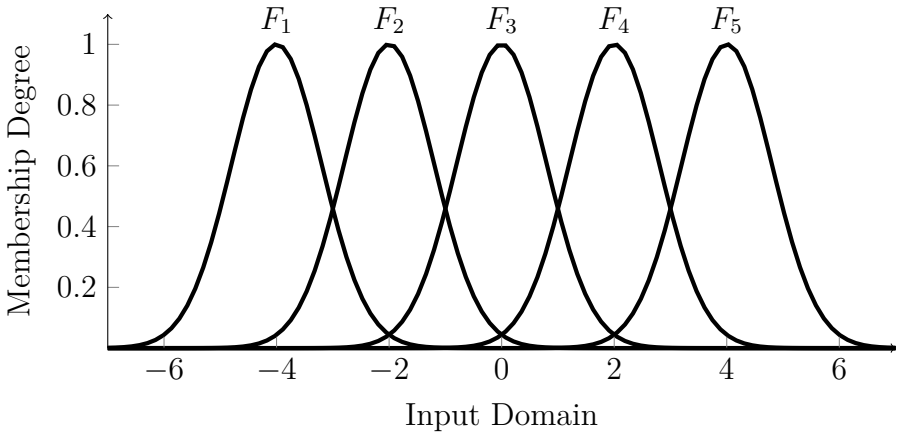

Figure 2.2: Generic input domain partition using Type-1 Fuzzy Sets.

2.3 Type-1 Fuzzy Logic Systems

One of the most used approaches to manipulate linguistic information is to use FLSs based on *If-Then* rules, a method that can be easily used to develop models and control algorithms in a way closer to human perception and thinking. There exist also alternatives to the use of rule based systems as is proposed by Delgado et al. in [29]. In their work, it is developed an arithmetic approach based on Extension Principle [30], a method that redefines common algebraic operations such as addition, multiplication, among many others to the domain of Fuzzy Sets. Even though sometimes it is hard to define *If-Then* rules into compact algebraic operations, the proposal of Delgado is particularly useful in situations where the problem has a high dimensionality, i.e. the number of existing rules used to describe the system is so high that it may result in a computationally inefficient process.

A FLS based on Type-1 FSs consists of four main elements, as depicted in figure (2.3) and briefly described as follows.

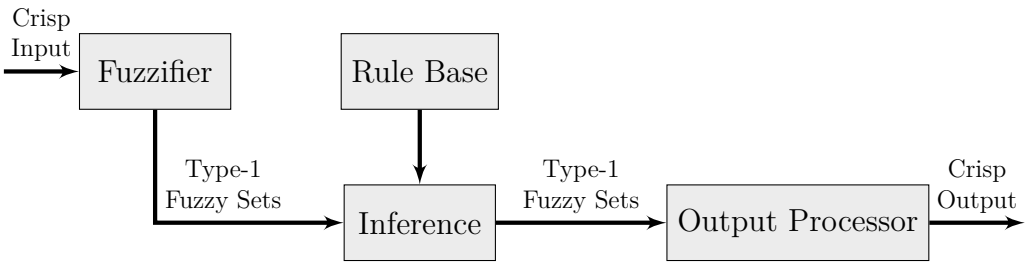

Figure 2.3: Type-1 Fuzzy Logic System structure.

- The Fuzzifier, which is an interface which maps a crisp number into a fuzzy domain defined by a Fuzzy Set. The most widely method is the *singleton fuzzifier*, in which measurements are considered perfect and therefore modeled as crisp values, i.e, as singletons.

- The Rule-Base, which is the heart of a FLS and is composed by information given by experts or extracted from numerical data, is often organized as several *If-Then* statements, where the IF-part of a rule is its antecedent, and the THEN-part of the rule is its consequent.

- The Inference Engine, which is the mechanism that implements the algebras required to manipulate Fuzzy Sets. In the same way humans use many inferential procedures, there exist several methods to do so based on FL - the Mamdani and the Takagi-Sugeno inference mechanisms are the two most popular ones [31].

- The Output Processor, which is the final stage of the FLS and implements the defuzzification procedures to aggregate the output fuzzy set into a single crisp value adequate to the FLS application scenario (usually a process's output prediction in modeling applications or the actuation value of a control system).

2.3.1 Fuzzifier

As pointed out, the singleton fuzzifier is the most used method to implement the Fuzzifier stage of a FLS due to its conceptual simplicity and easy manipulation in the subsequent stages of the FLS. Alternatively other functions to perform this operation could be used, as gaussian functions or triangular ones, but then calculating the firing levels of each antecedent membership function would be a far more complex process [30]. For this reason, singletons are considered in this work, and defined as:

$$\mu_{A_x}(x) = \begin{cases} 1, & x = x' \\ 0, & otherwise \end{cases} \tag{2.1}$$

where x' is the input value. This concept is depicted in figure (2.4).

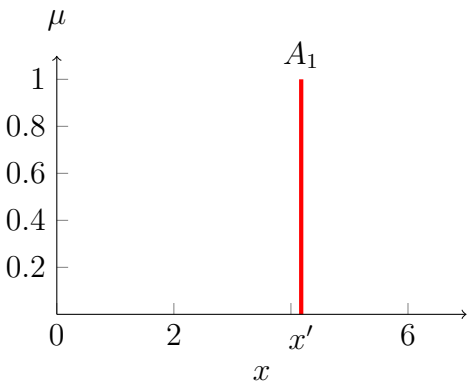

Figure 2.4: Depiction of a Singleton input.

2.3.2 Rule-Base

Playing a central role in the structure of a FLS, rules are a simple way to gather the knowledge that defines the behavior of a fuzzy system in a specific application. These rules are developed around different types of fuzzy sets, associated with the linguistic terms that appear in their antecedent and consequent parts, interconnected by operators that establish the relationship dependencies between fuzzy terms.

The most used rule structure is presented in equation (2.2)

$$R^i : IF\, x_1\, is\, F_1^i\, and\, \cdots\, and\, x_j\, is\, F_j^i,\, THEN\, y^i\, is\, G^i \tag{2.2}$$

where R^i represents the i^{th} fuzzy rule, F_j^l and G^i are linguistic terms characterized by Type-1 Fuzzy Sets, $i = [1, \cdots, M]$ where M is the number of fuzzy rules, $j = [1, \cdots, N]$ where N is the number of antecedents, x_j are the fuzzy system inputs and y^i is the rule output.

The linguistic terms F and G can assume several different shapes such as triangular, trapezoidal or gaussian. The latter form was employed in this work, having its definition presented in equation (2.3).

$$g(c, \sigma, x) = exp\left[-\frac{1}{2}\left(\frac{x-c}{\sigma}\right)^2\right] \tag{2.3}$$

The presented rule structure is just one example of many possible ways to embed knowledge in a Fuzzy Logic System. Similarly to our natural language, it is possible to establish other combinations between Fuzzy Sets using *or* relationships, consider the negation of fuzzy sets or even using *non-obvious* connectives like *unless* or comparative terms [30]. Though, in most scenarios, such logical statements can be represented using the more regular structure of equation (2.2).

2.3.3 Inference Engine

The manipulation of fuzzy sets can be performed according to several different algebraic operations depending on the possible combinations of operators used for implementing the rule's connective terms, implication methods and rule aggregation. By considering that we have two Type-1 FS F_1 and F_2 characterized by the MFs $\mu_{F_1}(x)$ and $\mu_{F_2}(x)$,

$$F_1 = \int_{x \in X} \mu_{F_1}(x)dx \qquad F_2 = \int_{x \in X} \mu_{F_2}(x)dx \tag{2.4}$$

the basic logic operations (union, (*s-norm*), intersection (*t-norm*) and complement (*c-norm*)) that provide the support for FS's manipulation can be defined as follows:

$$\begin{aligned} \mu_{F_1 \cup F_2}(x) &= max\left[\mu_{F_1}(x), \mu_{F_2}(x)\right],\ x \in X \\ \mu_{F_1 \cap F_2}(x) &= min\left[\mu_{F_1}(x), \mu_{F_2}(x)\right],\ x \in X \\ \mu_{\overline{F}}(x) &= 1 - \mu_F(x),\ x \in X \end{aligned} \tag{2.5}$$

The intersection operator can also be implemented based on the algebraic product and defined as:

$$\mu_{F_1 \cap F_2}(x) = \mu_{F_1}(x) * \mu_{F_2}(x),\ x \in X \tag{2.6}$$

Since the most usual way to represent a rule is to use the *and* connectives, the *t-norm* operators are the most used ones. Regardless the followed implementation, since the membership grades $\mu_{F_1}(x)$ and $\mu_{F_2}(x)$ are crisp numbers, any of the operations presented in equations (2.5) and (2.6) yields a crisp number. More particularly, when these operators are used to aggregate several fired FSs from the antecedent part of the rule, the obtained result is typically referred to as the i^{th} rule firing level f^i. Figure (2.5) depicts the the use of the *t-norm* in a two antecedent operation.

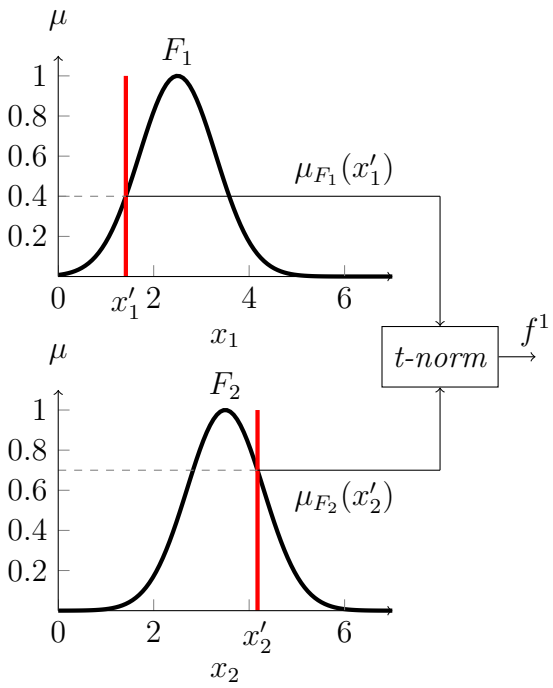

Figure 2.5: Operation between singleton input and the antecedents of a Type-1 FLS using a *t-norm* operator (minimum or product).

When both rule's antecedents and consequent are expressed using Type-1 FS, the implication of the rule's firing level over the consequent FS is typically obtained using one of the Mamdani implication methods - the Mamdani minimum or the Mamdani product. These methods are based on the *t-norm* operators previously described and are applied between the rule's firing level f^i and its consequent FS, $G^i(x)$.

$$\begin{aligned} f^i \to G^i(x) &= min\left[f^i, \mu_{G^i}(x)\right],\ x \in X \\ f^i \to G^i(x) &= f^i * \mu_{G^i}(x),\ x \in X \end{aligned} \tag{2.7}$$

Depending whether minimum or product *t-norm* is used, one obtains a clipped or a scaled version of the consequent MF, as depicted in figure (2.6).

The inference process ends up by obtaining a fuzzy set determined by the aggregation of the output of all the fired FLSs rules. One of the most used methods to do so is by using a *t-conorm* - the fuzzy union, which is no more than the finding the maximum value of the overlapped FSs. Figure (2.7) depicts this procedure.

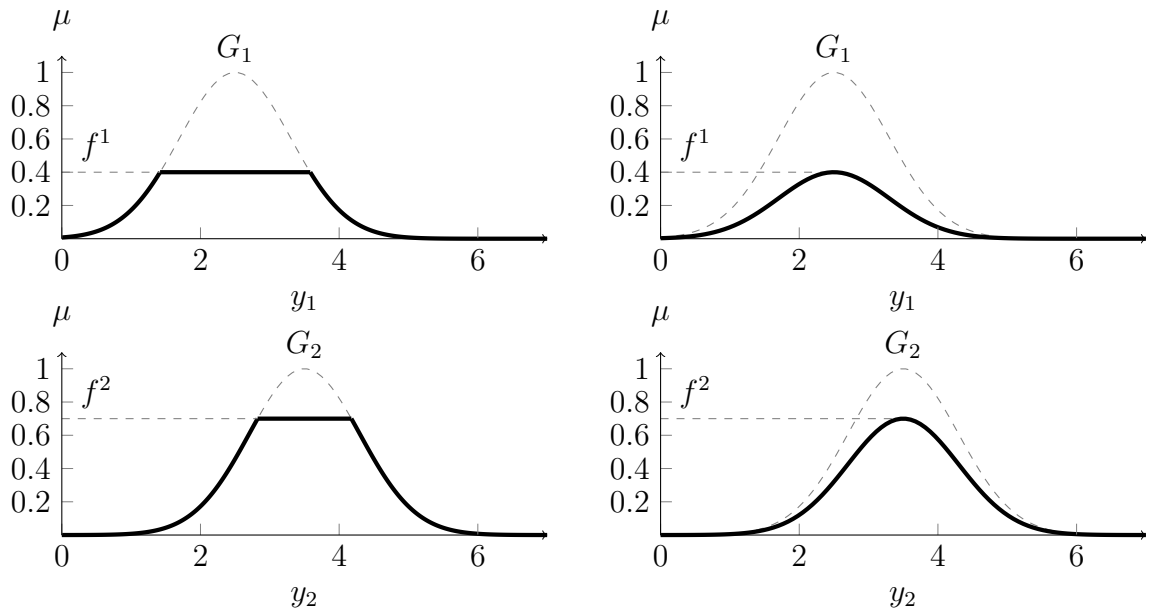

(a) Fired output sets using the minimum *t-norm*.

(b) Fired output sets using the product *t-norm*.

Figure 2.6: Mamdani inference operations using Type-1 FSs.

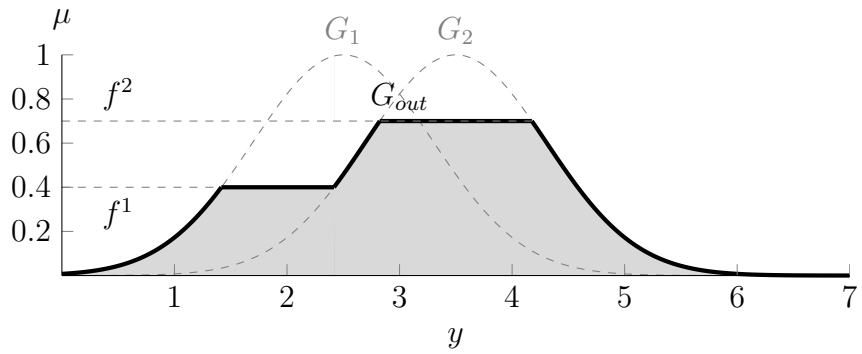

Figure 2.7: Type-1 Fuzzy Set fired consequents' aggregation procedure, after using the Mamdani minimum implication.

Still, this final step is not consensual among authors, existing some that give preference to aggregate the output of every rule before defuzzification while others perform the aggregation as part of the defuzzification procedure. Given this fact there exist several different methods to implement FLS defuzzification stage, as will be following discussed.

2.3.4 Output Processor

The Output Processor is employed to obtain a crisp output from the FS resulting from the inference procedure - a process known as defuzzification. Literature is rich in defuzzifiers methods but when considering applications in modeling and control domains, its computational efficiency is one of the main exclusion criterion. From the available methods, the Centroid and the Center-of-Sets defuzzifiers are the most frequently used ones [30], and are good examples of the two different aggregation/defuzzification approaches previously referred.

The Centroid defuzzifier obtains a crisp value by finding the centroid of a Type-1 FS resulting from the union of the consequent fuzzy sets. By sampling the resulting G_{out} FS into K points, as depicted in figure (2.8), its centroid is given by:

$$y_C = \frac{\sum_{i=1}^{K} x_i \mu_{G_{out}}(x_i)}{\sum_{i=1}^{K} \mu_{G_{out}}(x_i)} \tag{2.8}$$

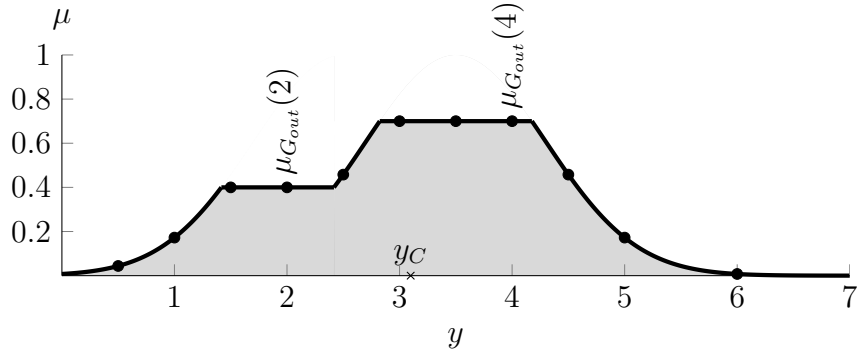

Figure 2.8: Defuzzification procedure based on the centroid method applied to the G_{out} Fuzzy Set.

Alternatively, the Center-of-Sets defuzzifier does not rely on prior aggregation of every fired consequent FS. Instead, it replaces every rule's consequent Type-1 FS by a singleton placed at its centroid which amplitude is given by the respective rule's firing level. The defuzzifier output value is then obtained by calculating the centroid of the Type-1 FS comprised of these singletons, given by:

$$y_{COS} = \frac{\sum_{i=1}^{M} c^i f^i}{\sum_{i=1}^{M} f^i} \tag{2.9}$$

where c^i is the centroid of the i^th consequent FS, M is the number of rules of the FLS and f_i is each rule's firing level. This procedure is depicted in figure (2.9).

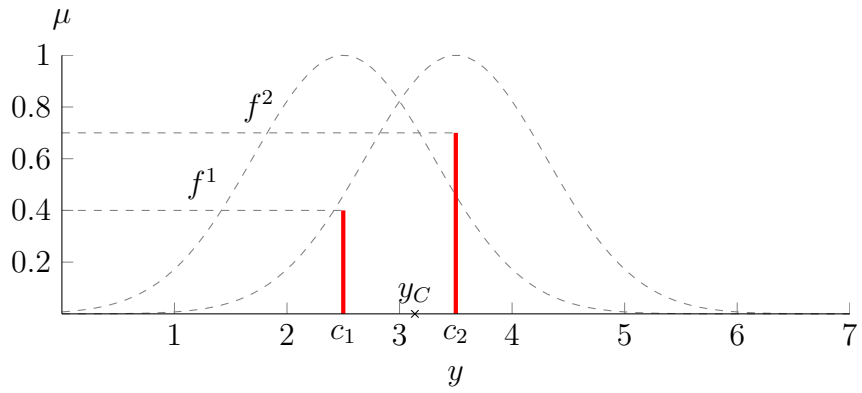

Figure 2.9: Defuzzification procedure based on the Center-of-Sets method, using the centroid of each fired consequent Fuzzy Sets separately

The latter approach is usually preferred when implemented in computationally constrained systems since the centroid of each consequent's FS can be calculated *a priori*, before the fuzzy system is deployed. Hence, the FLS's output is obtained as a weighted average of the pre-calculated centroids.

2.3.5 Considerations about Type-1 Fuzzy Logic Systems

The importance of the additive structure that a Fuzzy Logic System presents goes far beyond its rules' intelligibility. By using several rules, one is in fact defining several fuzzy patches and average the ones that overlap, ultimately performing a multi-variable function approximation. Such procedure's accuracy improves as the fuzzy patches grow in number and shrink in size.

Although Type-1 FSs have been found to provide good results in uncertainty modeling, there are several opinions referring that using them as a model for a linguistic label is an incorrect scientific theory [32]. As is pointed out in Jerry Mendel's line of reasoning, it is easy to understand the reasons for this refutation:

- A Type-1 FS representation for a word is well-defined by its Membership Function that is totally certain once all of its parameters are specified.
- Words mean different things to different people and so are uncertain.

- Therefore, it is a contradiction to say that something certain can model something that is uncertain.

The same way the variance provides a measure of dispersion about the mean, the uncertainty of a linguistic term also needs to be captured, which is not possible to be represented when a single static MF is used. In Fuzzy Set's theory, this second order uncertainty can be modeled by Type-2 Fuzzy Sets.

2.4 Type-2 Fuzzy Sets

The concept of Type-2 Fuzzy Sets was developed by Zadeh already in 1975 as an extension of Type-1 FSs [33] but it only gained broader audience much more recently with the several developments proposed by Mendel and Karnik [34]. Type-1 FSs introduced an important fuzziness degree to create linguistic partitions of a crisp domain. Nonetheless, the MFs used to do so are themselves crisp since they are totally defined without considering any uncertainty on their parameters. Type-2 FS overcome this limitation by defining a secondary degree of fuzziness, i.e. the membership value for each input of a FS is itself defined as a FS in the [0,1] domain [30]. To better understand this new dimensionality, suppose the process of defining a concept as a Type-1 FS by polling a group of experts. After gathering all the responses, certainly it will be noticed that the endpoints of the membership function will vary from person to person. The union of all embedded Type-1 FSs eventually will end up in a blurred area, known as Footprint of Uncertainty (FOU), that is bounded by two MFs, namely the Upper Membership Function (UMF) and the Lower Membership Function (LMF). Furthermore, each membership function given by a person can be assigned with a variable weight according to the amount of confidence associated to its opinion, defining this way the secondary degree of fuzziness. For this reason, a Type-2 FS representation embeds additional degrees of freedom which can better handle uncertainties caused by noisy data and changing environments as is required for example when developing a process's model. Figure (2.10) gives a better overview of the new concepts introduced by Type-2 FSs, which can be generically represented by equation (2.10).

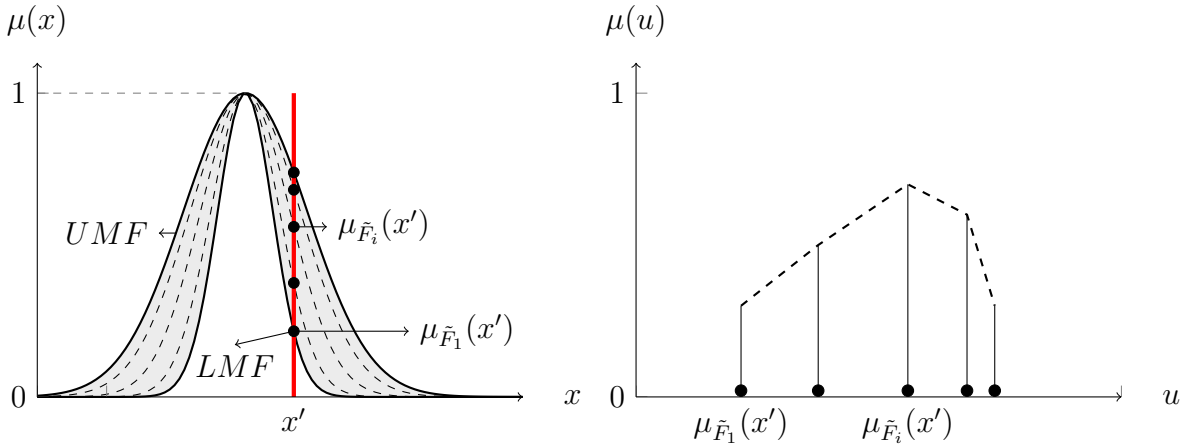

(a) FOU of a Type-2 Fuzzy Set, evincing several embedded Fuzzy Sets.

(b) Vertical slice over the FOU, evincing the variable secondary membership value of each embedded Fuzzy Set.

Figure 2.10: Representation of an Type-2 Fuzzy Set.

$$\tilde{F} = \int_{u \in X} \mu(u)du = \int_{u \in X} \left[\int_{x \in J_x} g(x)dx \right] du \qquad J_x \subseteq \Re \; and \; X \subseteq [0,1] \tag{2.10}$$

where $g(x)$ is one of the possible primary MFs.

Until late nineties the research on Type-2 FSs was of highly mathematical and theoretical nature, having few publications dedicated to it [35]. The main investigation line was focused on the development of logical operators, with important works from Mizumoto and Tanaka [36], Dubois and Prade [37] and more recently Karnik and Mendel [34]. Another important topic that has received few attention from the literature is the process of acquisition of the Type-2 FSs' membership functions. From the few works published about this topic, Turksen [38] proposes that a Type-2 FS representation could be constructed with the mean and standard deviations of scatter points obtained from surveys and, more recently, Wagner and Hagras [39] published a work proposing a recursive algorithm to define an optimal approximation of the second degree membership function based on the collected data histogram for the cases of linguistic variables and noisy sensor measurements. The representation and manipulation algebras of Type-2 FSs are not closed problems, existing some recent proposals such as [4, 40, 3] which introduce simplifications in the Type-2 FSs's representation while maintaining the uncertainty in information representation over the inference stages.

2.5 Type-2 Fuzzy Logic Systems

The success of Type-1 FLSs naturally led to the development of FLSs based on Type-2 FSs. The structure of a Type-2 FLS shares the same core components of its Type-1 counterpart, namely: a Fuzzifier, a Rule-Base, an Inference Engine and ultimately the Output Processor. While in Type-1 FLSs their final stage resumes to a defuzzification procedure, in the Type-2 case the Output Processor embraces an additional stage so a Type-2 FS is firstly converted into an equivalent Type-1 FS. This procedure is implemented by a Type-Reduction (TR) algorithm, which will be presented further in this document. The interdependency of the referred blocks is depicted in figure (2.11).

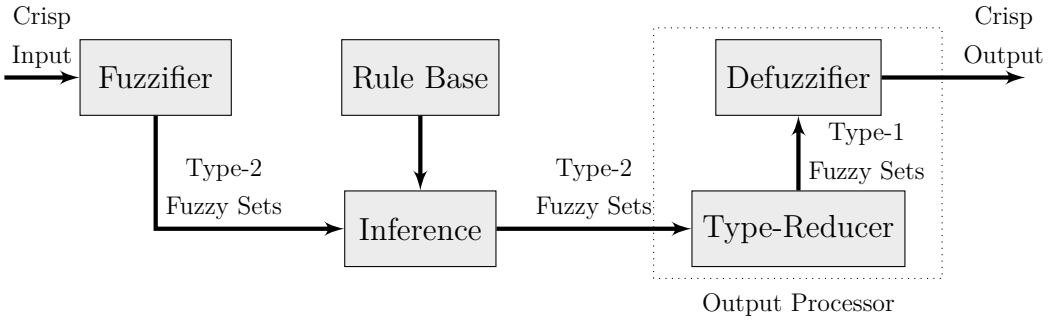

Figure 2.11: Type-2 Fuzzy Logic System structure.

Type-2 FSs can be used either on antecedent, consequent or both levels of the Type-2 FLS, depending on whether is advantageous to account for uncertainties at the referred parts of the rules. As a consequence of its additional degrees of freedom, it has been argued that Type-2 FLSs have a great potential to produce better performing systems. The main reasons for this statement are the following:

- Given the fact that a Type-2 FS embeds itself a large number of Type-1 FS under the same label, it is possible to cover the same range of operation of a Type-1 FS with a smaller number of labels and rules, reducing the complexity of modeling, tuning and understanding a rule base system when comparing to a similar performing Type-1 FS. This rule reduction capability is particularly advantageous in situations when the number of system inputs increases, as it reduces the number of possible combinations of the linguistic labels that describe each input.

- In a Type-2 FLS, since each input and output is indirectly represented by a large number of Type-1 FSs, more complex input/output relationships that could not be obtained with in a Type-1 FLS can now be modeled without necessarily increase the number of rules [2].

While the additional degrees of freedom of Type-2 FSs shown greater potential to supplant conventional methodologies [3, 4], especially in complex non-linear modeling tasks, generally their use calls for a greater computational effort. Since Type-2 FS membership degrees are given as a function of a Type-1 FS, the formalisms of elementary fuzzy computations such as the the union, intersection and complement are performed in a three-dimensional space, requiring far more complex procedures based on Zadeh's Extension Principle to implement such algebras. Moreover, the accuracy of the TR procedure depends on the number of discretization points of the FS input domain, which naturally is as better as many evaluation points are used - but the computational complexity also increases significantly. For that reason, a great amount of research in Type-2 Fuzzy Logic domains has been put towards developing more efficient representations in order to overcome this bottleneck and further extend its applicability to scenarios where the available computational resources are insufficient to cope with the time constants of the application scenarios.

In the past decade, Type-2 FSs' theory publication rate increased significantly, putting stronger efforts towards the reduction of its theoretical complexity and inherent computational effort - the two main problems that kept this uncertainty modeling tool away from real world applications until recent years. In fact, shortly after the first publications, most of the authors focused on a simplified representation known as Interval Type-2 Fuzzy Sets (IT2FSs). In a IT2FS, the MFs uncertainty is restricted to the FOU and considers the third dimension of the Fuzzy Set as uniformly distributed with a membership value '1' [35]. As so, each primary membership is associated with the same third dimension, and each fuzzy set is characterized solely by its LMF and UMF. This concept is depicted in figure (2.12).

Interval Type-2 FS can also be represented based on triangular, gaussian, trapezoidal or sigmoidal MFs. However, while one can define an arbitrary FOU as a piecewise function, the use of the referred traditional shapes simplify further model adjustments in training procedures. For this reason, literature mostly uses gaussian MFs since their FOU can be

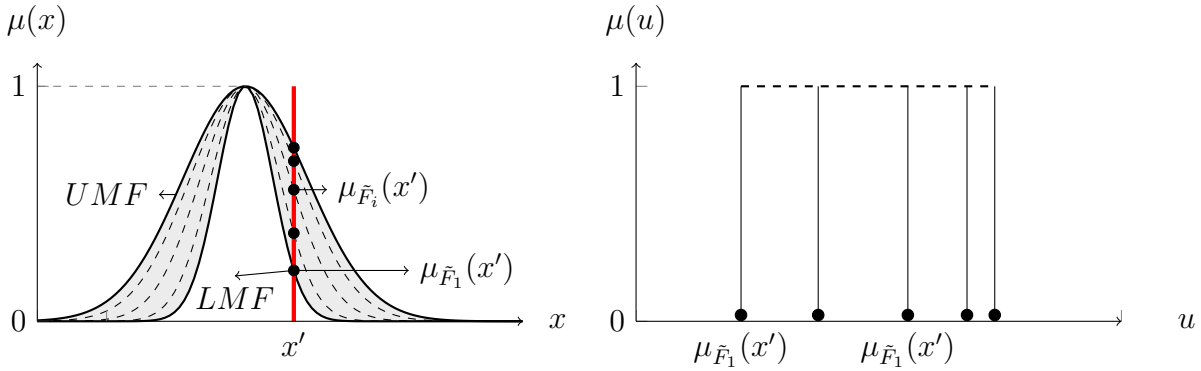

(a) FOU of an Interval Type-2 Fuzzy Set, evincing several embedded Fuzzy Sets.

(b) Vertical slice over the FOU, evincing the constant secondary membership value of each embedded Fuzzy Set.

Figure 2.12: Representation of an Interval Type-2 Fuzzy Set.

modeled by varying their mean and standard deviation, as presented in equation (2.11).

$$\begin{aligned} \tilde{F}_i(c_i, \sigma_i, x) &= exp\left[-\frac{1}{2}\left(\frac{x - c_i}{\sigma_i}\right)^2\right] \\ &= G(c_i, \sigma_i, x),\ \sigma_j^i \in [\sigma 1_i, \sigma 2_i]\ and\ c_i \in [c1_i, c2_i] \end{aligned} \tag{2.11}$$

Figure (2.13) illustrates the resulting Type-2 FS by varying each one of the referred parameters individually.

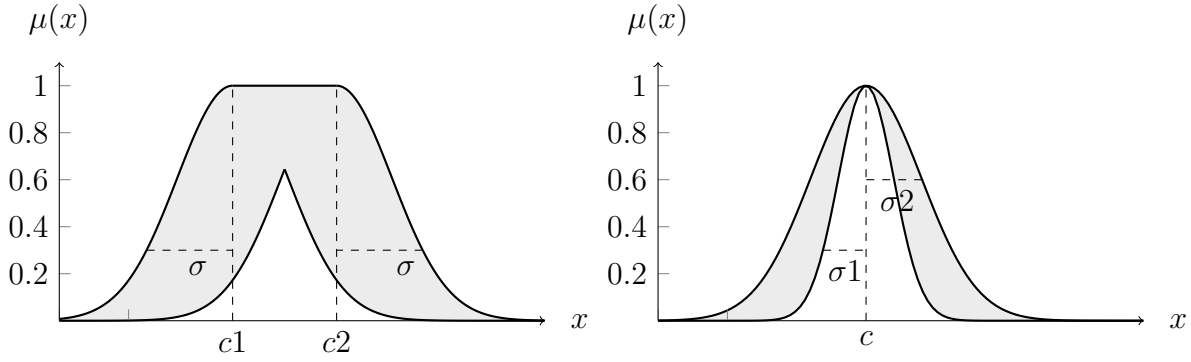

(a) Gaussian MF with uncertain mean.

(b) Gaussian MF with uncertain standard deviation.

Figure 2.13: Two possible representations of an Interval Type-2 Fuzzy Set based on gaussian membership functions.

The use of an interval based representation significantly reduced the complexity of all

the calculations required in the FLSs and, for that reason, turned Interval Type-2 Fuzzy Logic Systems (IT2FLSs) feasible in practical scenarios. Despite the changes in the nature of the MFs, the basic principles of fuzzy logic remain valid and, consequently, IT2FSs' manipulation procedures are very similar to the ones already presented regarding its Type-1 counterpart. Following, a brief analysis of the Type-2 FLS based on the Mamdani inference will be performed assuming that both antecedent and consequent FSs are of Type-2 nature.

2.5.1 Fuzzifier

Similarly to the Type-1 FLS, the most simple way to implement the fuzzifier of a Type-2 FLS is to map a crisp input into a Singleton FS, as defined in equation (2.12). While information uncertainty is not explicitly considered in the fuzzification stage, it is indirectly accounted for in the rule's FSs representations.

$$\mu_{\tilde{A}_x}(x) = \begin{cases} 1, & x = x' \\ 0, & otherwise \end{cases} \tag{2.12}$$

where x' is the system's input value.

2.5.2 Rule-Base

As a natural extension of Type-1 FLS, Type-2 FLSs also synthesize their Rule-Base in a set of *If-Then* rules, establishing the relations between the system's input and output. Regardless the Fuzzy Sets nature, the way which rules are formed remains the same. Therefore, a Type-2 FLS rule is represented as follows:

$$R^i : IF\, x_1\, is\, \tilde{F}_1^i\, and\, \cdots\, and\, x_j\, is\, \tilde{F}_j^i,\, THEN\, y^i\, is\, \tilde{G}^i \tag{2.13}$$

where R^i represents the i^{th} fuzzy rule, $\tilde{F}_j^i$ and $\tilde{G}^i$ are linguistic terms characterized by Interval Type-2 FSs, $i = [1, \cdots, M]$ where M is the number of rules, $j = [1, \cdots, N]$ where N is the number of antecedents, x_j are the FLS inputs and y^i is the rule output.

2.5.3 Inference Engine

The main difference between a Type-1 FLS and a Type-2 FLS resides in their inference engine. From section 2.2, one concluded that the result of the j^{th} input and corresponding

antecedent operations in the i^{th} rule yields a crisp number (μ_j^i) referred as membership degree. In an IT2FS the result of this operation is an interval given by $\tilde{\mu}_j^i$ as follows:

$$\tilde{\mu}_{F_j^i}(x_j) = \left[\underline{\mu}_{\tilde{F}_j^i}(x_j), \overline{\mu}_{\tilde{F}_j^i}(x_j)\right] \tag{2.14}$$

where x_j is the j^{th} FLS system input.

Despite the apparent complexity of this result, an interval based representation allows the direct use of the basic fuzzy logic operations (union, (s-norm), intersection (*t-norm*) and complement (c-norm)) as previously defined in equations (2.5) and (2.6) by considering the upper and lower bounds of the IT2FS separately. As so, the *t-norm* operator, which is used to perform the intersection of the antecedent FS is defined as:

$$\underline{f}^i = T_{j=1}^N \underline{\mu}_{\tilde{F}_j^i}(x_j) \qquad \overline{f}^i = T_{j=1}^N \overline{\mu}_{\tilde{F}_j^i}(x_j) \tag{2.15}$$

where T is a *t-norm* (product or minimum). The result of input and antecedent operations (for the minimum and product *t-norm*) is depicted in figure (2.14).

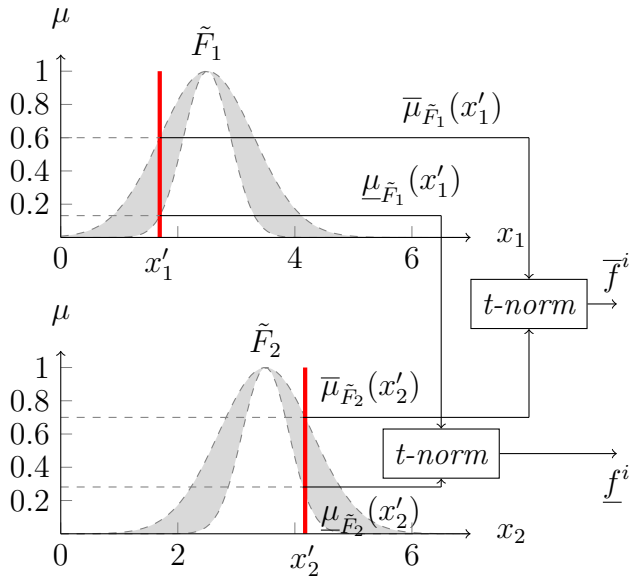

Figure 2.14: Representation of the operation between singleton input and the antecedents of a Type-2 FLS using a t-norm operator (minimum or product).

Similarly, the Mamdani implication methods - the Mamdani's minimum and product, can be directly used with IT2FS by applying the t-norm operator to the rule's firing level $\tilde{f}^i$ and the consequent $\tilde{G}_i$. This procedure is performed by considering the upper and lower bounds of $\tilde{f}^i$ and $\tilde{G}_i$ separately, as presented in figure (2.15) for the minimum and product *t-norms*.

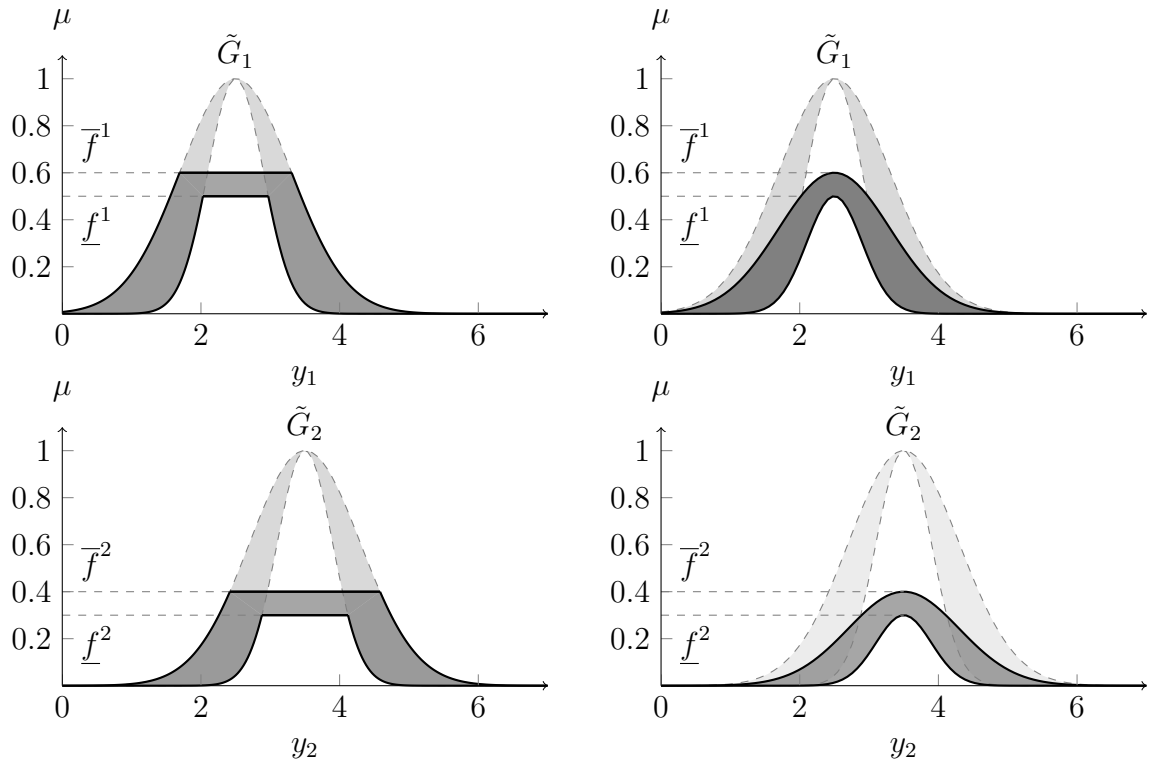

(a) Fired output sets using the minimum *t-norm*.

(b) Fired output sets using the product *t-norm*.

Figure 2.15: Mamdani inference operations using Type-2 FSs.

The inference process ends up by obtaining the Fuzzy Set determined by the aggregation of the output of all the fired fuzzy sets. Similarly to the Type-1 FLS case, one can merge the contribution of each rule by finding the maximum value of the overlapped FSs, as depicted in figure (2.16). To obtain a crisp output after this procedure, one will have to apply a TR algorithm firstly, as will be discussed in the following subsection.

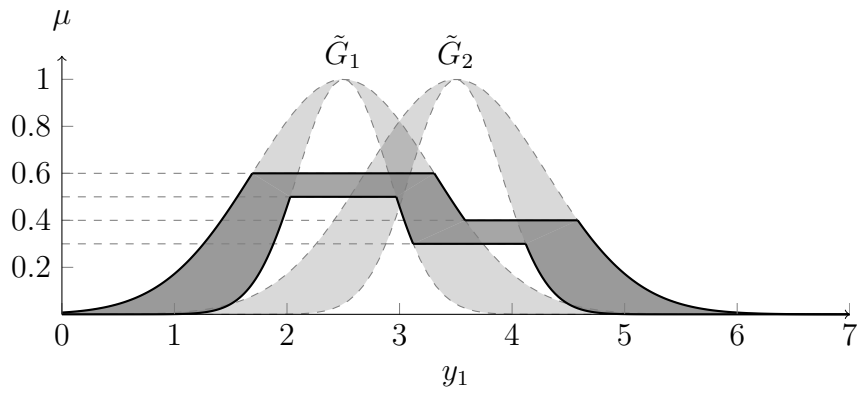

Figure 2.16: Type-2 Fuzzy Sets fired consequents' aggregation procedure, after using the Mamdani minimum implication.

2.5.4 Type-Reduction

In order to develop practical applications based on the Type-2 FLs, it becomes necessary to obtain a crisp value from the combination of all fired FS. To accomplish this goal, it is firstly necessary to obtain the centroid of a Type-2 FS, represented as an interval often referred to as type-reduced set. The Karnik-Mendel (KM) algorithm [41], which can be seen as an extension of Type-1 defuzzification procedure, is currently the most accurate TR method found in literature. Though, given its iterative nature, it is the most complex stage of the fuzzy inference process, requiring extensive calculations even when the simpler IT2FSs are used.

Karnik-Mendel Type-Reduction

The KM algorithm is an iterative process which allows one to obtain an interval of uncertainty for the centroid of an Interval Type-2 FS given by $[y_l, y_r]$. Similarly to the Type-1 FSs defuzzification case, Karnik and Mendel [30] proposed several methods to perform the Type-2 FSs' TR based on well known approaches from the Type-1 FLS defuzzification procedures, namely: Height and Modified Height TR, Centroid TR and Center-of-Sets TR. Despite equally valid, the choice of the defuzzification method has significant implications in the result's quality. The Height and Modified Height are the less complex ones to implement. However, it is known that when a single rule is triggered, these methods may return inconsistent results [30]. The Centroid one requires a large amount of calculations because, for each new system input, it has to firstly merge the consequent part FS of

every rule and only then obtain the centroid of the resulting FS. Finally, the Center-of-Sets TR is usually the employed method since it performs a smaller amount of operations when compared with the Centroid one. Its efficiency is due to the *a priori* computation of each consequent FS's centroid as, since its value is independent from the system's input variables, this result can be used as a constant in the Center-of-Sets TR. As so, the only procedure that has to be performed after each new input into the system is a weighted average of the stored centroids according to a combination of the upper and lower firing levels of each rule. Since the Center-of-Sets TR inevitably requires one to compute the centroid of each consequent Type-2 FS once, the Centroid TR will be hereby presented.

Similarly to the Centroid defuzzification procedure, the Centroid TR starts by obtaining K samples from a Type-2 FS. Since the FOU of a Type-2 FS embeds several Type-1 FS, to perform the TR one has firstly to obtain two Type-1 FS whose centroid best approximates the upper and lower bounds of the Type-2 FS centroid. Using as example the $\tilde{G}_{out}$ FS, this procedure starts by using its sampled upper and lower bounds to find the optimal values for the switching points [L,R], as depicted in figure (2.17).

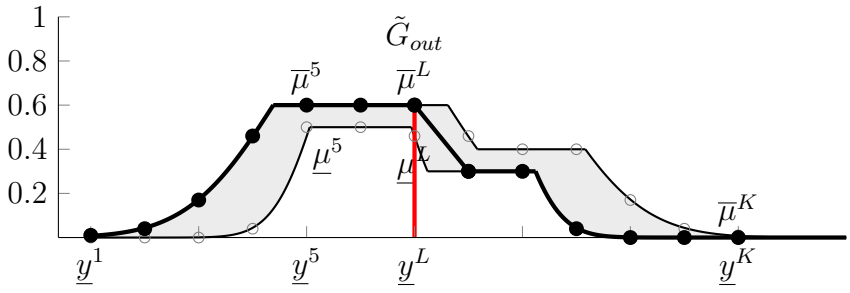

(a) Computing y_l: Switching from the upper bounds of the firing intervals to the lower bounds.

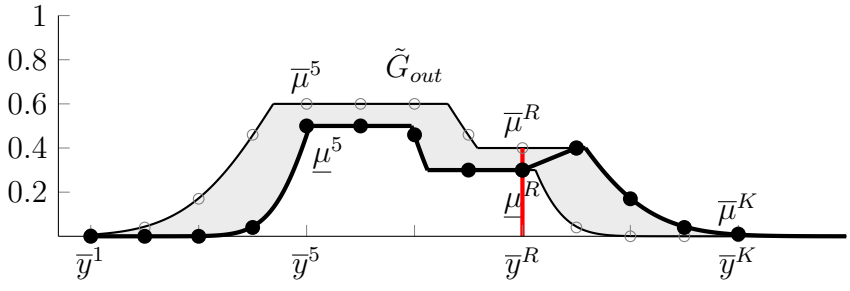

(b) Computing y_r: Switching from the lower bounds of the firing intervals to the upper bounds.

Figure 2.17: Switching points in computing y_l and y_r.

The candidate points are obtained as follows in equations (2.16) and (2.17).

$$y_l(k) = \frac{\sum_{i=1}^{k} \underline{y}^i \overline{\mu}^i_{\tilde{G}_{out}} + \sum_{i=k+1}^{K} \underline{y}^i \underline{\mu}^i_{\tilde{G}_{out}}}{\sum_{i=1}^{k} \overline{\mu}^i_{\tilde{G}_{out}} + \sum_{i=k+1}^{K} \underline{\mu}^i_{\tilde{G}_{out}}} \tag{2.16}$$

$$y_r(k) = \frac{\sum_{i=1}^{k} \overline{y}^i \underline{\mu}^i_{\tilde{G}_{out}} + \sum_{i=k+1}^{K} \overline{y}^i \overline{\mu}^i_{\tilde{G}_{out}}}{\sum_{i=1}^{k} \underline{\mu}^i_{\tilde{G}_{out}} + \sum_{i=k+1}^{K} \overline{\mu}^i_{\tilde{G}_{out}}} \tag{2.17}$$

where k is an integer in [1,K - 1] interval, where K is the number of discretization points. Then, the optimal interval bounds can be obtained by y_l and y_r, as following presented:

$$y_l = \min_{k \in [1, M-1]} y_l(k) \equiv y(L) \equiv \frac{\sum_{i=1}^{L} \underline{y}^i \overline{\mu}^i_{\tilde{G}_{out}} + \sum_{i=L+1}^{K} \underline{y}^i \underline{\mu}^i_{\tilde{G}_{out}}}{\sum_{i=1}^{L} \overline{\mu}^i_{\tilde{G}_{out}} + \sum_{i=L+1}^{K} \underline{\mu}^i_{\tilde{G}_{out}}} \tag{2.18}$$

$$y_r = \max_{k \in [1, M-1]} y_r(k) \equiv y(R) \equiv \frac{\sum_{i=1}^{R} \overline{y}^i \underline{\mu}^i_{\tilde{G}_{out}} + \sum_{i=R+1}^{K} \overline{y}^i \overline{\mu}^i_{\tilde{G}_{out}}}{\sum_{i=1}^{R} \underline{\mu}^i_{\tilde{G}_{out}} + \sum_{i=R+1}^{K} \overline{\mu}^i_{\tilde{G}_{out}}} \tag{2.19}$$

where L and R are switch points satisfying

$$y^L \leq y_l < y^{L+1} \tag{2.20}$$

$$y^R \leq y_r < y^{R+1} \tag{2.21}$$

The choice of whether we start from the upper or lower firing levels when finding the left and right bounds of each switching point has a very simple explanation. Take y_l as an example: y_l has to be the minimum value of the FLS output. Since $\underline{y}^i$ is ordered ascendantly along the horizontal axis of figure (2.12), a large weight (upper bound of the firing interval) should be chosen in the left of the switch point and a small weight (lower bound of the firing interval) for its right side. As finding all the centroid $[y_l, y_r]$ candidates is a computationally inefficient approach, an iterative procedure to find the optimal switching points is presented in Table (2.1).

Step	For computing y_l	For computing y_r
1.	Initialize	Initialize
	$\mu^i_{\tilde{G}_{out}} = \dfrac{\underline{\mu}^i_{\tilde{G}_{out}} + \overline{\mu}^i_{\tilde{G}_{out}}}{2}$	$\mu^i_{\tilde{G}_{out}} = \dfrac{\underline{\mu}^i_{\tilde{G}_{out}} + \overline{\mu}^i_{\tilde{G}_{out}}}{2}$
	and compute	and compute
	$y = \dfrac{\sum_{i=1}^{M} \underline{y}^i \mu^i_{\tilde{G}_{out}}}{\sum_{i=1}^{M} \mu^i_{\tilde{G}_{out}}}$	$y = \dfrac{\sum_{i=1}^{M} \overline{y}^i \mu^i_{\tilde{G}_{out}}}{\sum_{i=1}^{M} \mu^i_{\tilde{G}_{out}}}$
2.	Find $l \in [1, M-1]$ such that	Find $r \in [1, M-1]$ such that
	$\underline{y}^l < y < \underline{y}^{l+1}$	$\overline{y}^r < y < \overline{y}^{r+1}$
3.	Set	Set
	$\mu^i_{\tilde{G}_{out}} = \begin{cases} \overline{\mu}^i_{\tilde{G}_{out}}, & n \leq l \\ \underline{\mu}^i_{\tilde{G}_{out}}, & n > l \end{cases}$	$\mu^i_{\tilde{G}_{out}} = \begin{cases} \underline{\mu}^i_{\tilde{G}_{out}}, & n \leq r \\ \overline{\mu}^i_{\tilde{G}_{out}}, & n > r \end{cases}$
	and compute	and compute
	$y' = \dfrac{\sum_{i=1}^{M} \underline{y}^i \mu^i_{\tilde{G}_{out}}}{\sum_{i=1}^{M} \mu^i_{\tilde{G}_{out}}}$	$y' = \dfrac{\sum_{i=1}^{M} \overline{y}^i \mu^i_{\tilde{G}_{out}}}{\sum_{i=1}^{M} \mu^i_{\tilde{G}_{out}}}$
4.	If $y' = y$, stop and set $y_l = y$ and $L = l$; otherwise, set $y = y'$; and go to step 2.	If $y' = y$, stop and set $y_r = y$ and $R = r$; otherwise, set $y = y'$; and go to step 2.

Table 2.1: Iterative Karnik-Mendel algorithm.

Despite the improvements brought by Interval Type-2 FS representations, the KM algorithm still requires a large number of iterations to find the optimal type-reduced FS. Therefore, several enhancements and simplifications were proposed in the recent years for the sake of reducing its computational footprint.

Optimized Type-Reduction Algorithms

With the development of simpler and alternative algorithms, Type-2 Fuzzy Logic definitely gathered the attention of a broader number of researchers, having a direct impact in an increasing number of applications in domains such as modeling, control and classification and pattern recognition observed in recent years.

The Type-Reduction methods found in literature can be grouped into two main categories:

- Enhancements to the KM algorithm, which improve directly the original formulation of the KM by choosing a better initialization and termination conditions, to reduce the number of iterations and optimize the computing technique to speed up each iteration of the TR process;
- Alternative TR algorithms, which unlike the iterative KM algorithms, are mostly presented in a closed-form representation and provide faster results than the KM method;

In [42] a thorough analysis about the current TR algorithms' state-of-the-art is done and it was observed that enhanced versions of the KM algorithm are, in general, faster than its original formulation. Yet, the gains may vary depending on the size of the FLS rule base. From the presented approaches, the Enhanced Opposite Direction Searching Algorithm (EODS) [43] shown itself as the fastest one achieving gains up to 70% (relative to the original KM) when the FLS has less than 100 rules - as is used in most part of non-linear processes' modeling applications. It is important to highlight that, despite their algorithmic differences, enhanced versions of the KM algorithms give exactly the same outputs as its original formulation.

While KM algorithms have been widely adopted, some closed-form methods that bypass this TR procedure have been proposed. However, since their methodologies may be significantly different than the original KM algorithms their outputs may also be quite different - a compromise between accuracy and complexity of the method may be necessary. For example, Wu and Tan [44] introduced a method which eliminates TR by defining a collection of Type-1 FS embedded by the footprint of uncertainty. Alternatively, Wu-Mendel Uncertainty Bound method [45] directly uses the uncertainty bounds of the FS and was shown to be the closed-form method giving the closest approximation to the KM and presented an execution turnaround time very close to a similar sized Type-1 FLS. Despite

their good performance, a closed-form approach is not used in this work since the best performing ones hinder the decomposition of the model output as sum of locally linear models. The capability of decomposing the system in such way is of great advantage to the present work as it allows an efficient implementation of the online training procedures and the synthesis of the control law based on the Generalized Predictive Control theory.

2.5.5 Defuzzifier

After applying one of the possible TR methods, the obtained Interval Fuzzy Set still has to be converted into a crisp number so it becomes suited to the most part of the FLS application scenarios. Anyway, this procedure is fairly straightforward, and the defuzzified value obtained by simply computing the average of the interval's left and right endpoints.

$$y_{out} = \frac{y_r + y_l}{2} \tag{2.22}$$

2.6 Comparative Analysis

The noise reduction properties of Type-2 Fuzzy MFs have been several times pointed in literature as one of its main advantages when compared to its Type-1 counterparts. To attest the influence of the antecedent part membership functions' FOU width in the rule activation level when the FLS's inputs are corrupted by disturbances, a comparative analysis will be performed by probing its input domain with different magnitude noise levels. This comparison will be based on Gaussian-shaped FS with uncertain mean (as presented in figure (2.13a), where its FOU is bounded by the upper and lower MFs as defined in equations (2.23) and (2.24)

$$\underline{\mu}_{\tilde{F}}(x) = \begin{cases} G(c2, \sigma, x), & x < \frac{c1+c2}{2} \\ G(c1, \sigma, x), & x \geq \frac{c1+c2}{2} \end{cases} \tag{2.23}$$

$$\overline{\mu}_{\tilde{F}}(x) = \begin{cases} G(c1, \sigma, x), & x < c1 \\ 1, & c1 \leq x \leq c2 \\ G(c2, \sigma, x), & x > c2 \end{cases} \tag{2.24}$$

In a similar approach as presented in [46], this procedure will be based on a simple FLS comprising a single input and two rules defined by two overlapping MFs ($\tilde{F}_1$ and $\tilde{F}_2$) such

that, for a certain input value x, the following conditions are satisfied:

$$\overline{\mu}_2 = 1 - \underline{\mu}_1 \tag{2.25a}$$

$$\underline{\mu}_2 = 1 - \overline{\mu}_1 \tag{2.25b}$$

where $\overline{\mu}_i$ and $\underline{\mu}_i$ are the upper and lower firing levels of $\tilde{F}_i(x)$, respectively.

To simplify this evaluation, it is considered that the output is given by Nie Tan closed form Type-Reduction [47] presented in equation (2.26),

$$y = \frac{\sum_{i=1}^{M}(\underline{f}^i + \overline{f}^i)y^i}{\sum_{i=1}^{M}(\underline{f}^i + \overline{f}^i)} \tag{2.26}$$

where y_i is the output of each rule and $\underline{f}^i$ and $\overline{f}^i$ are equivalent to $\overline{\mu}_i$ and $\underline{\mu}_i$, respectively, since the system solely has one antecedent. Therefore, based on equations (2.25) and (2.26), the contribution of each rule to the model output is weighted by equation (2.27).

$$\begin{aligned} r_i(x) &= \frac{\underline{f}^i + \overline{f}^i}{\sum_{k=1}^{M}(\underline{f}^k + \overline{f}^k)} \\ &= \frac{\underline{\mu}^i(x) + \overline{\mu}^i(x)}{2} \end{aligned} \tag{2.27}$$

Considering that the system's input is corrupted by a gaussian noise of magnitude n, the firing strength becomes:

$$r_i(x+n) = \frac{\underline{\mu}_i(x+n) + \overline{\mu}_i(x+n)}{2} \tag{2.28}$$

Based on equations (2.27) and (2.28), one can evaluate the relationship between the firing level distortion caused by the input noise and the FOU width for a single rule by obtaining the Normalized Squared Error (NSE) as presented in equation (2.29).

$$NSE = \int_{n=-n1}^{n1}\int_{x=x_1}^{x_2}\left[\frac{r_i(x) - r_i(x+n)}{r_i(x)}\right]^2 dxdn \tag{2.29}$$

The solution of equation (2.29) is obtained numerically by varying in the same proportion the values c_1 and c_2 relatively to a Type-1 Fuzzy Set initially set with center on c and then corrupting the input variable with a noise signal with different Signal-to-Noise Ratios (SNRs) (defined relatively to the maximum input value of the fuzzy set's domain). The maximum uncertainty percentage relatively to the FS upper and lower MF's center was limited to 10% as with higher values a great portion of the input space a large portion of the upper and lower membership degrees become closer to one and zero respectively (thus not providing a desirable input space partition for a TS system). Figure (2.18) presents the dependency of the NSE on the noise level and the uncertainty ratio, and the results are obtained by averaging 50 runs for every parameters' combination.

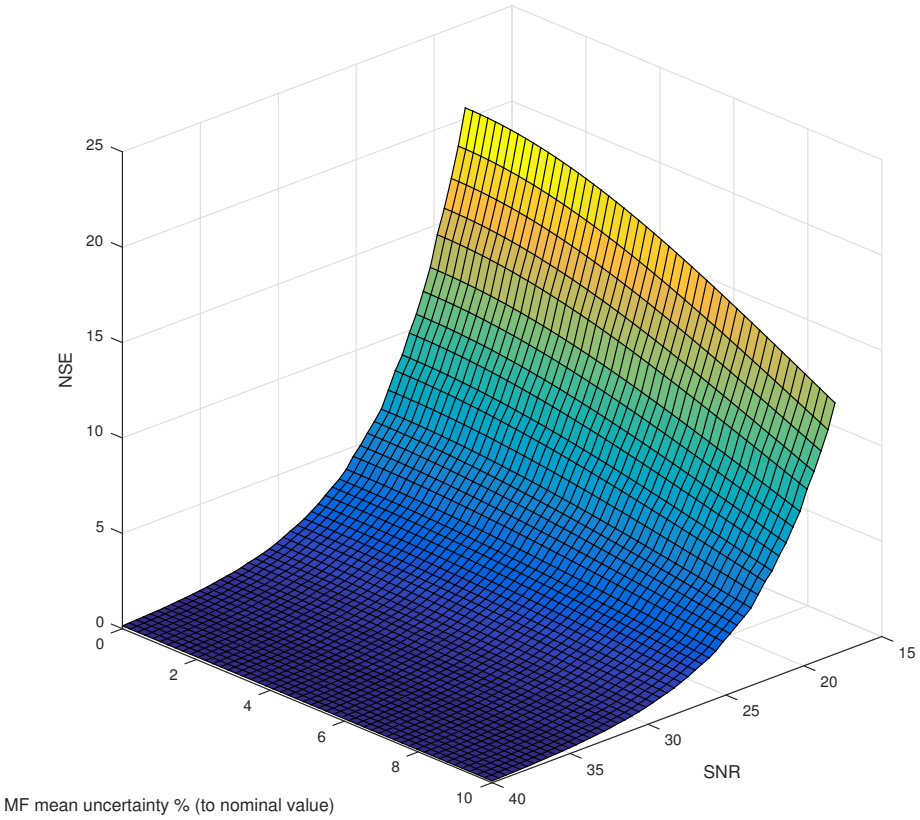

Figure 2.18: Surface of the NSE of the evaluated system depending on the input noise level and the antecedent parameter's FOU width.

For a better comparison between the different scenarios, a bi-dimensional projection perspective of the previous surface is presented in figure (2.19) while the results relative to the 10% uncertainty level summarized in Table (2.2).

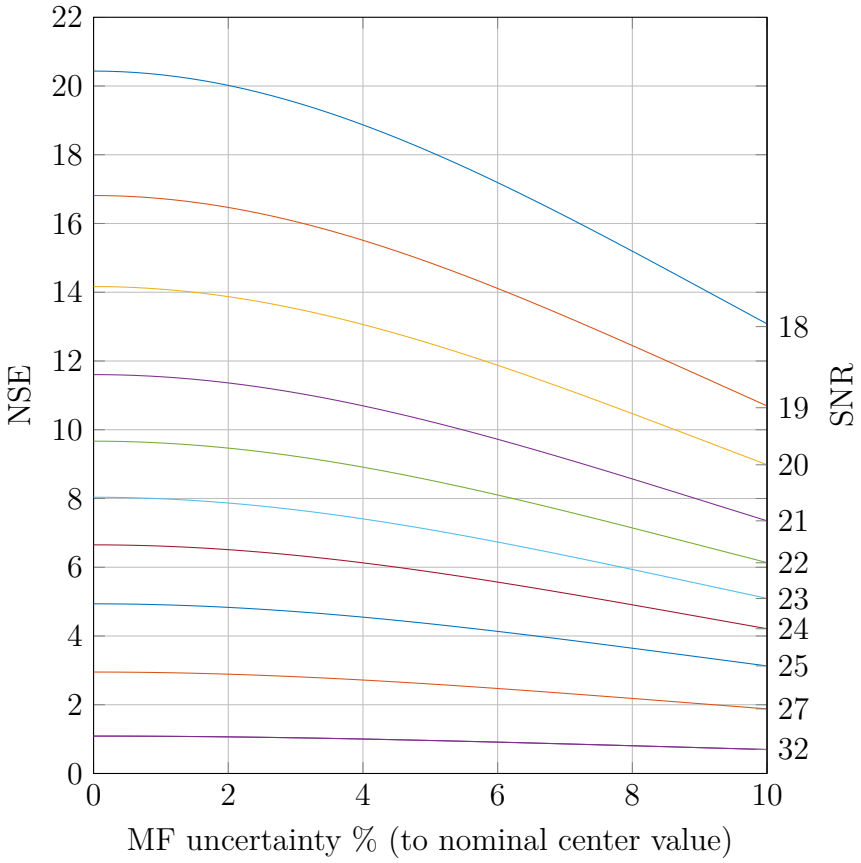

Figure 2.19: Dependency of the firing degree NSE on the membership function's center uncertainty ratio and the noise level corrupting the input signals.

Table 2.2: Distortion level for different SNR considering 10% uncertainty over the membership function's center.

	SNR									
	18	19	20	21	22	23	24	25	27	32
NSE	13.11	10.64	8.98	7.35	6.13	5.09	4.21	3.13	1.88	0.70
σ	0.98	0.81	0.72	0.47	0.46	0.39	0.38	0.24	0.13	0.05

From the presented results two main conclusions can be obtained regarding the noise properties of Type-2 Fuzzy Sets:

- For a given SNR, increasing its FOU reduces the distortion observed at each rule firing level when comparing to the Type-1 counterpart which served as starting point (when a 0% uncertainty factor is considered in the MF's center);
- For reduced noise levels, the use of Type-2 FS at the antecedent part of the rule base does not bring significant improvements comparing to its Type-1 counterpart, as is evinced by the flatter region observed in figure (2.19) as SNR is increased.

2.7 Conclusions

This chapter presented the fundamental theory of Type-1 FLSs and how its extension to the Type-2 FL formalisms can be performed. In the recent years, Type-2 FL has been acclaimed as a significant improvement over the fundamental Fuzzy Logic Theory. Despite the lack of an irrefutable theoretical proof of it, the fact is that most recent publications present practical applications where the use of Type-2 FL is advantageous, mostly in scenarios where uncertain information representations are manipulated - the evaluative scenario concluding this chapter points also in that direction. Therefore the concepts here introduced will be further developed in the succeeding chapters, by integrating them with more flexible structures in terms of learning capabilities.

Chapter 3

Takagi-Sugeno Fuzzy Logic Systems

3.1 Introduction

The achievements obtained by Fuzzy Logic undoubtedly changed the way expert information is represented, manipulated, and interpreted in computational systems. Nevertheless, the initialization of Mamdani FLSs' main parameters, namely its membership functions and their interdependency relations, is a process that depends on the knowledge of an expert (which may be subjective and is ultimately limited by its know-how). Takagi and Sugeno [26] were among the first researches who recognized that Fuzzy Logic Systems could be further enhanced by autonomous learning techniques. Together, they proposed a new structure for the consequent part of the rules, introducing also methodologies to autonomously create and improve the FLSs' performance based on heuristic and non-linear optimization algorithms for the antecedent part of the rule-base and a Kalman Filter for the consequent one. It is however for their innovative FLS's structure that supports their work that Takagi and Sugeno are nowadays known in Fuzzy Systems' literature (effectively coining the concept of Takagi-Sugeno Fuzzy Logic Systems), serving their work as the stepping stone for many successful research topics.

As regards to learning ability, Artificial Neural Networks (ANNs) stand in the exact opposite side of traditional FLS. ANNs can model any arbitrary function representing a system's input/output behavior by means of a network of several activation functions, with parameters which can be autonomously tuned based on simple concepts as the error back-propagation. It is a problem, though, that the knowledge of these systems is stored in an opaque fashion for the system's designer since the learning results are represented by a large set of parameter values with hardly any interpretable features. To overcome

such limitation and improve Fuzzy System's adaptability, different structures inspired by Multi-Layer Neural Networks have been presented over the last years. These hybrid architectures, referred to as Neuro-Fuzzy Systems [48], reveal themselves as an approach that benefits from the readability of a fuzzy rule and the learning ability of ANNs. Among many Neuro-Fuzzy architectures, the most referred ones are the Fuzzy Adaptive Learning Control Network (FALCON) [49], the Generalized Approximate Reasoning based Intelligence Control (GARIC) [50], Neural Fuzzy Controller (NEFCON) [51], the Self Constructing Neural Fuzzy Inference Network (SONFIN) [52] and ultimately the Adaptive Network based Fuzzy Inference System (ANFIS) [53].

This multitude of implementations of Neuro-Fuzzy systems is in its essence similar but present some fundamental differences [54]: while some use ANNs as a pre or post-processing stage for the Fuzzy Logic Systems, other focus on the reorganization of well known fuzzy structures such as the Mamdani FLS or the Takagi-Sugeno FLS into an equivalent Multi-Layer Neural Network so its simple training principles can be used to update the Fuzzy System's parameters. Some authors take the system's learning capabilities further ahead, proposing algorithms to develop Neuro-Fuzzy Systems in a completely autonomous approach, providing system-wide adaption mechanisms to optimize their structure. However, most of them focus on the parameter level adaption, leaving the structure problem up to an application expert analysis (effectively making use of the Fuzzy Systems intelligibility).

The ANFIS architecture is one of the most successful Neuro-Fuzzy systems' implementations due to its functional equivalence to the Takagi-Sugeno FLSs, providing a simple methodology to convert *If-Then* rules into an adaptive Radial Basis Function Network (RBFN). Due to the typical TS FLS formulation, where each rule's output is given by a function of its input variables, the conversion of the inference and aggregation procedures is fairly straightforward. A similar procedure could also be performed according to the Mamdani type of FLS but its applicability it is restricted to very specific types of defuzzification procedures (Center-of-Sets) for it to become a computationally efficient alternative approach. As will be clear further in this work, the balance between computational speed and methodology accuracy are major concerns when a fuzzy system is used as a model in real-time systems, thus making the Takagi-Sugeno systems better candidates than the Mamdani ones to accomplish such task.

Since the structures of Takagi-Sugeno FLSs and ANFISpl are deeply related, this chapter will begin by presenting the former one, starting with the Type-1 Fuzzy Sets which will be then extended to the several possible architectures based on Type-2 Fuzzy Sets.

According to the more general Type-2 TS FLS, the formal equivalence between the traditional *If-Then* rule base structure and the ANFIS will be then evinced. Ultimately, the procedures employed during the training of the TS Fuzzy Systems will be presented.

3.2 Type-1 Takagi-Sugeno Fuzzy Logic Systems

Takagi-Sugeno FLS are a type of Fuzzy Systems' representation which, along with the Mamdani one, became the *de facto standards* in fuzzy modeling and control applications. Similarly to the Mamdani FLS, the Takagi and Sugeno [26] one establishes an input-output relation based on a set of *If-Then* rules. In the latter case, while the system's input space is partitioned by Type-1 FS, the consequent part of each rule is usually given by a first order polynomial. Even though it is possible to use higher-order polynomials, first-order ones are widely preferred due to their closeness with linear modeling approaches [55]. Equation (3.1) presents the structure of a first-order Type-1 TS model rule.

$$\begin{aligned} R^i: \quad & IF\ x_1\ is\ F_1^i\ and\ \cdots\ and\ x_j\ is\ F_j^i \\ & THEN\ y^i\ =\ c_1^i x_1\ +\cdots+\ c_j^i x_j \end{aligned} \tag{3.1}$$

where R^i represents the i^{th} fuzzy rule, F_j^i are linguistic terms characterized by Type-1 FS, c_j^i are the consequent polynomial parameters, $i = [1, \cdots, M]$ where M is the number of fuzzy rules, $j = [1, \cdots, N]$ where N is the number of antecedents, x_j are the fuzzy system inputs and y^i is the rule output.

One important result upcoming from the algebraic nature of the rule's consequent part is that the defuzzification mechanism in TS FLSs is inherently implemented at the output of each rule, not requiring further steps as in the Mamdani case to convert a fired output Type-1 FS into an equivalent crisp value. Consequently, the global output of a Type-1 TS FLS can be obtained in a straightforward way using the Center-of-Sets defuzzification, which is no more than a weighted average of the output of the M rules according to their firing level, as follows in equation (3.2):

$$y(\mathbf{x}) = \frac{\sum_{i=1}^{M} f^i y^i}{\sum_{i=1}^{M} f^i} = \frac{\sum_{i=1}^{M} f^i (c_1^i x_1 + c_2^i x_2 + \cdots + c_N^i x_N)}{\sum_{i=1}^{M} f^i} \tag{3.2}$$

where f^i is the rule's firing level, defined as:

$$f^i = T_{k=1}^{N} \mu_{F_k^i}(x_k) \tag{3.3}$$

and $T_{k=1}^{N}$ denotes a *t-norm*, a operator which merges the firing levels of each rule's antecedent. Similarly to the aggregation procedures presented on the previous chapter, the minimum and product operators are usually employed. The latter the most commonly used and also adopted in this work. As so, f^i becomes:

$$f^i(\mathbf{x}) = \mu_{F_1^i}(x_1) * \mu_{F_2^i}(x_2) * \cdots * \mu_{F_N^i}(x_N) \tag{3.4}$$

In figure (3.1) the main concepts supporting the TS FLS inference mechanism are depicted.

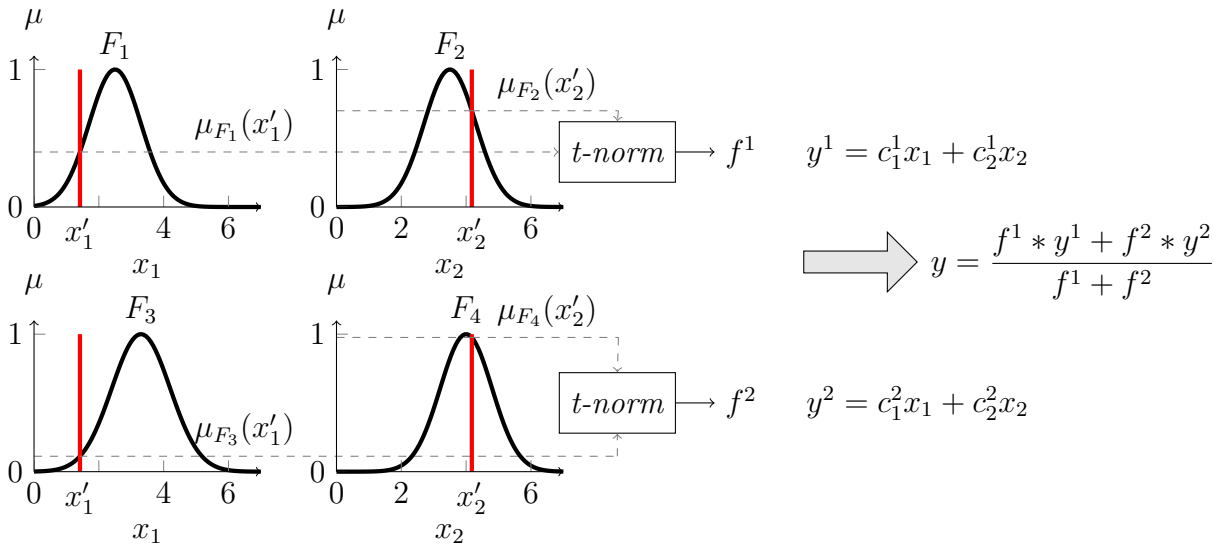

Figure 3.1: Example of a two rules - two antecedent Type-1 Takagi-Sugeno FLS.

While providing a relatively simple model structure and maintaining an important level of intelligibility, Takagi–Sugeno FLS also offer an efficient and accurate way of modeling non-linear behaviors. The antecedent part of the *If-Then* rules allows one to partition a system's input space using several input/output linear function which are valid approximations of the global non-linear system under different operating regions. Considering a particular local model output, given by y^i and defined for an operation point in the vicinity of $\mathbf{x}$, its validity for the current operating regime (given by the input vector $\mathbf{x} = [x_1, x_2, \cdots, x_N]$) is as higher as its firing level (f^i) is closer to unity, and consequently lower when the local

approximation is no longer valid. Figure (3.2) presents a simple case where such approach can be used to model a non-linear input/output relationship.

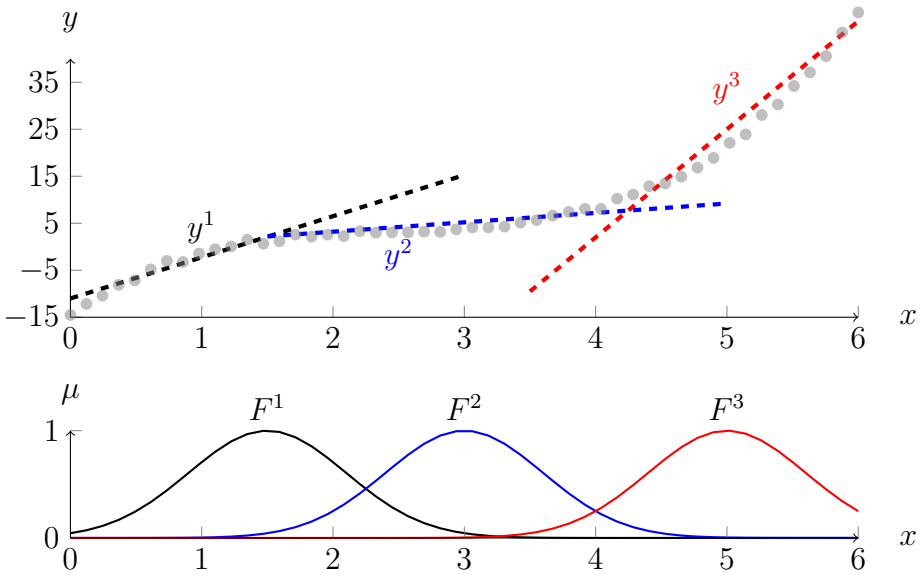

Figure 3.2: Example of a three rule (M=3) partition with a single input (N=1) TS FLS to model a non-linear function.

Therefore, the overall non-linear behavior of the system can be obtained by a smooth interpolation of simpler local linear subsystems which are up to a certain degree transparent, overcoming the limitations of some black-box non-linear modeling approaches such as Neural-Networks or Volterra series, where the model dimensionality can increase significantly and the relationships between variables become intractable. Attesting the theoretical and practical utility of TS FLSs, it has also been proved that they are also universal approximators [53], demonstrating their capability of approximate any reasonable function with subjective accuracy depending on the number of rules and the training level considered.

3.3 Type-2 Takagi-Sugeno Fuzzy Logic Systems

Inspired by its simplicity when developing rule based systems, researchers further extended the Type-1 TS FLS structure with the Type-2 FL formalisms to accommodate higher levels of uncertainty in the system's parameters. As is discussed in [30], this transition is fairly natural since the basic principles of the fuzzy logic are independent of the nature of the membership functions, requiring only little changes in the inference engine and defuzzifier blocks to cope with new information representations. When developing a Type-2 TS FLS, its parameter's uncertainty can be accounted at different parts of the rule-base - at its antecedent ('A') or consequent ('C') level. Table (3.1) summarizes the possible combinations that can be made with the information representation methods.

	A2-C1	A2-C0	A1-C1
Antecedent	Type-2 Fuzzy Sets	Type-2 Fuzzy Sets	Type-1 Fuzzy Sets
Consequent	Type-1 Fuzzy Sets	Crisp numbers	Type-1 Fuzzy Sets

Table 3.1: Characterization of Type-2 TS FLSs according to the type of parameters used in the Antecedent and Consequent parts of the rule base.

The literature of Type-2 TS FLSs tends to put more emphasis in the former two representations (A2-C1 and A2-C0) since they effectively make use of Type-2 FSs. However, by using Type-1 FSs at the consequent part of the rule, the A1-C1 structure also accounts with higher level of uncertainty in the parameters and, for that reason, is included in the spectrum of Type-2 TS FLSs. The A2-C1 and A2-C0 TS FLSs distinguish themselves in their consequent part: in the A2-C0 case, the consequents are a linear combination of crisp values (a polynomial in its traditional sense), whereas in the A2-C1 the consequent part is a linear combination of Type-1 FSs. In the latter case, the Type-1 FS resulting from the output of each rule can be obtained by using the Extension Principle [30]. However, since the calculations necessary to obtain a crisp output can become quite complex, their simpler interval representations are often preferred in practical applications. In the following subsections the more general A2-C1 structure will be firstly detailed, referring then to the simpler A2-C0 and A1-C1 cases.

3.3.1 A2-C1 Structure

In order to better understand how the typical FLS main blocks are implemented under a Takagi-Sugeno structure, the information processing stages of this system will be thoroughly analyzed considering IT2FSs and Interval Type-1 Fuzzy Sets (IT1FSs) at the antecedent and consequent parts of the rule base, respectively. Extending the generic rule described in equation (3.1) to the present case, an A2-C1 TSFLS rule is defined as follows:

$$\begin{aligned} R^i: \quad & IF\ x_1\ is\ \tilde{F}_1^i\ and\ \cdots\ and\ x_j\ is\ \tilde{F}_j^i, \\ & THEN\ y^i\ =\ C_1^i x_1\ +\cdots+\ C_j^i x_j(k) \end{aligned} \tag{3.5}$$

where R^i represents the i^{th} fuzzy rule, $\tilde{F}_j^i$ are IT2FSs, C_j^i are the consequent polynomial parameters given by IT1FSs, $i = [1, \cdots, M]$ where M is the number of fuzzy rules, $j = [1, \cdots, N]$ with N reprsenting the number of antecedents, x_j the fuzzy system inputs and y^i the rule output. Each fuzzy set C_j^i is characterized by its center (c_j^i) and spread (s_j^i) values as presented in equation (3.6)

$$C_j^i = [c_j^i - s_j^i; c_j^i + s_j^i] \tag{3.6}$$

Despite the interval representation of the rule's consequent part parameters, ultimately the output of this stage can be summarized as two separate polynomials yielding an upper and lower bound for each rule output, represented as:

$$\begin{aligned} \overline{y}^i &= \sum_{j=1}^{N} (c_j^i * x_j + s_j^i * |x_j|) \\ \underline{y}^i &= \sum_{j=1}^{N} (c_j^i * x_j - s_j^i * |x_j|) \end{aligned} \tag{3.7}$$

The main difference between Type-2 TS FLSs and their Type-1 counterpart lies in the aggregation mechanisms used to merge the output of each rule. Similarly to the Type-2 Mamdani FLS case, to obtain the output of a Type-2 TS FLS is also required an intermediate step, based on a Type-Reduction procedure, to account with the additional degrees of freedom provided by the Type-2 FSs.

Type-Reduction

The implementation of the Type-Reduction algorithm for a Interval Type-2 Takagi-Sugeno Fuzzy Logic System is, in its essence, very similar to the procedure already presented in the previous chapter. Considering the more general A2-C1 TS FLS, each bound

of its output, $\overline{y}$ and $\underline{y}$ is obtained separately by a Center-of-Sets Type-Reduction according to the upper and lower outputs of each rule ($\underline{y}^i$, $\overline{y}^i$) and their respective firing levels ($\underline{f}^i$, $\overline{f}^i$). To find the set of upper and lower firing levels that give the best estimation of the system's output, the output of each rule ($\underline{y}^i$ and $\overline{y}^i$) must be firstly reordered ascendantly, yielding geometric representations similar to the ones presented in figure (3.3). This procedure is mandatory when using a Type-Reduction algorithm based on the Karnik-Mendel principles.

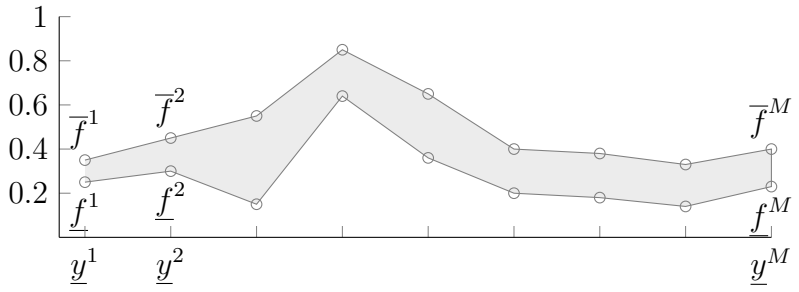

(a) Lower bound output of every system's rule ($\underline{y}^i$) sorted in ascending order.

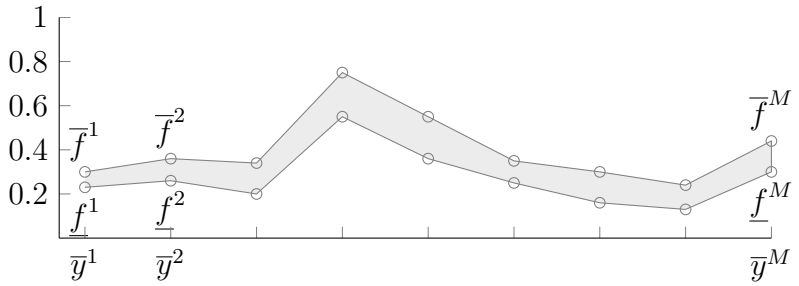

(b) Upper bound output of every system's rule ($\overline{y}^i$) sorted in ascending order.

Figure 3.3: Polygons obtained after reordering each rule's output in order to apply the Karnik-Mendel Type-Reduction procedure.

This polygon can be interpreted as a special IT2FS, as the area bounded by the rule's upper and lower firing levels in fact resemble one. Hence, the principles of Karnik-Mendel Type-Reduction can be applied to this set of points so the optimal switching points (L and R) are found. In this procedure is usual practice to ensure that $\underline{y}^i$ and $\overline{y}^i$ have no duplicate elements, which can be easily achieved by combining the weights of duplicate elements.

Then, $\underline{y}$ and $\overline{y}$ are obtained as presented in equations (3.8) and (3.9).

$$\underline{y} = \frac{\sum_{i=1}^{L} \underline{y}^i \overline{f}^i + \sum_{i=L+1}^{M} \underline{y}^i \underline{f}^i}{\sum_{i=1}^{L} \overline{f}^i + \sum_{i=L+1}^{M} \underline{f}^i} \tag{3.8}$$

$$\overline{y} = \frac{\sum_{i=1}^{R} \overline{y}^i \underline{f}^i + \sum_{i=R+1}^{M} \overline{y}^i \overline{f}^i}{\sum_{i=1}^{R} \underline{f}^i + \sum_{i=R+1}^{M} \overline{f}^i} \tag{3.9}$$

where L and R are the switch points satisfying

$$\underline{y}^L \leq \underline{y} < \underline{y}^{L+1} \tag{3.10}$$

$$\overline{y}^R \leq \overline{y} < \overline{y}^{R+1} \tag{3.11}$$

In figure (3.4) the optimal Type-Reduced Fuzzy Sets are represented in bold for the upper and lower outputs:

Due to the compact yet accurate representation of the Type-2 TS FLS consequents, Type-Reduction procedures require fewer calculations comparatively to the Mamdani case presented in the previous chapter.

Defuzzifier

After applying one of the Type-Reduction methods, the obtained Interval Fuzzy Set still has to be converted into a crisp number so it becomes suited to the most part of the FLS application scenarios. This procedure is fairly straightforward, yielding the defuzzified value by simply computing the average of the interval's left and right endpoints.

$$y_{out} = \frac{\underline{y} + \overline{y}}{2} \tag{3.12}$$

When such level of uncertainty representation is not necessary, simpler Type-2 TS FLSs can be obtained by simplifying either the antecedent or the consequent part of the FLS, as will be presented in the following sections.

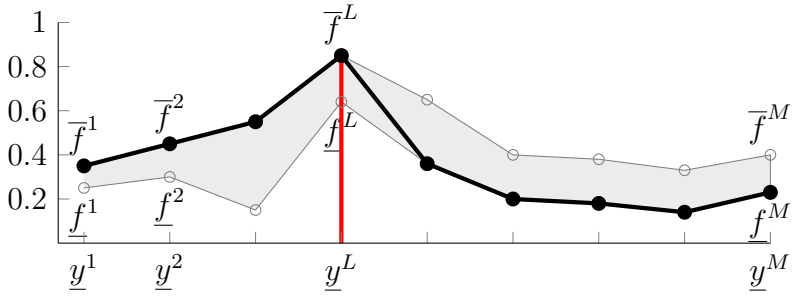

(a) Computing $\underline{y}$: Switching from the upper bounds of the firing intervals to the lower ones.

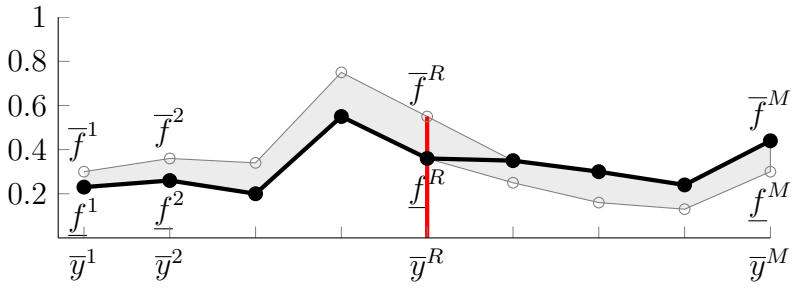

(b) Computing $\overline{y}$: Switching from the lower bounds of the firing intervals to the upper ones.

Figure 3.4: Computation of the optimal output bound in the A2-C1 case using the Karnik-Mendel Type-reduction.

3.3.2 A2-C0 Structure

As a particular case of the A2-C1 structure where the consequent functions are polynomials with crisp-number parameters, the A2-C0 FLSs distinguish themselves by their consequent part structure which is defined as follows:

$$\begin{aligned} R^i: \quad & IF\ x_1\ is\ \tilde{F}_1^i\ and\ \cdots\ and\ x_j\ is\ \tilde{F}_j^i, \\ & THEN\ y^i\ =\ c_1^i x_1\ + \cdots +\ c_j^i x_j(k) \end{aligned} \tag{3.13}$$

where R^i represents the i^{th} fuzzy rule, $\tilde{F}_j^i$ are IT2FSs, c_j^i are the consequent polynomial parameters, $i = [1, \cdots, M]$ where M is the number of fuzzy rules, $j = [1, \cdots, N]$ where N is the number of antecedents, x_j are the fuzzy system inputs and y^i is the rule output.

Despite yielding just a single output for each rule, this approach also considers an uncertainty degree bounded by the rule's firing level interval. For this reason and by establishing a parallelism with the A2-C1 case, the procedure to calculate the bounds of

the system output, $[\underline{y}, \overline{y}]$, is the same as presented in equations (3.8) and (3.9) except that now $\underline{y}^i = \overline{y}^i = y^i$. It is important to note that, despite this equivalence, the limits R and L for the Type-Reduction are not necessarily equal, as is depicted in figure (3.5).

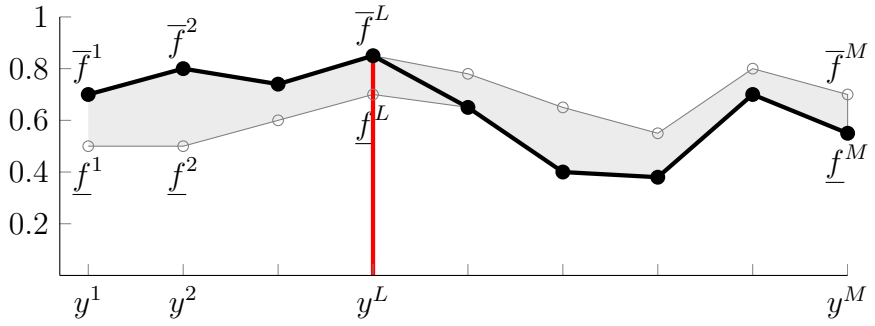

(a) Computing $\underline{y}$: Switching from the upper bounds of the firing intervals to the lower bounds.

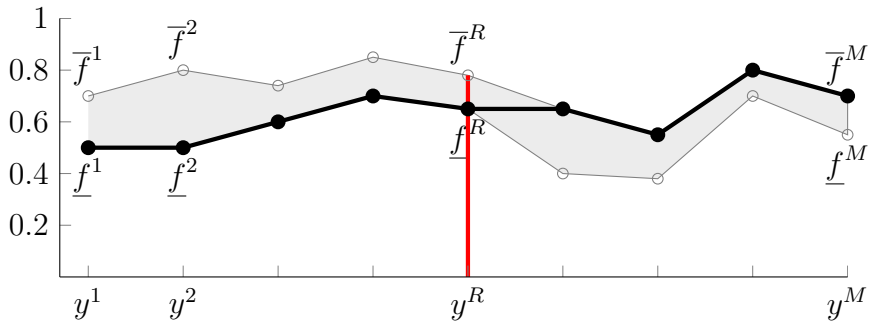

(b) Computing $\overline{y}$: Switching from the lower bounds of the firing intervals to the upper bounds.

Figure 3.5: Computation of the optimal output bounds in the A2-C0 case using the Karnik-Mendel Type-reduction.

3.3.3 A1-C1 Structure

Considering now the last case where both antecedent and consequent part parameters' are Type-1 FSs, each FLS's rule can be written as:

$$\begin{aligned} R^i: \quad & IF\ x_1\ is\ F_1^i\ and\ \cdots\ and\ x_j\ is\ F_j^i, \\ & THEN\ y^i\ =\ C_1^i x_1\ +\cdots+\ C_j^i x_j(k) \end{aligned} \tag{3.14}$$

where R^i represents the i^{th} fuzzy rule, F_j^i are Type-1 FSs, C_j^i are the consequent polynomial parameters, $i = [1, \cdots, M]$ where M is the number of fuzzy rules, $j = [1, \cdots, N]$ where N is the number of antecedents, x_j are the fuzzy system inputs and y^i is the rule output.

In this scenario, all the model uncertainty is considered in the consequent part of the rule and, thus, the firing level of each rule is given by a crisp number as was defined previously in equation (3.3). Similarly to the A2-C1 case, the output of each rule is given by an IT1FS yielding an interval bounded by $[\underline{y}^i, \overline{y}^i]$. Each one of these values can be obtained as presented in equation (3.15).

$$\begin{aligned} \overline{y}^i &= \sum_{j=1}^{N} (c_j^i * x_j + s_j^i * |x_j|) \\ \underline{y}^i &= \sum_{j=1}^{N} (c_j^i * x_j - s_j^i * |x_j|) \end{aligned} \tag{3.15}$$

Since the firing levels are crisp values, the extended output of the FLS does not require the use of the Karnik-Mendel algorithm, as given by equation (3.16):

$$Y = \left[\frac{\sum_{i=1}^{M} f^i \underline{y}^i}{\sum_{i=1}^{M} f^i}, \frac{\sum_{i=1}^{M} f^i \overline{y}^i}{\sum_{i=1}^{M} f^i} \right] \tag{3.16}$$

which ultimately resumes to

$$y = \frac{\underline{y} + \overline{y}}{2} = \frac{\sum_{i=1}^{M} f^i (\sum_{j=1}^{N} c_j^i * x_j)}{\sum_{i=1}^{M} f^i} \tag{3.17}$$

Comparing the results from equations (3.2) and (3.17), it is possible to conclude that the output of an Interval A1-C1 TSFLS and the traditional Type-1 TS FLS are in fact identical. For this reason, in applications where the interest is in obtained the defuzzified output of the FLS one may choose the latter model since there is no effective advantage in implementing this more complex approach. Nonetheless, if there is interest in evaluating the uncertainty degree of the obtained output, such information can be inferred by evaluating the width of the extended output given by equation (3.16), which can only be obtained from the A1-C1 FLS [56].

3.4 ANFIS based on Type-2 TS Fuzzy Logic Systems

As a formal extension of the well known Type-1 TS Fuzzy Logic Systems, Type-2 TS FLSs can also be represented according to a layered architecture which best characterizes a Multi-Layer Neural System. This structure is generically depicted in figure (3.6) and will be presented as follows.

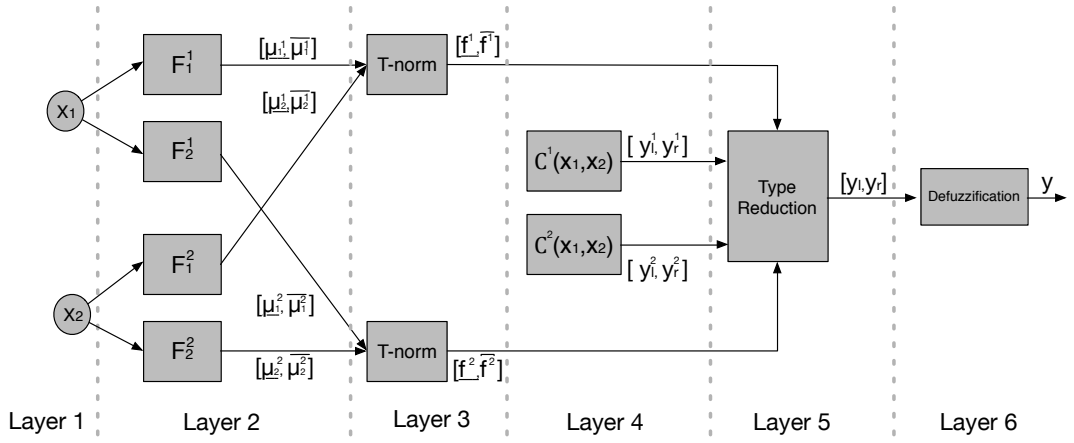

Figure 3.6: Parallelism between the Type-2 TS FLS and the ANFIS structures.

Layer 1: This layer, also known as the input layer, is defined by N nodes which embrace the crisp values relative to each input variable x_j.

Layer 2: In this layer, the fuzzification operation is performed by evaluating the membership degree of each input variable x_j in the respective fuzzy set considered in the antecedents part of the M FLS rules. Assuming that each fuzzy set is defined by a Gaussian function with fixed mean and uncertain standard deviation, as defined in equation (3.18).

$$\begin{aligned} \tilde{F}_j^i(c_j^i, \sigma_j^i, x_j) &= exp\left[-\frac{1}{2}\left(\frac{x_j - c_j^i}{\sigma_j^i}\right)^2\right] \\ &= G(c_j^i, \sigma_j^i, x_j),\ c_j^i \in [c1_j^i, c2_j^i] \end{aligned} \tag{3.18}$$

Unlike a Type-1 FS, where the measured membership grade is given by a number, when using IT2FSs this metric is represented as an interval of uncertainty given by:

$$[\underline{\mu}_j^i, \overline{\mu}_j^i] = [G(c1_j^i, \sigma_j^i, x_j), G(c2_j^i, \sigma_j^i, x_j)] \tag{3.19}$$

Layer 3: In this layer, the upper and lower bounds of each rule firing strength is calculated. This interval is obtained by using the *product t-norm* operator [30] over the upper and lower membership values of each rule antecedents, as is presented on equations (3.20) and (3.21).

$$\underline{f}^i = \underline{\mu}_1^i(x_1) * \underline{\mu}_2^i(x_2) * ... * \underline{\mu}_N^i(x_N) \tag{3.20}$$

$$\overline{f}^i = \overline{\mu}_1^i(x_1) * \overline{\mu}_2^i(x_2) * ... * \overline{\mu}_N^i(x_N) \tag{3.21}$$

At the output of this layer, it is obtained and interval $[\underline{f}^i, \overline{f}^i]$ denoting the uncertainty regarding each rule firing level.

Layer 4: Each node of the fourth layer implements the inference mechanism according to the Takagi-Sugeno principles. Considering the A2-C1 structure, the result is a linear combination of IT1FSs, yielding an interval bounded by $[\underline{y}^i, \overline{y}^i]$, whose limits are obtained based on equations (3.22) and (3.23) respectively.

$$\overline{y}^i = \sum_{j=1}^{N} (c_j^i * x_j + s_j^i * |x_j|) \tag{3.22}$$

$$\underline{y}^i = \sum_{j=1}^{N} (c_j^i * x_j - s_j^i * |x_j|) \tag{3.23}$$

Layer 5: The fifth layer of the A2-C1 TS FLS is responsible for combining together the output of each rule according to their upper and lower firing level bounds. This procedure is performed by using the iterative Karnik-Mendel algorithm (or one of its enhanced versions) or a closed-form approximation such as the Wu-Mendel's Uncertainty Bound Type-Reducer previously presented.

Layer 6: Finally, in the sixth layer the output of the Type-2 TS FLS is defuzzified using the average of the two endpoints $\underline{y}$ and $\overline{y}$, hence:

$$y = \frac{\underline{y} + \overline{y}}{2} \tag{3.24}$$

As was already referred, one advantage of this structure is the possibility of developing adaptation mechanisms for the model parameters based on the approximation error of the network to a input-output data dependency. The succeeding section will depict such procedures.

3.5 Training algorithms for TS Fuzzy Systems

As was previously shown, the multi-layered architecture of Takagi-Sugeno Fuzzy Logic Systems is formally equivalent to the Feed-Forward Artificial Neural Network structure. Hence, the same algorithms used in ANN's training (mostly based on the output error back-propagation) are natural candidates for the development of the TS model's adaptation. In multi-layered systems, the training methods which minimize the error between the desired output and the model's output are typically implemented in two separate steps [57]. Firstly the Feed-Forward computations are performed, obtaining the values of every intermediate node of the model, followed by a backwards parameter's adaptation based on the observation of the output error. The model adaption can be considered as a single optimization problem, by training every parameter according to the information given by the gradient and Hessian of the output error (using the Gradient descent, Gauss-Newton or Levenberg-Marquardt methods for instance [57]). However, a more efficient and stable procedure can be alternatively employed - since the estimation obtained by a TS system can be expressed as a weighted combination of several locally linear functions, the model training can be divided into two smaller separate problems. Apart from reducing the procedure's complexity for the consequent part parameters', such approach also minimizes possible numerical problems related with the larger number of estimated parameters and the possibility of the non-linear optimization methods to be stuck into local minima. The referred approach, known as Hybrid Training [48] is performed as follows:

- At a given sampling instant, considering the parameters of the model's antecedent part fixed, the output of the TS Fuzzy model results from the weighted contribution of several linear models according to the firing level of their respective rules. Therefore, the consequent part parameters can be trained using a least squares method such as the Recursive Least Squares (RLS).

- Afterwards, by fixing the consequent parameters, the non-linear part of the model can be trained by back-propagating the output error to each one of the antecedent parameters using methods based on the error signal derivatives.

As was clear from the previous sections, the extension of TS Fuzzy Systems to the Type-2 Fuzzy Logic concepts introduced a significant amount of additional unknown parameters. The estimation of their optimal values can be performed by directly employing optimization algorithms [9, 58] or recursively trained [59, 60]. Yet, considering a Type-2

TS Fuzzy model estimation solely as an error minimization problem is an approach which misses the initial purpose of embedding uncertainty intervals over Type-1 FLS and, when applied without supervision, may result in Footprints-of-Uncertainty that no longer have a valid meaning for the model's interpretability. Hence, as every membership function is ultimately obtained by varying one or several parameters of a Type-1 FS, the training methods further presented focus on the Type-1 TS model structure. The obtained parameters can then be used as a starting point for the development of its Type-2 TS Fuzzy model, by expanding the uncertainty intervals by a fixed factor so the overall model performance is improved. Despite simplicity and intuitiveness of this approach, it is currently not discussed in literature. Nonetheless, it is fairly simpler than the Type-2 TS training procedures currently available and it was found to provide superior numerical robustness in the development of model based controllers.

In the following sections, the local training procedures used in the development of a Type-1 TS Fuzzy model will be presented.

3.5.1 Model initialization

The initialization of the antecedent part of the Type-1 FLS plays an important role in the definition of the system's structure as it will ultimately set the minimum number of rules necessary to accurately model the input-output dependency of a system. Since its appropriate dimension is hardly known at the beginning of the design stage, it is common practice to use one-pass clustering algorithms over a large input-output dataset in order to extract natural groupings of data from it. Although clustering is usually employed in classification problems, it is also often used as an initialization procedure of the FLSs' rule base. Despite the differences in nomenclature and information organization, a n-dimensional cluster is functionally equivalent to the antecedent part of a rule with n input variables. As so, such approach will be used to obtain the appropriate number of rules as well as defining the center and variance of each membership function of the model's input space.

Literature is rich in clustering algorithms which, despite their different nomenclatures, ultimately are variations of the original Fuzzy C-Means (FCM) clustering algorithm [61]. The FCM algorithm is an iterative optimization method used to find the optimal centers of the membership functions that partition the input space of a FLS, which aims to minimize the cost function presented in equation (3.25).

$$J = \sum_{k=1}^{K} \sum_{i=1}^{C} \mu_{ik}^{m} \|x_k - v_i\|^2 \tag{3.25}$$

where K is the number of data points, C is the number of clusters, x_k is the k^{th} n-dimensional data point, v_i is the i^{th} cluster center, μ_{ik} is the degree of the membership of the k^{th} data in the i^{th} cluster and m is a constant greater than 1 (typically $m = 2$) that defines the width of the cluster. Provided the desired number of clusters and an initial guess for each cluster center v_i, the FCM algorithm will converge to a solution which represents either a local or global minimum of the given cost function.

As in every non-linear optimization problem, the quality of the solution found is highly related with the choice of the initial values of the clusters' centers. By using the Mountain Method [62], such constraint is overcome by simply using a grid partition of a n-dimensional input space as a starting point for the clusters' parameters. However, the computational complexity of such approach can escalate very easily, growing exponentially with the number of input variables of the system. The Subtractive Clustering algorithm [63] circumvents the dimensionality issues of the previous method by considering each data point (and not each one of the possible grid partitions) as a potential cluster center. The computational complexity depending on the dimensionality of the data set but, more importantly, unrelated with the input space dimensionality.

In the Subtractive Clustering algorithm, the possible cluster centers are found according to a metric that evaluates the potential of each data point in assuming such role. Such metric is presented in equation (3.26).

$$P_i = \sum_{j=1, j \neq i}^{n} exp\Big[-\alpha \|x_i - x_j\|^2\Big] \tag{3.26}$$

where

$$\alpha = \frac{4}{r_a^2} \tag{3.27}$$

and r_a is a positive constant related with the radius of influence of each possible cluster center candidate. Thus, the points with higher number of neighbor points will present an higher potential value, having more chances to be selected as cluster centers. After the potential of every point is calculated, the data point with higher potential value is selected as the first cluster. Let x_1^* be the location of the first cluster center and P_1^* its potential,

The potential of every remaining data point is revised by equation (3.28),

$$P_i \Leftarrow P_i - P_1^* exp{-\beta}\|x_i - x_1^*\|^2 \tag{3.28}$$

where

$$\beta = \frac{4}{r_b^2} \tag{3.29}$$

and r_b is a positive constant. This second step effectively penalizes the data points closer to the first cluster reducing their potential of be selected as cluster centers in the successive iterations of the algorithm. To avoid the selection of closely spaced clusters, r_b should be greater than r_a usually in the proportion of $r_b = 1.5r_a$. This procedure is repeated until the potential of the k^{th} cluster is a small fraction of the first cluster extracted, as presented in equation (3.30).

$$P_k^* < \varepsilon P_1^* \tag{3.30}$$

The value of this threshold, ε, will ultimately define the number of data points accepted as cluster centers and set the dimensionality of the rule base.

As far as it concerns to the remaining parameters that define a gaussian fuzzy MF - the variance, its value can be obtained considering the equivalence between equation (3.31) and the clustering metric presented in equation (3.26). Having a gaussian membership function defined as

$$F(x, c, \sigma) = exp\left[-\frac{(x-c)^2}{2\sigma^2}\right] \tag{3.31}$$

the variance of the membership functions obtained via Subtractive Clustering is given by equation (3.32).

$$\sigma^2 = \frac{r_a^2}{8} \tag{3.32}$$

While the use of the Subtractive Clustering significantly contributed to the development of smaller yet well performing TS systems, not every input variable is strictly relevant for an accurate non-linear input space partitioning. If every input variable present at the consequent part regressive model is considered, one can easily end up in a combinatorial problem which leads to a very large structure and even reduce its extrapolation capabilities. Therefore, it is of great importance to establish a balance between the model accuracy and

its complexity. Based on this premise, in [64] is proposed a methodology where only the regressors having a non-linear impact in the parameters of the consequent part of the TS systems are considered in the rule extraction procedure, as those are in fact the state variables that define the necessity of employing different linear approximations over different operating scenarios. Opposing to the Mamdani inference procedure, pruning the antecedent part of a TS structure does not necessarily impairs its approximation capability since the consequent one inherently establishes the output interdependency with every input variable considered.

3.5.2 Training of the Antecedent part of the Rule Base

After the initialization stage, the parameters of the antecedent part can be fine-tuned using a non-linear optimization algorithm such as the Gradient Descent or the Levenberg-Marquardt [65, 66]. Since the input space of a TS Fuzzy Model is less likely to present significant variations over the time, the initial antecedent parameters estimations are usually fairly close to the optimal ones. Thus, while it may be argued that the Gradient Descent training might present a slower convergence towards the optimal solution than Hessian based methods such as the LM, for the majority of applications this is not a restrictive drawback as the adaptiveness of the model resides mostly at its consequent part. Therefore, the Gradient Descent update rules for the variance and the center of each antecedent part of Type-1 FS can be obtained based on the minimization of the squared error of the prediction model as is following presented:

$$c_j^i(k+1) = c_j^i(k) - \eta \frac{\partial E}{\partial c_j^i} \tag{3.33a}$$

$$\sigma_j^i(k+1) = \sigma_j^i(k) - \eta \frac{\partial E}{\partial \sigma_j^i} \tag{3.33b}$$

where E is the prediction error and η is the learning coefficient, usually chosen in the interval $0 < \eta \leq 0.2$ [57].

The partial derivatives of each free parameter present in the antecedent part of the rule base are obtained as considering that

$$E = \frac{1}{2}\sum_{k=1}^{K}(y^d(k) - y(k))^2 \tag{3.34}$$

and

$$G(c_j^i, \sigma_j^i, x_j) = exp\left[-\frac{1}{2}\left(\frac{x_j - c_j^i}{\sigma_j^i}\right)^2\right] \tag{3.35}$$

Therefore,

$$\frac{\partial E}{\partial \sigma_j^i} = \frac{\partial E}{\partial y}\frac{\partial y}{\partial f^i}\frac{\partial f^i}{\partial \mu_j^i}\frac{\partial \mu_j^i}{\partial \sigma_j^i} \tag{3.36}$$

$$\frac{\partial E}{\partial c_j^i} = \frac{\partial E}{\partial y}\frac{\partial y}{\partial f^i}\frac{\partial f^i}{\partial \mu_j^i}\frac{\partial \mu_j^i}{\partial c_j^i} \tag{3.37}$$

where

$$\frac{\partial E}{\partial y} = -1 \tag{3.38}$$

$$\frac{\partial y}{\partial f^i} = \frac{y^i \sum_{i=1}^{M} f^i - \sum_{i=1}^{M} f^i y^i}{\left(\sum_{i=1}^{M} f^i\right)^2} \tag{3.39}$$

$$\frac{\partial f^i}{\partial \mu_j^i} = \prod_{k=1, k\neq j}^{N} \mu_k^i \tag{3.40}$$

$$\frac{\partial \mu_j^i}{\partial c_j^i} = \frac{\left(x_j - c_j^i\right)}{(\sigma_j^i)^2} G(c_j^i, \sigma_j^i, x_j) \tag{3.41}$$

$$\frac{\partial \mu_j^i}{\partial \sigma_j^i} = \frac{\left(x_j - c_j^i\right)^2}{(\sigma_j^i)^3} G(c_j^i, \sigma_j^i, x_j) \tag{3.42}$$

At this stage, the importance of the Forward Pass for the training of every antecedent part parameter is clearer, since the values of parameters μ_j^i and f^i depend on the execution of one iteration of the TS system for a given a set of input values.

3.5.3 Training of the Consequent part of the Rule Base

When a system to be identified is linear on its parameters, procedures based on the squared error minimization such as the RLS algorithm are know to provide the best convergence to the solution which better approximates a specific input/output behavior [12]. Takagi-Sugeno FLSs fall into this category since, by considering that at given instant the antecedent part firing levels' are constant, the output of the system is no more than a weighted combination of linear functions given by each rule's consequent part.

The training procedure for the consequent part of the rule base can be translated into a least squares optimization problem according to two different ways: using either a global or a local optimization approach, as presented in equations (3.43) and (3.44) respectively.

$$\theta = arg\ min \sum_{k=1}^{K} \left(y_k^* - \sum_{n=1}^{N} f^i \varphi \hat{\theta}_i \right) \tag{3.43}$$

where y^* is the system output to approximate, φ_i is the n-dimensional observation vector, $\theta = [\theta_1\ \theta_2\ \cdots\ \theta_N]$ is the concatenation of all the individual rule's parameter vectors, f_i is the normalized firing level of each rule, N is the number of rules of the system and K is the length of the training dataset.

$$\theta_i = arg\ min \sum_{k=1}^{K} \left(f^i y_k^* - f^i \varphi \hat{\theta}_i \right) \tag{3.44}$$

where y^* is the system output to approximate, φ is the n-dimensional observation vector, and θ_i is the parameter vector of each individual rule, f^i is the normalized firing level of each rule, N is the number of rules of the system and K is the length of the training dataset.

In the former approach, as is employed for example in [59], every consequent functions parameters' are trained as a whole, in a single regression problem, while in the latter case the training of the consequent part of each rule constitutes a separate optimization problem. In terms of error minimization, the choice of the method used is not crucial but, if each rule output is to be interpreted as a local model, then the employed approach ultimately defines its usability. As is argued in [67] and [68], a globally optimal model by no means guarantees a locally adequate behavior of the sub-models that constitute the TS structure, often leading to over-fitting problems and meaningless parameters estimates which can ultimately result in numerical instability as verified in [59]. A simple interpretation of this problem is depicted in figure (3.7).

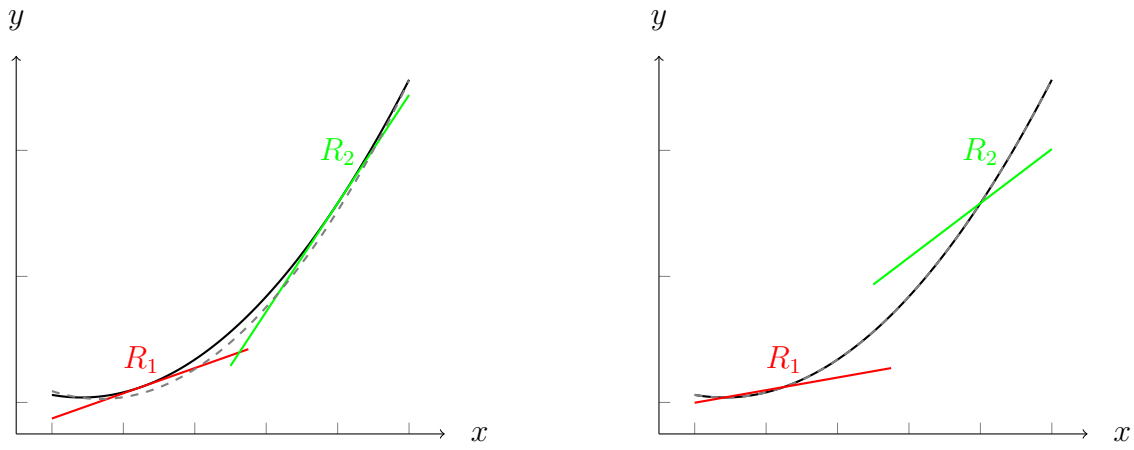

Figure 3.7: The result of local (left) and global (right) optimization of the consequent parameters for a single input two rule's system. The dashed line is the output of the system.

From the depicted scenario, the consequents estimated by local optimization properly describe the local behavior of the function, while giving a less accurate global fitting. For the global optimization approach, the opposite holds - a better fit is obtained but the consequent part functions are not relevant for a local description of the system's behavior. As will be clearer in the further chapters, the validity of the local models will be important to perform the synthesis of model based controllers. To tackle this requirement, constrained and multi-criteria optimization methods can be applied to the global training approach [68] in order to restrict the domains of freedom in the parameters. However, the training procedure becomes a quadratic optimization problem instead of a least squares one, increasing both the complexity and the required computational effort to solve it. For this reason, establishing a compromise between modeling accuracy and method complexity, the local training approach will be followed in the present work using a weighted RLS algorithm.

While the RLS algorithm provides an efficient mean of performing a local training of each rule consequent part, it is known that its conventional formulation lacks the required adaptability to track time varying parameters [12] since it gives the same importance to all the previous samples for the current time estimation. To overcome this issue, modified versions of the cited algorithm introduced an exponential weight that reduces the significance of past samples according to their obsolescence [12]. Yet, in practical scenarios where the system excitation is insufficient or not uniform over the whole parameters' space, this information loss mechanism can lead to numerical stability problems due to a phenomenon referred in the literature as covariance matrix windup [12]. Therefore, several heuristics

have been proposed to overcome this problem either by adjusting the algorithm forgetting factor considering the evolution of the estimation error or by monitoring the evolution of the covariance matrix [12]. Approaches based on the latter method are considered more robust and, among the existing methods, the Directional Forgetting mechanism [69, 70] stands out for its simplicity, stability and capability of maintaining the adaptability of the estimator to fast and slow parameter's variations. Despite its superior capabilities in ensuring the model's learning capability over long training epochs, Hybrid TS model learning techniques continue to put emphasis in methods that periodically reset the covariance matrix of the estimator to maintain is stability and adaptability - an approach which can be simply seen as a "reboot of the estimator". Few publications tackle this problem using the Recursive Least Squares with Directional Forgetting (RLSDF) algorithm [71, 72] but, given its proven superiority, it will be used during this work and defined as follows.

Considering that, at each sampling instant, the estimated output results from the weighted contribution of several linear models according to each rule's normalized firing level, f^i, the output of the model is given as presented in equation (3.45).

$$y = \frac{\sum_{i=1}^{M} f^i y^i}{\sum_{i=1}^{M} f^i} \tag{3.45}$$

Following a local training based approach, the cost function J to be minimized is defined as the sum of the cost functions J_i of each sub-model, as presented in (3.46):

$$J = \sum_{i=1}^{R} J_i \tag{3.46}$$

where

$$J_i = (y^* - \varphi^T \hat{\theta}_i) f^i \lambda_i (y^* - \varphi^T \hat{\theta}_i) \tag{3.47}$$

which can ultimately be rewritten as

$$J_i = (\sqrt{f^i} y^* - \sqrt{f^i} \varphi^T \hat{\theta}_i) \lambda_i (\sqrt{f^i} y^* - \sqrt{f^i} \varphi^T \hat{\theta}_i) \tag{3.48}$$

where, for the i^{th} system's rule, f^i is the normalized activation level, φ the n-dimensional observation vector, $\hat{\theta}_i$ the n-dimensional parameter's vector of the locally linear sub-model and λ_i a weight related to the estimator forgetting factor. Assuming that the model has R rules, the same number of linear models must be estimated and, consequently, the same number of cost functions must be optimized.

As so, at the time instant k, the parameters of the discrete-time linear predictor for the i^{th} rule can be recursively obtained using the weighted RLSDF algorithm as follows in equation (3.49).

$$\hat{\theta}_i(k) = \hat{\theta}_i(k-1) + K(k)\varepsilon_i(k) \tag{3.49a}$$

$$\varepsilon_i(k) = \sqrt{f^i}y^*(k) - \sqrt{f^i}\varphi(k)^T\hat{\theta}_i(k) \tag{3.49b}$$

$$r_i(k) = fi\varphi^T(k)P_i(k-1)\varphi(k) \tag{3.49c}$$

$$K(k) = \frac{\sqrt{f^i}P_i(k-1)\varphi(k)}{1 + r_i(k)\alpha_i(k)} \tag{3.49d}$$

$$P_i(k) = P_i(k-1) - K(k)\sqrt{f^i}\varphi^T(k)\alpha_i(k)P_i(k-1) \tag{3.49e}$$

$$\alpha_i(k) = \begin{cases} \lambda_i - \dfrac{1-\lambda_i}{r_i(k)}, & r_i(k) > 0 \\ 1, & r_i(k) = 0 \end{cases} \tag{3.49f}$$

The parameter λ_i represents the algorithm forgetting factor and it is usually chosen in the interval $0.95 \leq \lambda_i \leq 1$. The value of this coefficient establishes a commitment regarding the algorithm's capability in tracking fast/slow variations of the model parameters.

3.6 Conclusions

The development of rule-base systems according to the Takagi-Sugeno structure significantly expanded the domains of application of Fuzzy Logic Systems due to their closeness to well known linear modeling theory and applicability of simple training algorithms (derived for their equivalent ANFIS structure) which refine the systems performance in an autonomous way. By inheritance of Type-1 TS FLSs' main properties and due to their information uncertainty representation features, Type-2 FLSs based on the Takagi-Sugeno structure have a greater potential to excel in system modeling tasks.

Since every Type-2 TS FLSs is ultimately defined by embedding a FOU over its Type-1 counterpart parameters, the procedure of defining a Type-2 FLS is significantly simplified if one focus on the centers of the uncertainty intervals. Such approach seems to be disregarded by the related literature but, despite its simplicity, it is not less valid than the currently available ones. In fact, it provides to the practitioner a deeper insight regarding the influence of the uncertainty factors on the quality and accuracy of the developed systems and is computationally less demanding due to the smaller number of parameters that must be tuned. Such dependency will be clearer in the succeeding chapters, by studying the applicability of Type-2 FLSs in modeling and control applications.

Chapter 4

System Modeling using Type-2 Takagi-Sugeno Fuzzy Systems

4.1 Introduction

The development of computational models capable of accurately describe a process's dynamic response is a task ultimately dependent on its physical phenomena complexity and the type of disturbances that may affect its operation. According to the literature [73], there exist several different approaches to obtain such system's description:

- Physical models;
- Black-Box models;
- Grey-Box models;

When a deep knowledge about the physical laws underlying the system's behavior is present, it becomes possible to develop models based on a set of differential equations describing the rate of change of the system's state variables and additional algebraic equations for relating all the implicated processes. The development of fundamental models typically requires a large number of parameters but, once each one of them is available, either estimated from experimental scenarios or well known physical constants, it becomes possible to extrapolate results from a large range of operation regions. Although having some knowledge about the system dynamics is a desirable feature, in some particular applications the model identification procedures become a computational and time demanding

task. Thus, they may require specific test conditions so the influence of individual parameters is isolated, a condition which is even more problematic when the system presents non-linear behavior since the superposition principles are no longer valid. Consequently, a large number of possible combinations of input variables has to be necessarily tested, ultimately posing a large search space for numerical optimization algorithms to obtain the set of parameter that best approximate the process response. For this reason, the use of physical modeling methods in the development of prediction models and controller synthesis is very restricted.

In what concerns to the parameters' interpretability, Black-Box models advocate the opposite point of view in a model development procedure in the sense that the it is developed on an information processing point of view, without any considerations regarding the process's physical properties. As so, a mathematical description of the system is developed aiming to find the best relationships among variables that best fits the input/output data obtained from the process. Typically, such descriptions can be represented using polynomial structures, either based on linear Auto-Regressive with eXogenous inputs (ARX) structures, or Non-Linear Auto-Regressive with eXogenous inputs (NARX) such as Feed-Forward Neural Networks, Wiener or Hammerstein models [73]. In any of its forms, an input-output model can be generically represented as:

$$\hat{y}(k) = f(y(k-1), \cdots, y(k-n_y), u(k-d-1), \cdots, u(k-d-n_u), v(k-1), \cdots, v(k-n_c)) \quad (4.1)$$

where f defines the variables' interdependency, $\hat{y}$ is the predicted output, y are the process's past outputs, and its exogenous inputs are given by the actuation values u and the measured external disturbances v. The parameters n_y, n_u, n_c are chosen according to the relevancy of the past values to the present estimation and d represents the process's dead-time. Obtaining a Black-Box model is a procedure which encompasses several stages, typically grouped as: structure selection, parameter identification and model validation [57]. Due to its iterative nature, such procedure is not a single-pass one, an typically requires several experiments before a robust yet simple model is obtained.

While there may exist scenarios where the process's dynamic behavior is totally unknown and a Black-Box modeling approach is ultimately used to develop a model, most of the times the little knowledge available about the process can significantly reduce the number of iterations required to find an optimal model. By combining the fundamental

and Black-Box modeling principles, an approach known as Grey-Box modeling, empirical relations (which usually have a limited region of validity) can be established among the relevant system variables, reducing the model structure size while closely approximate the plant dominant dynamics in a specific operation region. Knowing how disturbances affect its operation, the noise's spectral distribution, the non-linearities over the expected operation regime or the memory that the system has concerning past inputs or outputs are some of the parameters that may give some important hints to accomplish this task [57].

The parameters of a Grey-Box model do not present any physical meaning. Nevertheless, when such models are developed according to linear systems' identification theory, important relations can be established between their parameters and the dynamic response of the system (as stability and transient response analysis) [12]. For this reason, despite the improved modeling capabilities of non-linear approaches, linear ones continue to have a large adoption due to their simpler structure and easier theoretical analysis. As was presented in chapter 3, Takagi-Sugeno FLSs stand in between both methods, providing a simple framework to approximate non-linear input-output relations based on the use of several locally linear transfer functions. Considering their use in process modeling applications, the linear consequent part of the model can also be developed according to a Grey-Box principles, thus extending important developments from linear modeling and control theory to TS FLSs.

4.2 Locally linear models based on Type-2 TS Fuzzy Logic Systems

The use of TS FLSs in system modeling applications is a natural process since a dynamic interpretation of its structure is obtained by replacing its input variables with the relevant regression variables. Considering the particular case of developing linear systems based on the ARX structure, the consequent part of the TS model is commonly represented as in equation (4.2):

$$A(z^{-1})y(k) = B(z^{-1})z^{-d}u(k) + C(z^{-1})v(k) \tag{4.2}$$

where $u(k)$ and $y(k)$ are the control and output sequences of the plant, d is the dead time of the system and $v(k)$ is a process disturbance. A, B, and C are the polynomials

represented in the backward shift operator z^{-1}:

$$\begin{aligned} A(z^{-1}) &= 1 + a_1 z^{-1} + a_2 z^{-2} + \cdots + a_{n_a} z^{-n_a} \\ B(z^{-1}) &= b_1 z^{-1} + b_2 z^{-2} + \cdots + b_{n_b} z^{-n_b} \\ C(z^{-1}) &= 1 + c_1 z^{-1} + c_2 z^{-2} + \cdots + c_{n_c} z^{-n_c} \end{aligned} \tag{4.3}$$

where the parameters n_a and n_b are related to the order of the estimated ARX model and n_c related with the expected type of disturbance.

As was already referred, the interpolation features provided by Takagi-Sugeno models are well known to provide good approximations of non-linear models as long an adequate number of rules are employed. Nonetheless, in modeling applications, the parameters of each locally linear approximations used at every rule's consequent part will be very likely affected by uncertainty factors due to time varying conditions of the modeled processes. Type-2 TS FLSs inherently encode in their structure the mechanisms necessary to represent such variability and their inclusion in system modeling applications is performed by assuming the existence of a uncertainty factor over the parameters of a Type-1 TS Fuzzy model. The antecedent part of the model can be extended by varying either the variance or the mean value of the membership functions that partition the model's input space while the consequent parameters can be generically defined in an interval representation $\tilde{p}$, as presented in equation (4.4),

$$\tilde{p} = [p - s; p + s] \equiv [\underline{p}; \overline{p}] \tag{4.4}$$

where the center of the interval (p) is given by the coefficients of the polynomials A, B and C presented in (4.3), and s is the width of the considered uncertainty interval, which can be defined as a percentage of the parameter p. Ultimately, a Type-2 TS Fuzzy Model can represent each rule consequent by two polynomial functions associated with the upper and lower bounds of its parameters which, complemented with the Type-reduction mechanisms, constitute a compact and effective way of embedding several possible models that best approximate a specific operation point of a process. A generic definition of the i^{th} rule of a system with M *If-Then* rules and N antecedents is presented as follows:

$$\begin{aligned} &IF && y(k-1) \; is \; \tilde{F}_1^i \; and \; \cdots \; and \; u(k-1) \; is \; \tilde{F}_N^i, \\ &THEN && \begin{aligned} \underline{A}^i(z^{-1})\underline{y}^i(k) &= \underline{B}_i(z^{-1})u(k) + \underline{C}_i(z^{-1})v(k) \\ \overline{A}^i(z^{-1})\overline{y}^i(k) &= \overline{B}_i(z^{-1})u(k) + \overline{C}_i(z^{-1})v(k) \end{aligned} \end{aligned} \tag{4.5}$$

and:

$$[\underline{A}^i, \overline{A}^i](z^{-1}) = [1,1] + [\underline{a}_{1i}, \overline{a}_{1i}] + [\underline{a}_{2i}, \overline{a}_{2i}]z^{-1} + \cdots + [\underline{a}_{n_a i}, \overline{a}_{n_a i}]z^{n_a} \tag{4.6a}$$

$$[\underline{B}^i, \overline{B}_i](z^{-1}) = [\underline{b}_{1i}, \overline{b}_{1i}]z^{-1} + \cdots + [\underline{b}_{n_b i}, \overline{b}_{n_b i}]z^{n_b} \tag{4.6b}$$

$$[\underline{C}^i, \overline{C}_i](z^{-1}) = [1,1] + [\underline{c}_{1i}, \overline{c}_{1i}]z^{-1} + \cdots + [\underline{c}_{n_c i}, \overline{c}_{n_c i}]z^{n_c} \tag{4.6c}$$

4.2.1 Development of the interpolated Interval Type-2 Fuzzy Model

One of the advantages upcoming from the existence of a system's model is the possibility of developing control techniques capable of adapt their performance to different operating conditions. Model based control techniques such as Pole-Placement [74] or Model Predictive Control [14] are some examples of so. From the point of view of the system's behavior prediction, Takagi-Sugeno FLSs provide a simple mechanism of interpolating its output based on the weighted contribution of several locally linear models. However, when a model is used in a model-based control framework, it is important not to have solely the predicted output but also the parameters of an equivalent model that provides so. Fortunately, since the TS FLSs' rule aggregation is of linear nature, one can obtain a single linear model where each parameter results from the weighted contribution of every locally linear model partially activated at the current operating region [75]. Naturally, transitory regions that activate several partitions of the input space result from the contribution of several models and, therefore, present higher levels of uncertainty. For this reason, [16] overcame this issue and improved the model's accuracy by merging a set of the best performing linear models at each region obtained by a genetic algorithm. By combining multiple TS fuzzy models, one can improve the overall identification performance of the model, since the expected error upcoming from the use of multiple models will (in the worst case scenario) not exceed the expected error of the individual models [76]. The present work aims to extend such principle by using the model uncertainty representation according to the Type-2 TS FLSs' principles.

Since a Type-2 FLS output is ultimately represented by a bounded output, two average models of the plant ($\tilde{\overline{y}}(k)$ and $\tilde{\underline{y}}(k)$) will be obtained. Hence, defining the upper and lower bounds separately and the C polynomial chosen to be 1, an average estimated model ($\tilde{y}$) is represented as:

$$\tilde{y}(k) = [1 - \tilde{A}(z^{-1})]y(k-1) + \tilde{B}(z^{-1})u(k) \tag{4.7a}$$

where,

$$\tilde{A}(z^{-1}) = 1 + \tilde{a}_1 z^{-1} + \tilde{a}_2 z^{-2} + \cdots + \tilde{a}_{n_a} z^{n_a} \tag{4.8a}$$

$$\tilde{B}(z^{-1}) = \tilde{b}_1 z^{-1} + \cdots + \tilde{b}_{n_b} z^{n_b} \tag{4.8b}$$

The coefficients of the polynomials $\tilde{A}(z^{-1})$ and $\tilde{B}(z^{-1})$ are obtained by averaging the M consequent models, separately for the upper and lower bounds, according to their respective normalized firing level. This procedure is presented in the equations (4.9).

$$\tilde{a}_k = \frac{\sum_{i=1}^{M} w^i a_k^i}{\sum_{i=1}^{M} w^i}, \qquad k = 1, \cdots, n_a \tag{4.9a}$$

$$\tilde{b}_k = \frac{\sum_{i=1}^{M} w^i b_k^i}{\sum_{i=1}^{M} w^i} \qquad k = 0, \cdots, n_b \tag{4.9b}$$

For the lower average model, the weights w that define the contribution of each sub-model for the expression of $\tilde{y}(k)$ and the parameters a_k^i and b_k^i are given by:

$$w \equiv \underline{w} = [\overline{f}^1, \overline{f}^2, \cdots, \overline{f}^L, \underline{f}^{L+1}, \cdots, \underline{f}^M],\ a_{ki} \equiv \underline{a}_{ki},\ b_{ki} \equiv \underline{b}_{ki} \tag{4.10}$$

while for the upper average model, the parameters are given by:

$$w \equiv \overline{w} = [\underline{f}^1, \underline{f}^2, \cdots, \underline{f}^R, \overline{f}^{R+1}, \cdots, \overline{f}^M],\ a_k^i \equiv \overline{a}_k^i,\ b_k^i \equiv \overline{b}_k^i \tag{4.11}$$

The values of the boundaries L and R are given by the Type-Reduction algorithm, previously presented in the chapter 2.

4.2.2 Development of the *n-step* ahead predictor

When the developed model is integrated on a model predictive control framework, the accuracy of the system's predicted behavior given by a locally linear model ultimately defines the success of the control law in accomplishing the desired closed loop performance metrics. However, the use of locally linear models to approximate a non-linear system's response several steps ahead of current sampling instant, particularly during transient conditions, is usually a sub-optimal approach. Nevertheless, as in some modeling and control applications locally linear approximations usually yield computationally efficient methods without significant loss in accuracy, such commitment is often considered [77].

Literature highlights two different ways of using locally linearized models to predict the behavior of a system during a future time window [77]:

- By considering a fixed linearized model constant over the prediction window (obtained at the extrapolation instant);
- By performing successive linearizations of the model at each new expected operating point over the prediction window.

While potentially more accurate, the latter approach has a larger computational burden directly dependent on the length of the prediction window. In addition, in mildly non-linear scenarios when such approach is integrated in a closed loop control algorithm it is known for not yielding significant improvements comparing to the former method [77]. For this reason, the present work will focus on the use of locally linear models which are assumed as constant over the whole prediction window.

Considering the simpler case based on a linearized Type-1 TS fuzzy model, one can obtain an approximation of the system's predicted response by evaluating its free response, assuming that future control actions will remain equal to the current control action $u(k)$ and disturbances ε are constant. Based on the incremental model presented in equation (4.13), the system's free response can easily be obtained recursively as presented in equations (4.14).

Considering the one step-ahead predictor for a second order system given by equation (4.2) and assuming its dead-time equal to 0, two consecutive iterations of the predictor can be written as:

$$\hat{y}(k) = -a_1 y(k-1) - a_2 y(k-2) + b_1 u(k-d-1) + b_2 u(k-2) + \varepsilon(k) \tag{4.12a}$$

$$\hat{y}(k+1) = -a_1 y(k) - a_2 y(k-1) + b_1 u(k) + b_2 u(k-1) + \varepsilon(k+1) \tag{4.12b}$$

Thus, an incremental model can be obtained by subtracting two consecutive iterations, yielding:

$$\hat{y}(k+1) = (1-a_1)y(k) - (a_2-a_1)y(k-1) + a_2 y(k-2) + b_1\Delta u(t) + b_2\Delta u(t-1) + \varepsilon(k+1) - \varepsilon(k), \tag{4.13}$$

where $\Delta = 1 - z^{-1}$. Considering that a constant disturbance is present over the prediction window (N_p), the developed predictor will be offset-free (since $\varepsilon(k+1) - \varepsilon(k) = 0$). Thus, the free response (f(k+n)) over the future *n-steps* is given by:

$$f(k+1) = (1-a_1)y(k) - (a_2-a_1)y(k-1) + a_2 y(k-2) + b_1\Delta u(k) + b_2\Delta u(k-1) \tag{4.14a}$$

$$f(k+2) = (1-a_1)f(k+1) - (a_2-a_1)y(k) + a_2 y(k-1) + b_2\Delta u(k-1) \tag{4.14b}$$

$$f(k+3) = (1-a_1)f(k+2) - (a_2-a_1)f(k+1) + a_2 y(k) \tag{4.14c}$$

$$f(k+4) = (1-a_1)f(k+3) - (a_2-a_1)f(k+2) + a_2 f(k+1) \tag{4.14d}$$

$$f(k+N_p) = (1-a_1)f(k+N_p-1) - (a_2-a_1)f(k+N_p-2) + a_2 f(k+N_p-3) \tag{4.14e}$$

Regarding the application of the extrapolation hereby presented to Interval Type-2 TS Fuzzy Models, the obtained results remain valid by developing a *n-step* ahead predictor considering the parameters of the upper and lower bounds of the model separately and average the obtained estimations.

4.3 Application scenarios

To assess the improvements attained with the use of IT2FLSs, two non-linear processes will be used as support for the development of the *n-step* ahead predictors. The Fermentation Reactor [77] and the Coupled Tanks systems [78] are two traditional benchmark frameworks frequently used in the literature to evaluate the performance and robustness of non-linear modeling and control methodologies. To provide a comparative standpoint in the results discussion, two additional n-step ahead predictors will be implemented based on a linear ARX model and a Type-1 TS Fuzzy Model.

4.3.1 Fermentation Reactor modeling

Yeast fermentation is a biochemical process that, having ethanol and carbon-dioxide as a sub-product, has significant value for several branches of food industry such as bakeries, breweries and distilleries as well as to other domains such as pharmaceutical and chemical plants. The yeast fermentation reaction is itself a composition of several interdependent physical/chemical processes and, for that reason, requires fairly complex models to be accurately simulated. In the work of [79], an extended model of this reaction is developed by complementing its kinetic properties (from which most part of the models existent in literature [80] are based) with the heat transfer equations that directly influence the fermentation process. The biochemical reactions occurs in a reactor which is modeled as a stirred tank with constant substrate feed flow and a constant outlet flow containing the product (ethanol), substrate (glucose) and biomass (suspension of yeast), as generically depicted in figure (4.1).

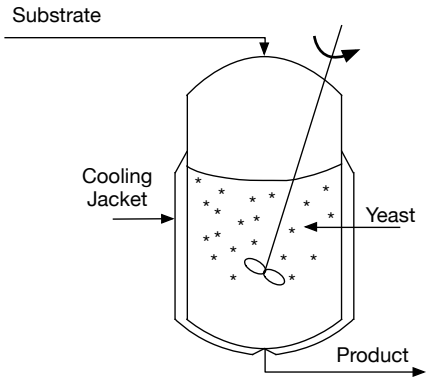

Figure 4.1: Diagram of the continuous fermentation reactor.

The first-principle model of the yeast fermentation process is defined by the following set of non-linear differential equations (4.15):

$$
\begin{aligned}
\frac{dV(t)}{dt} &= F_i t - F_e(t) \\
\frac{dc_X(t)}{dt} &= \mu_X(t) c_X(t) \frac{c_S(t)}{K_S + c_S(t)} exp(-K_P c_P(t)) - \frac{F_e(t)}{V(t)} c_X(t) \\
\frac{c_P(t)}{dt} &= \mu_P c_X(t) \frac{c_S(t)}{K_{S_1} + c_S(t)} exp(-K_P c_P(t)) \\
\frac{c_s(t)}{dt} &= -\frac{1}{R_{SX}} \mu_X(t) c_X(t) \frac{c_s(t)}{K_{S_1} + c_S(t)} exp(-K_P c_P(t)) \\
&\quad - \frac{1}{R_{SP}} \mu_P c_X(t) \frac{c_S(t)}{K_{S_1} + c_S(t)} exp(-K_{P_1} c_P(t)) \\
&\quad + \frac{F_i(t)}{V(t)} c_{S,in}(t) - \frac{F_e(t)}{V(t)} c_S(t) \\
\frac{d_{CO_2}}{dt} &= k_{la}(t)(c^*_{O_2}(t) - c_{O_2}(t)) - \tau_{O_2}(t) - \frac{F_e(t)}{V(t)} c_{O_2}(t) \\
\frac{dT_r(t)}{dt} &= \frac{F_i(t)}{V(t)}(T_{in}(t) + 273) - \frac{F_e(t)}{V(t)}(T_r(t) + 273) + \frac{\tau_{O_2}(t) \Delta H_r}{32 \rho_r C_{heat,r}} \\
&\quad - \frac{K_T A_T (T_r(t) - T_{ag}(t))}{V \rho_r C_{heat,r}} \\
\frac{dT_{ag}(t)}{dt} &= \frac{F_{ag}(t)}{V_j}(T_{in,a} - T_{ag}(t)) + \frac{K_T A_T (T_r(t) - T_{ag}(t))}{V_j \rho_{ag} C_{heat,ag}}
\end{aligned}
\tag{4.15}
$$

where

$$
\begin{aligned}
c^*_{O_2} &= (14.6 - 0.3943 T_r(t) + 0.007714 T_r^2(t) - 0.0000646 T_r^3(t)) x 10^{-\sum (H_i I_i)(t)} \\
(H_i I_i)(t) &= 0.5 H_{Na} \frac{M_{Na}}{V(t)} + 2 H_{Ca} \frac{M_{Ca}}{V(t)} + 2 H_{Mg} \frac{m_{MgCl_2}}{M_{MgCl_2}} \frac{M_{Mg}}{V(t)} \\
&\quad + 0.5 H_{Cl} \left(\frac{m_{NaCl}}{M_{NaCl}} + 2 \frac{m_{MgCl_2}}{M_{MgCl2}} \right) \frac{M_{Cl}}{V(t)} + 2 H_{CO3} \frac{m_{CaCO3}}{M_{CaCO3}} \frac{M_{CO3}}{V(t)} \\
&\quad + 0.5 H_H 10^{-pH(t)} + 0.5 H_{OH} 10^{-(14 - pH(t))} \\
k_{la}(t) &= k_{la0} 1.024^{Tr(t) - 20} \\
\tau_{O_2}(t) &= \mu_{O_2} \frac{1}{Y_{O_2}} c_X(t) \frac{c_{O_2}(t)}{K_{O_2} + c_{O_2}(t)} \\
\mu_X &= A_1 exp(-\frac{E_{a_1}}{R(T_r(t) + 273)}) - A_2 exp(-\frac{E_{a_2}}{R(T_r(t) + 273)})
\end{aligned}
\tag{4.16}
$$

The model parameters and the nominal operation point of the system are presented in Tables (4.1) and (4.2), respectively.

Table 4.1: Parameters of the first-principle model of the yeast fermentation reactor.

$A_1 = 9.5x10^8$	$k_{la0} = 38\ l/h$	$M_{Mg} = 24g/mol$
$A_2 = 2.55x10^33$	$K_{la0} = 8.86\ mg/l$	$M_{MgCl_2} = 95g/mol$
$A_T = 1\ m^2$	$K_{la0} = 0.139\ g/l$	$M_{Na} = 23g/mol$
$C_{heat,ag} = 4.18\ J/(g\ K)$	$K_{la0} = 0.07\ g/l$	$M_{NaCl} = 58.5g/mol$
$C_{heat,r} = 4.18\ J/(g\ K)$	$K_{la0} = 1.03\ g/l$	$R = 8.31\ J/(mol\ K)$
$E_{a_1} = 55000\ J/mol$	$K_{la0} = 1.68\ g/l$	$R_{SP} = 0.435$
$E_{a_2} = 229999\ J/mol$	$K_{la0} = 3.6x10^5\ J/(h\ m^2\ K)$	$R_{SX} = 0.607$
$H_{Ca} = -0.303$	$m_{CaCO_3} = 100\ g$	$V_j = 50\ l$
$H_{Cl} = 0.844$	$m_{MgCl_2} = 100\ g$	$Y_{O2} = 0.97\ mg/mg$
$H_{C0_3} = 0.485$	$m_{NaCl} = 500\ g$	$\Delta H_r = 518\ kJ/mol\ O_2$
$H_H = -0.774$	$M_{Ca} = 40\ g/mol$	$\mu_{O_2} = 24\ l/h$
$H_{Mg} = -0.314$	$M_{CaCO_3} = 90\ g/mol$	$\mu_P = 24\ l/h$
$H_{Na} = -0.550$	$M_{Cl} = 35.5\ g/mol$	$\rho_{ag} = 24\ g/l$
$H_{OH} = 0.941$	$M_{CO_3} = 60\ g/mol$	$\rho_r = 24\ g/l$

Table 4.2: Nominal operating point of the yeast fermentation reactor.

$c_{O_2} = 3.106953\ mg/l$	$F_i = 51\ l/h$
$c_P = 12.515241\ g/l$	$pH = 6$
$c_S = 29.738924\ g/l$	$T_{ag} = 27.053939°C$
$c_{S,in} = 60\ g/l$	$T_{in} = 25\circ C$
$C_X = 0.904677\ g/l$	$T_{in,ag} = 20°C$
$F_{ag} = 18\ l/h$	$T_r = 29.4°C$
$E_{a_2} = 51\ l/h$	$V = 1000\ l$

Fermentation reactions are of exothermic nature and, since they are dependent on living organisms whose growth rate is highly sensitive to temperature variations, it is important to avoid temperature runaway of the reactor. Driven by this, temperature control is a key factor to ensure the reaction stability and can be efficiently used to indirectly obtain its sought products according to the demanded specifications. To do so and since sterility is often a crucial factor in such reactions, cooling jackets are usually employed as opposed to cooling coils into the fermenter itself [80]. Hence, from the perspective of a control algorithm, the reactor is a single-input single-output process: the coolant flow rate (F_{ag}) is the input (the manipulated variable) and the reactor's temperature (T_r) is the output (the controlled variable), as depicted in figure (4.2).

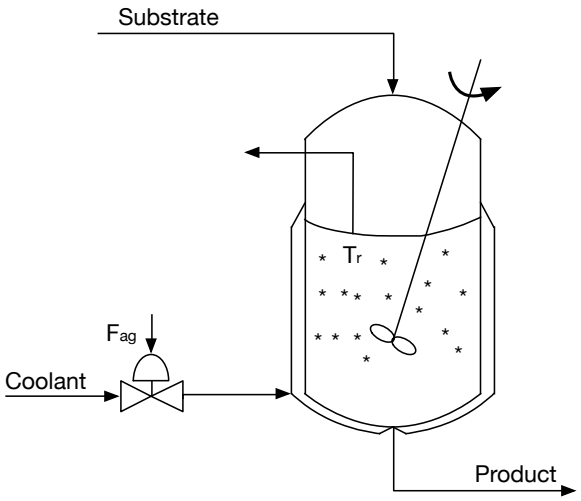

Figure 4.2: Diagram of the continuous fermentation reactor as a SISO system.

The dynamic behavior of the $T_r(F_{ag})$ dependency ultimately defines the complexity developed model. In the present scenario, both steady-state and dynamic properties of the process are of non-linear nature. As is shown by figures (4.3) and (4.4), the steady-state gain and the incremental gain are highly dependent on the current operating point.

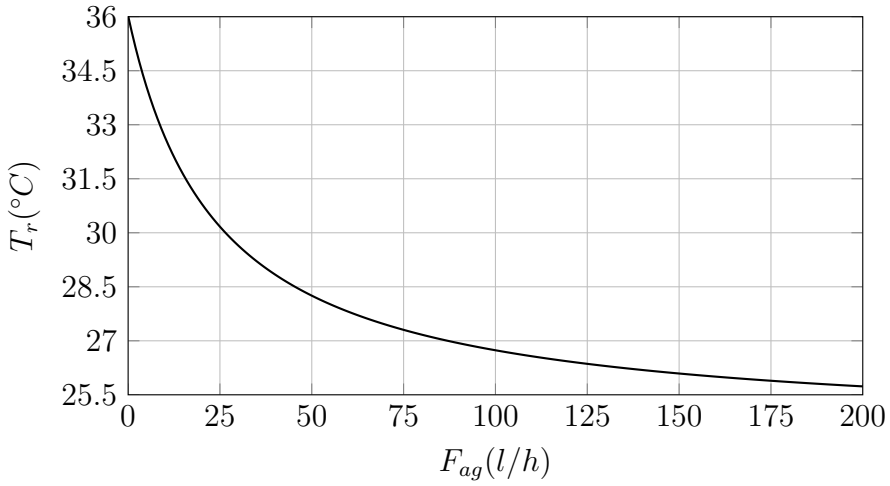

Figure 4.3: Steady-state gain $T_r(F_{ag})$ of the yeast fermentation reactor.

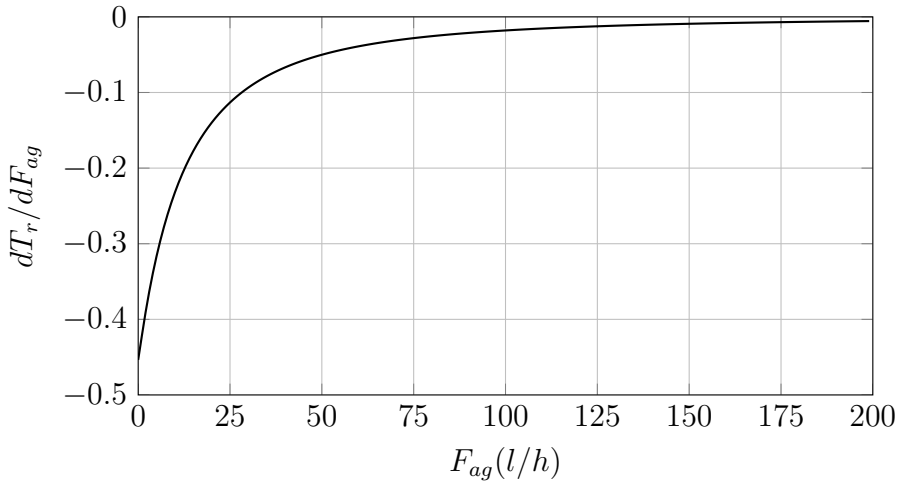

Figure 4.4: Dependence of the incremental gain with the operating point.

Yeast fermentation is a nonlinear process with relatively slow dynamic behavior which is mainly imposed by the glucose decomposition rate [79]. Consequently, when the reaction's operation point is changed, the attained settling time is in the scale of hours and, as so, one sample per hour is enough to capture the process's relevant dynamics.

In order to develop a model with "good" approximation capabilities over all the operational regimes of the process, a pseudo random sequence of control inputs was generated over the [0,200] l/h control range, with steps changing every 200 hours so the system reaches its steady-state. To better simulate the conditions of a real world scenario, the actuation variable was corrupted by gaussian noise with zero mean and variance of $0.1l/h$ while the reactor's temperature measurements were corrupted by gaussian noise with zero mean and $0.05°C$ variance. The training sequence is partially depicted in figure (4.5), evincing the slow dynamics of the reactor's temperature variations.

On related literature [77], the same model is also used as a benchmark system and it was found that a second order regressive models with no dead-time are typically used to model this system. Accordingly, the regression variables presented in equation (4.17) are considered during the identification of the model's consequent part parameters.

$$\hat{y}(k) = f(y(k-1), y(k-2), u(k-1), u(k-2)) \tag{4.17}$$

The Subtractive Clustering algorithm was used to partition the model's inputs space thus obtaining the centers and variance of the membership functions that define a Type-1 TS Fuzzy Model. This process considers solely the $y(k-1)$ and $u(k-1)$ regressors as

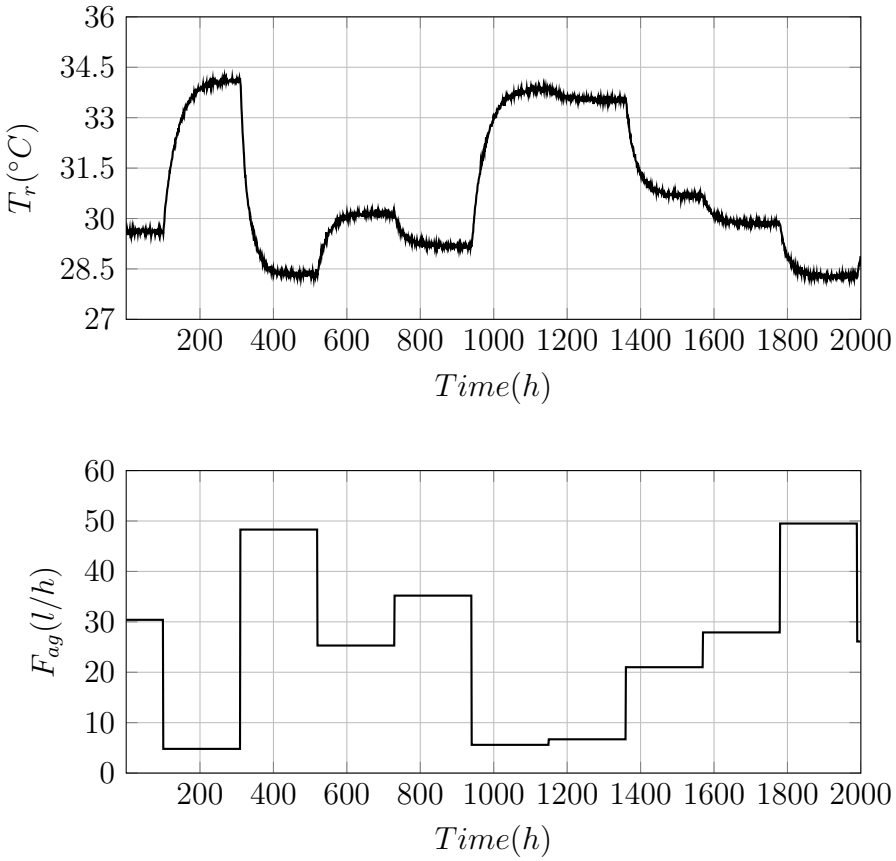

Figure 4.5: Partial depiction of the response of the system to a pseudo-random control sequence used for model extraction.

input variables, since little changes are observed over subsequent samples. The optimal input space partition was found considering a normalized cluster radius of 0.3, a squash factor of 1.25, an acceptance ratio of 0.5 and rejection rate of 0.15, yielding a total of 5 rules. The parameters of the membership functions that define the antecedent part of the model are presented in Table (4.3). Subsequently the consequent part parameters of the model were trained using the Recursive Least Squares procedure. The obtained Type-1 TS Fuzzy Model parameters will be then used as initialization of the Type-2 counterpart.

During the development of the Interval Type-2 TS Model its was found that its output is more sensitive to the width of the uncertainty interval of the consequent parameters. For this reason, and considering the conclusions obtained in chapter 2 regarding the width of the antecedent Type-2 MF, a 5% uncertainty over the antecedent function's center was assumed, yielding a good coverage of the model's input space. Regarding the choice of the uncertainty interval of the consequent part parameters, several trials where performed to

Table 4.3: Center and Variance of each MF used in the Type-1 TS Fuzzy Model input space partition.

	$F_{ag}(l/h)$ u(k-1)		$T_r(°C)$ y(k-1)	
	Center	σ^2	Center	σ^2
Rule 1	5.6	15.36	33.28	3.78
Rule 2	26.1	15.36	30.15	3.78
Rule 3	58.3	15.36	29.92	3.78
Rule 4	88.3	15.36	27.01	3.78
Rule 5	119.6	15.36	26.43	3.78

evaluate the influence of uncertainty ratio over the nominal value of the parameters. For each trial, it was considered that the system is at the steady-state operating point (where $F_{ag} = 32.5l/h$ and $T_r = 29.4°C$), performed then a step in the control signal (F_{ag}) in the range $\Delta u(k) \in [-32.5, 37.5]$. For each step, the change in the process output (T_r) is then obtained 10 sampling instants after. Due to the change of the process gain over different operation points, it is expected the model approximation capabilities to deteriorate when large changes in the operation point are performed. Therefore, long prediction horizons may reveal inadequate since the local linearization used in the extrapolation may no longer be valid. Figure (4.6) illustrates this procedure, revealing the influence of the uncertainty bounds in the prediction error of the Type-2 TS model.

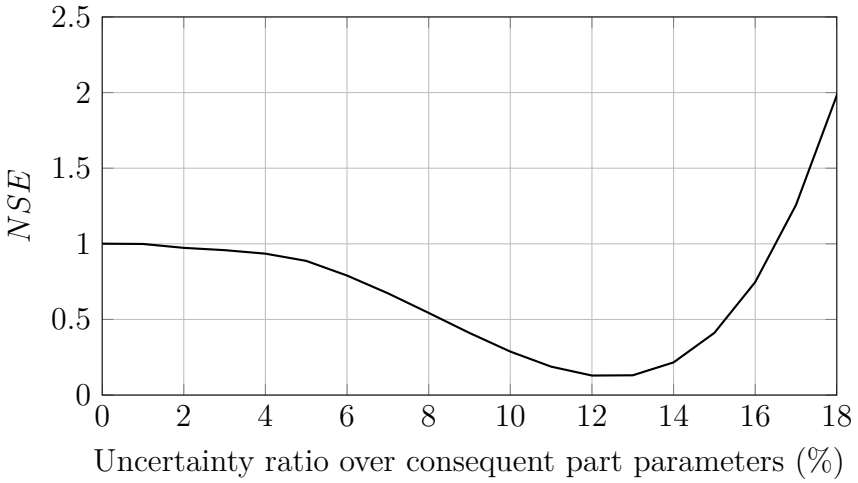

Figure 4.6: Normalized Squared Error of 10 step-ahead estimations using a Type-2 TS Fuzzy Model for different uncertainty ratios over the consequent part parameters, normalized to the Type-1 TS Fuzzy Model estimation error.

As is clear from the obtained results, which are normalized to the error obtained with a Type-1 TS model, increasing the uncertainty width of the Type-2 TS model's parameters is beneficial for the model prediction capabilities. This behavior is observed approximately up to 12% uncertainty ratio, from which its prediction capabilities start to deteriorate. Once again, the results obtained for the 0% value (NSE = 1) attest the equivalence between a Type-1 and a Type-2 TS model with 0% uncertainty ratio.

In figures (4.7), (4.8) and (4.9), are presented the Type-2 TS model 10 step-ahead predictions for several changes in the control signal in the conditions of the previous evaluation considering the 12%, 5% and 15% uncertainty ratios. These results are then compared with extrapolation obtained by two additional predictors (ARX and Type-1 TS FLS).

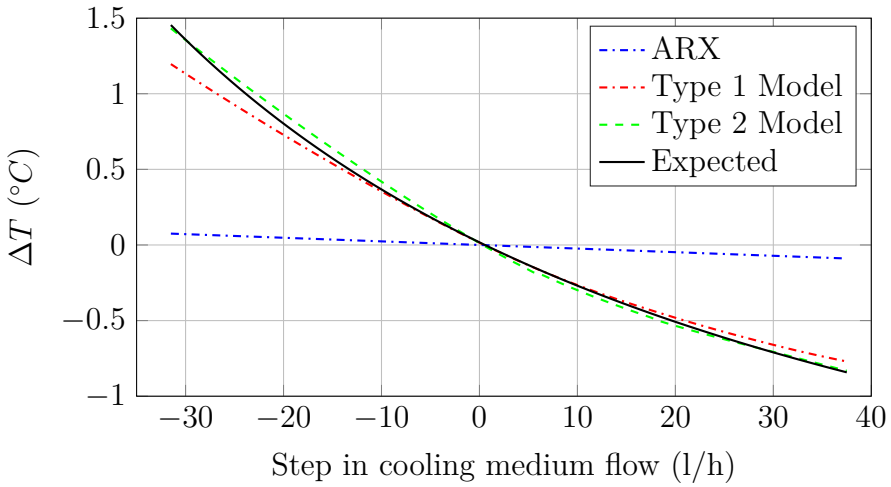

Figure 4.7: Reactor's temperature variation for different actuation steps over the nominal point ($29.4°C$). 10 step-ahead estimations given by predictors based on a linear ARX Model, Type-1 TS Fuzzy Model and a Type-2 TS Fuzzy Model with 12% uncertainty ratio over the consequent part parameters.

As is observed in figure (4.7), the use of a single linear ARX predictor clearly reveals an approach incapable of provide long term predictions due to the significant change of the process gain. On the contrary, for the given scenario, the TS Fuzzy Models evince their superior interpolation capabilities by providing better predictions of the local behavior of the system over the considered horizon. The results given also show that the Type-1 TS model predicts the system behavior with little error relatively to the real system behavior when the step in the cooling medium is limited to the interval $\Delta u(k) \in [-10, 10]$, starting to diverge as this amplitude increases. When a Type-2 TS model with an uncertainty factor of 12% over the consequent parameters is used, the model remains close to the real behavior

of the system over the whole considered interval. As will be evinced in the chapter 5 this improvement is important for the performance enhancements of the predictive controller developed based the Type-2 TS Fuzzy Model framework. On figures (4.8) and (4.9), the influence of the uncertainty interval width at the consequent part parameters is evaluated for 5% and 15% scenarios.

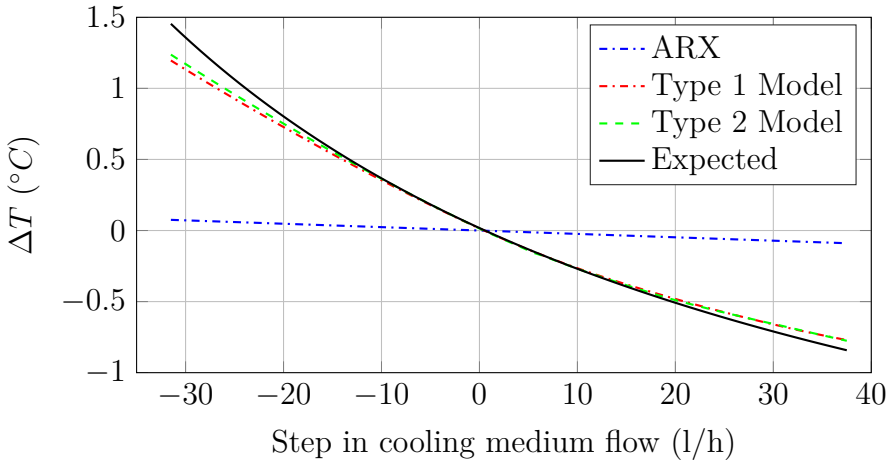

Figure 4.8: Reactor's temperature variation for different actuation steps over the nominal point ($29.4°C$). 10 step-ahead estimations given by predictors based on a linear ARX Model, Type-1 TS Fuzzy Model and a Type-2 TS Fuzzy Model with 5% uncertainty ratio over the consequent part parameters.

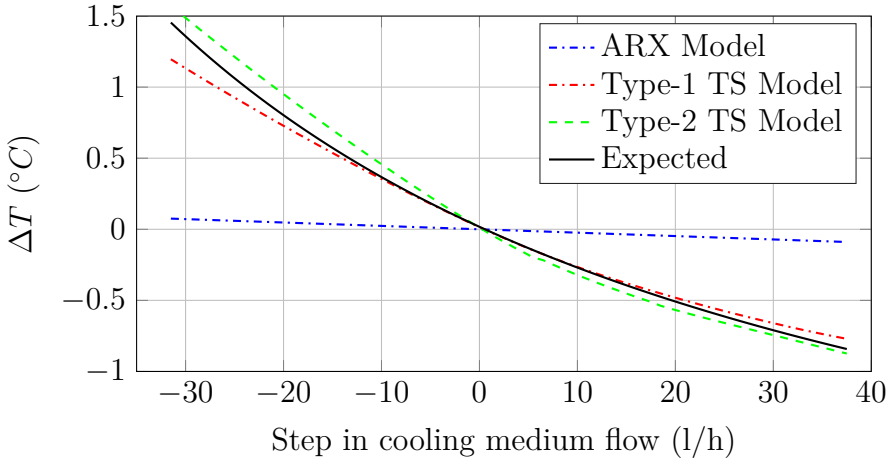

Figure 4.9: Reactor's temperature variation for different actuation steps over the nominal point ($29.4°C$). 10 step-ahead estimations given by predictors based on a linear ARX Model, Type-1 TS Fuzzy Model and a Type-2 TS Fuzzy Model with 15% uncertainty ratio over the consequent part parameters.

In the former figure the differences between the Type-1 and Type-2 TS Fuzzy Models are little (due to the small width of the considered intervals and consequent equivalence of the models). In contrast, when the uncertainty width is increased significantly, the Type-2 Fuzzy Model is no longer advantageous, as is evinced in the latter case where it presents a larger error over the prediction horizon than its Type-1 counterpart. While in this scenario the magnitude of the error is relatively small, the increase of the model's parameters uncertainty results in an increase of the predictor's error in the vicinity of the current operating point (for small variations of the cooling medium flow rate). When such model is integrated in a closed loop model-based controller and operating at steady-state, such predictor inaccuracies will ultimately produce a more active control signal - which is not necessarily desirable.

4.3.2 Coupled Tanks modeling

The control of the liquid level in tanks is a common problem in industries that require fluids to be pumped and stored between several deposits. Many times, such tanks are used to perform mixing reactions that, depending on their nature, can result in sudden volumetric changes of the liquids thus requiring a tight control of their level and flow rates to comply with the tank's storage capacities. The Coupled Tanks System (CTS) [78] used in this evaluation is based on a small scale system consists of two tanks, having each one an independent pump to control the inflow of liquid and an outlet at the bottom responsible for the liquid leakage. Additionally, the tanks are interconnected by a channel which allows the liquid to flow between them. A diagram of this setup is presented in figure (4.10).

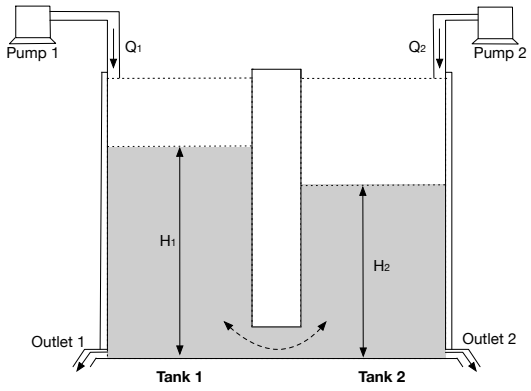

Figure 4.10: Diagram of the Coupled Tanks System.

Based on the Bernoulli's equations for a non-viscous, incompressible fluid in steady-

state flow, the dynamics of the CTS can be modeled by the resulting set of non-linear differential equations:

$$A_1 \frac{dH_1}{dt} = Q_1 - \alpha_1 \sqrt{H_1} - sgn(H_1 - H_2)\alpha_3 \sqrt{|H_1 - H_2|} \tag{4.18a}$$

$$A_2 \frac{dH_2}{dt} = Q_2 - \alpha_2 \sqrt{H_2} + sgn(H_1 - H_2)\alpha_3 \sqrt{|H_1 - H_2|} \tag{4.18b}$$

where A_1 and A_2 are the cross-sectional area of the tank 1 and 2; H_1 and H_2 are the liquid level in tank 1 and 2; Q_1 and Q_2 are the volumetric flow rate (cm^3/s) of Pump 1 and 2; α_1, α_2 and α_3 are proportionality coefficient corresponding to the $\sqrt{H_1}$, $\sqrt{H_2}$ and $\sqrt{H_1 - H_2}$ terms which depend on the discharge coefficients of each outlet and the gravitational constant. The reservoir model parameters were obtained from the setup described in [6], presented in Table (4.4):

Table 4.4: Parameters of the simulated Coupled Tanks System.

A1	A2	α_1	α_2	α_3
36.52 cm^2	36.52 cm^2	5.6186	5.6182	10

By choosing which pumps and rotary valves are directly manipulated, one can develop either a Single-Input Single-Output (SISO) or a Multiple-Input Multiple-Output (MIMO) system model to evaluate the variations of the liquid level of the tanks. In the present evaluation scenario, the Pump 1 will be the actuation variable and the liquid level of the Tank 2 the controlled one and is considered that the valves at the tank interconnection and respective outlets maintain a constant aperture. Using this configuration, the presented setup can be considered as a non-linear second order SISO system.

On related literature [78], this system is modeled using second order regressive models with no dead-time. Accordingly, the regression variables presented in equation (4.19) are considered during the identification of the model's consequent part parameters.

$$\hat{y}(k) = f(y(k-1), y(k-2), u(k-1), u(k-2)) \tag{4.19}$$

As is evinced by figures (4.11) and (4.12) the system's steady-state gain is of non-linear nature and its incremental gain highly dependent on the current operation point.

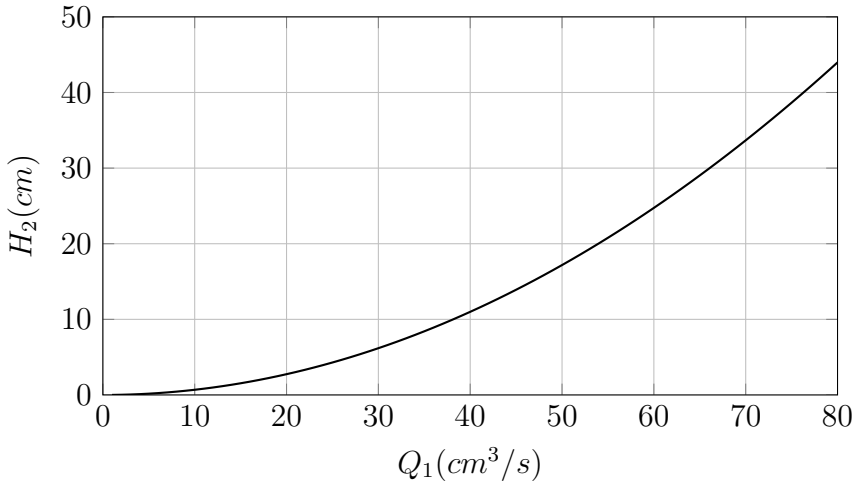

Figure 4.11: Steady-state gain $H_2(Q_1)$ of the Coupled Tanks System.

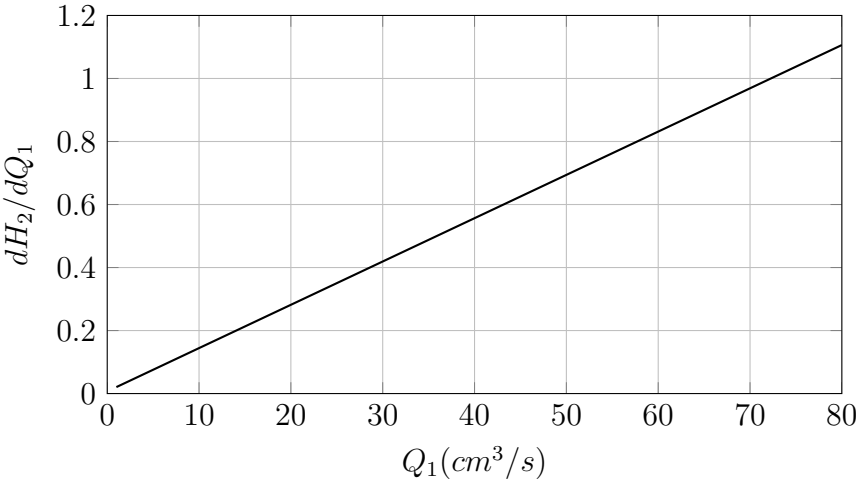

Figure 4.12: Dependence of the incremental gain with the operating point.

In order to extract a model capable of approximate the system's operation region, a pseudo random sequence of control inputs was generated (considering the maximum flow rate for the Pump 1 to be $80cm^3/s$), with steps changing every 200 seconds and the Pump 2 turned off. By evaluating several step responses, a sampling interval of 2 seconds was chosen as appropriate to capture the plant's behavior. An unmeasured gaussian disturbance is introduced in the control signal of Pump 1 with zero mean and variance of $0.5cm^3/s$ while the Tank 2 liquid level measurements are corrupted by a gaussian noise with zero mean and variance of $0.05cm$. Figure (4.13) partially details the changes in the Tank 2 level to a sequence of different liquid flow rates at the Tank 1 inlet.

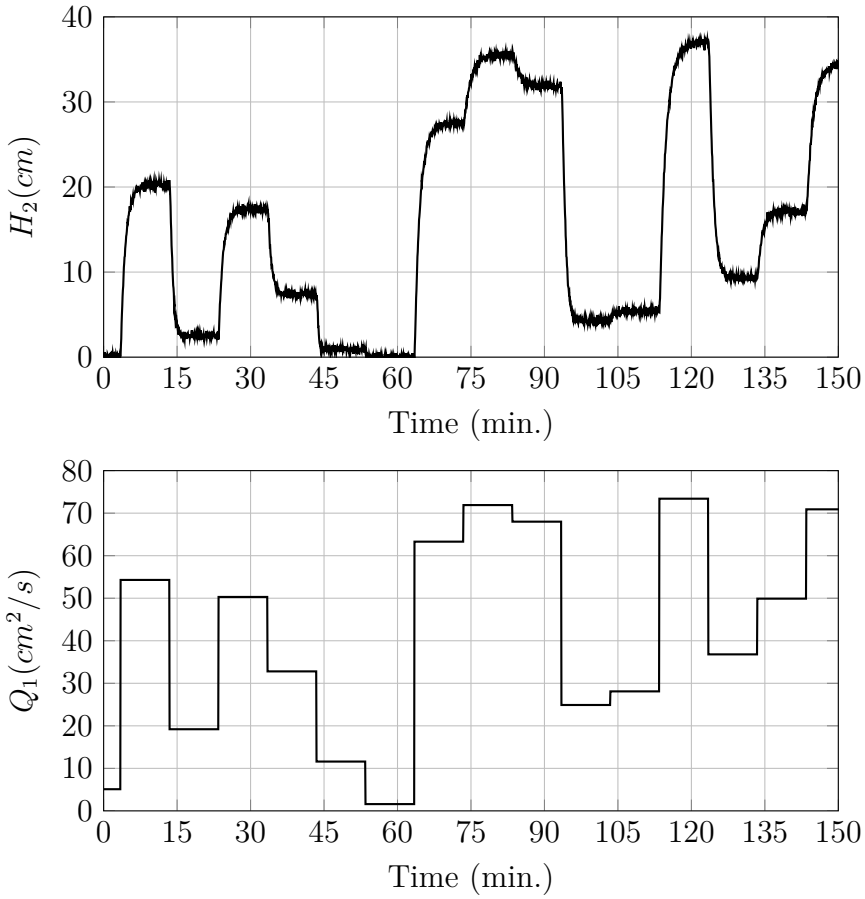

Figure 4.13: Response of the system to a pseudo-random control sequence used for model extraction.

Once again, for comparative purposes, three models were developed based on the linear ARX, Type-1 and Type-2 TS Fuzzy Models. The Type-1 TS Fuzzy model was obtained using the Subtractive Clustering algorithm considering solely the $y(k-1)$ and $u(k-1)$, followed by a training of the consequent part parameters based on the Recursive Least Squares Algorithm. The optimal input space partition was found assuming a normalized cluster radius of 0.3, a squash factor of 1.25, an acceptance ratio of 0.5 and rejection rate of 0.15, yielding a total of 4 rules, which come out to the antecedent part parameters presented in Table (4.5).

Similarly to the previous scenario, the influence of the uncertainty ratio ration over the Type-2 TS model parameters was evaluated by measuring the model's 10 step-ahead prediction error considering the system at the steady-state, with $Q_1 = 60cm^3/s$ and $H_2 = 24.7cm$ and control step variations in the interval $\Delta u \in [-50, 20]$. The Type-2 MF at the

Table 4.5: Center and Variance of each MF used in the Type-1 TS Fuzzy Model input space partition.

	$Q_1(cm^3/s$ u(k-1)		$H_2(cm)$ y(k-1)	
	Center	σ^2	Center	σ^2
Rule 1	8.6	11.30	0.79	6.20
Rule 2	32.8	11.30	7.51	6.20
Rule 3	54.1	11.30	19.92	6.20
Rule 4	71.9	11.30	35.06	6.20

antecedent part of the rule base were obtained considering a 5% uncertainty ratio over the Type-1 ones. The obtained results are represented in figure (4.14).

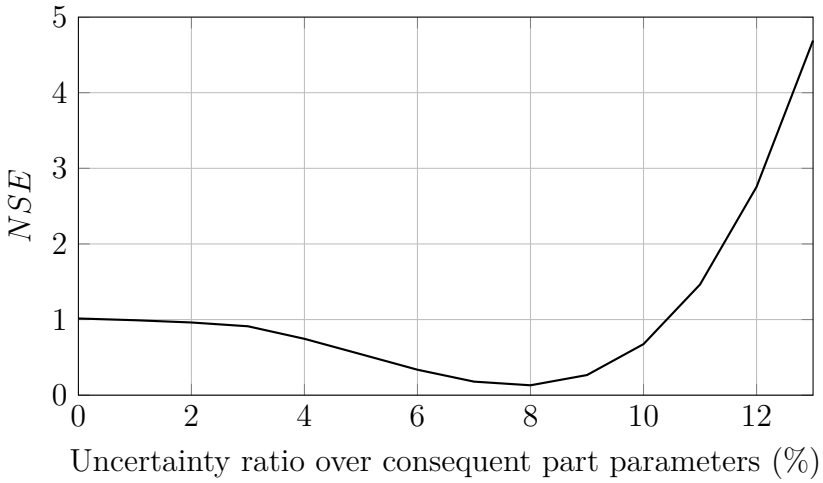

Figure 4.14: Normalized Squared Error of 10 step-ahead estimations using a Type-2 TS Fuzzy Model for different uncertainty ratio over the consequent part parameters, normalized to the Type-1 TS Fuzzy Model estimation error.

In comparison to the previous evaluation scenario, the uncertainty ratio introduced in the consequent part parameters has a similar influence over the prediction model's accuracy, showing that increasing its value is beneficial up to a certain value. In the Coupled Tanks model case, the optimal Type-2 TS model is obtained when a uncertainty ratio of 8% is used over the nominal parameters' values.

Figures (4.15), (4.15) and (4.17), whose Type-2 TS model results are obtained considering uncertainty widths of 8%, 4%, and 12% respectively, depict the prediction accuracy of the three evaluated models for different step changes over the nominal operation point.

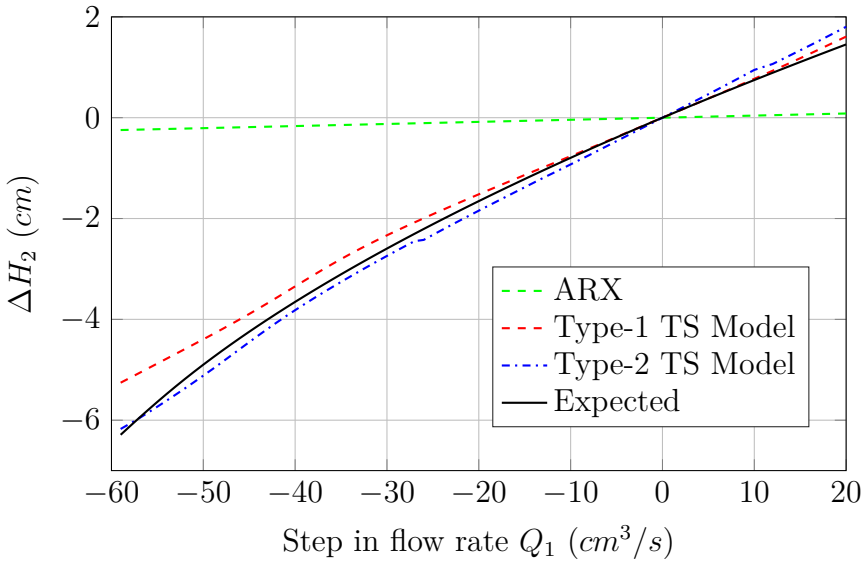

Figure 4.15: Tank 2 liquid level variation (nominal value of 24.7cm) due to a actuation steps in the Pump 1. Comparison between the estimations given by a predictor based on a linear ARX Model, Type-1 TS Fuzzy Model and a Type-2 TS Fuzzy Model with 8% uncertainty width over the nominal consequent part parameters.

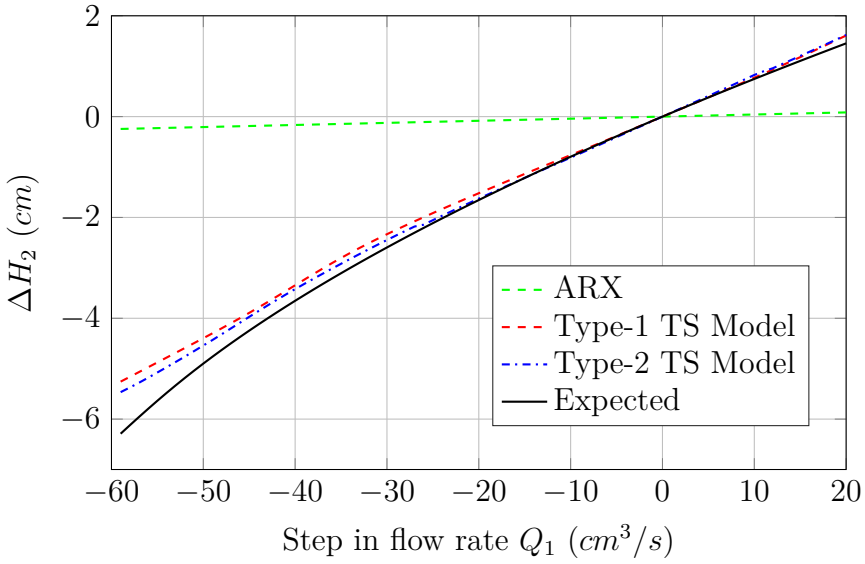

Figure 4.16: Tank 2 liquid level variation (nominal value of 24.7cm) due to a actuation steps on the Pump 1. Comparison between the estimations given by a predictor based on a linear ARX Model, Type-1 TS Fuzzy Model and a Type-2 TS Fuzzy Model with 4% uncertainty width over the nominal consequent part parameters.

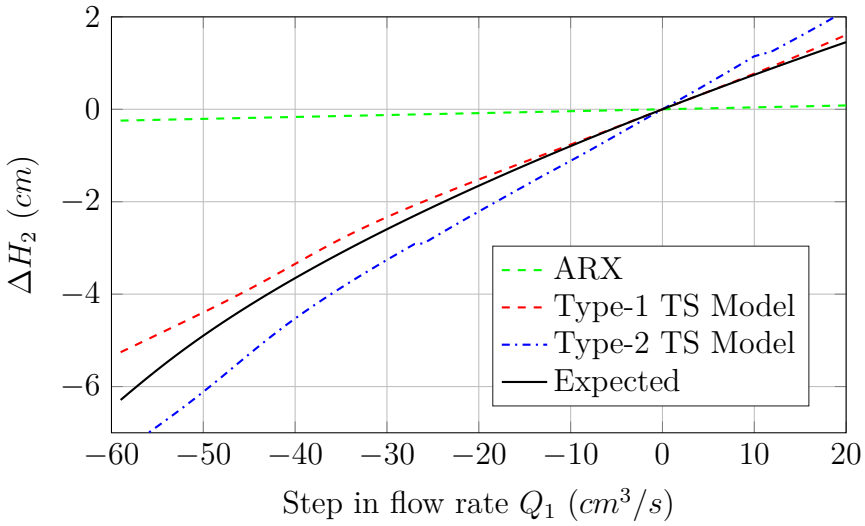

Figure 4.17: Tank 2 liquid level variation (nominal value of 24.7cm) due to a actuation steps in the Pump 1. Comparison between the estimations given by a predictor based on a linear ARX Model, Type-1 TS Fuzzy Model and a Type-2 TS Fuzzy Model with 12% uncertainty width over the nominal consequent part parameters.

Similarly to the previously evaluated scenario, it is clear that the considered uncertainty widths in the Type-2 TS Fuzzy Model significantly influence the performance of the developed predictor. Thehe scenario where the 8% uncertainty width is the one which presented best results and for that reason, will be used in the controller synthesis further presented.

4.4 Conclusions

In the present chapter an approach for the development of a predictive Type-2 TS Fuzzy Model based on the weighted contribution of locally linear models is presented. The evaluated scenarios show that the uncertainty width considered in the Type-2 TS Fuzzy Model parameters significantly influence the developed predictor's performance and, for this reason, the choice of this parameter may be subject to an optimization procedure. One main achievement of the presented results is that the prediction model's performance can be slightly improved based on the Type-2 Fuzzy Logic principles, without necessarily increasing the model complexity with new rules and regression parameters thus potentially providing a better support for model-based linear control methodologies. The succeeding chapter will develop such application, providing comparative results of a closed loop control system based on the described non-linear processes.

Chapter 5

Model Predictive Control using Type-2 Takagi-Sugeno Fuzzy Systems

5.1 Introduction

Model Predictive Control (MPC) is one of the most researched controller synthesis approaches which, based on an approximate model of a process, efficiently computes the best control strategy according to a set of predefined goals over a future time horizon. In fact, this is one of the most distinguishable features of MPC - while, traditionally, control systems determine the course of actions based on the evolution of the error of previous iterations, MPC is driven by evaluating the expected future error due to a chosen control trajectory in a receding horizon fashion. The success of MPC is in part due to the following factors [81]:

- Applicability to a broad class of systems which are difficult to control (i.e. processes with significant time-delays or non-minimum phase behavior).
- Ability to handle constraints imposed in the control as well in the system states.
- Algebraic approach to obtain a closed-loop controller.
- Easily extended to MIMO processes.
- Good tracking performance.
- Computational feasibility.

The genesis of MPC goes back to earlies 80'ies [82] as a result from the commitment of practitioners to solve specialized control needs of power plants and petroleum refineries.

Due to its origins, many of the MPC practical implementations are currently found in industry, mainly in scenarios where the time constants of the controlled processes are measured in the time scale of seconds. Examples of its practical feasibility are found in chemical, petrochemical, paper or in food processing industries [82] - applications where the control goals usually need to be stated not solely based on a reference signal (as in traditional control systems such as PID or even Pole-Placement) but also considering several natural evaluative metrics related with the quality of the final products and their cost.

Motivated by its high level of "simplicity" and flexibility in handling complex control scenarios, academia continued to put efforts in developing MPC beyond just industrial practices, proposing several extensions based on the most recent developments in system's modeling and optimization domains to address complex non-linear problems in any potential controllable scenario [77]. While in the past the available computational resources restrained their use in real-time applications, the theoretical results achieved were not unfruitful. Nowadays, the available computational power even in small embedded systems is turning some of the proposed non-linear MPC approaches into successful practical applications. Dynamic systems with *fast* time constants in automotive industry [83], such as in engine control, or in aerospace applications, as in Unmanned Aerial Vehicle flight control system, [84] are some examples of its recent applications.

MPC is not an unique technique but rather a set of different methodologies rooted on three common functional blocks, interconnected as presented in figure (5.1):

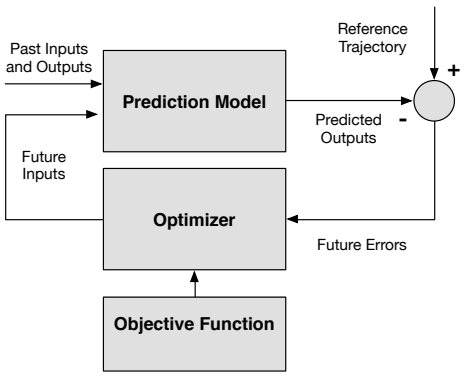

Figure 5.1: Basic structure of a Model Predictive Control algorithm.

Due to the predictive nature of this control approach, the model's process plays a central role in a MPC algorithm as it provides the mean to extrapolate the expected future

behavior of the system. The quality of its predictions ultimately determine the capability of achieve the control goals but also drive the level of computational complexity required to obtain the optimal control sequence. As was previously pointed, MPC algorithms were developed from practitioners and, for that reason, traditionally consider the simplest model capable of give accurate enough predictions. Linear models often satisfy this paradigm, assuming that their uncertainty and some gain scheduling in the control law suffices to overcome mildly non-linearities that industrial processes always present [85]. Among the linear modeling approaches found in the related literature, one can distinguish three main groups:

- Truncated Impulse Response Models - traditionally favored by industry applications, these models are obtained by performing simple tests such as the step response and easily interpretable but require far more data to tune their large number of parameters than the following two approaches.

- State Space Models - most widespread in the academic research, particular in the USA, allowing simple derivations for the controller and easily extended to the multivariable case.

- Transfer Function Models and polynomial methods - curiously these methods are preferred by academics in Europe, and clearly evince the influence of concepts such as dead-time and time constants in their representations. Furthermore, their structure can be easily constructed using both technological knowledge about the process and information provided by data-sets [77]. Due to the easiness in obtaining a regression model, such approach has a closer connection to popular black-box identification techniques what grants it an additional advantage in discrete-time process modeling. However, in multidimensional scenarios, transfer function models may lead to cumbersome and non minimal representations which are harder to interpret and manipulate.

Nevertheless, to address physical processes with stronger non linearities, literature also proposes several models based on non-linear structures such as Cascade (serial) models, Volterra series, Wavelets, Neural Networks and ultimately Fuzzy Systems [77]. Among the referred approaches, non-linear MPC implementations tend to give preference to neural models, existing already a wider consensus in the optimal approaches to use such structures in the predictive control domain [77]. This option is mainly due to their advantages in terms

of approximation accuracy (they are well known universal approximators), reasonably low number of parameters and a simple structure. Moreover, a great number of training and structure optimization algorithms are available for neural models, which make the modeling task a seamless process for practitioners less experienced with the physical details and the relevant variables of the controlled process.

On the other hand, the concept of incorporating Fuzzy Logic into neural models has become increasingly important in recent years and has been object of important studies regarding their stability and applicability in MPC [15]. In contrast to the pure neural networks or fuzzy systems, neuro-fuzzy models based on the Takagi–Sugeno structure have been proven suitable for the use in non-linear MPC, due to their ability in accurately approximate complex non-linear systems by merging *a priori* knowledge about the process, represent the inherent uncertainties regarding information and capability of autonomously improve the process's model. In [71, 86, 87] are presented some examples of the successful applications of MPC using fuzzy models.

Regarding the objective function, the first algorithm ever proposed according to the MPC principles, known as Model Algorithmic Control (MAC) [88] was designed to solely minimize the predicted deviations of the process from the reference trajectory in a least-squares sense. The Dynamic Matrix Control (DMC) [89] algorithm was in fact the first to use the two evaluative metrics that are nowadays considered as standard elements of a MPC objective function. The first one takes into account the differences between the predicted trajectory of the output variable and the set-point trajectory (i.e. the predicted control errors) over the prediction horizon N_p. The role of the second part of the objective function is to introduce a penalty term to reduce excessive (and hence disadvantageous) changes of the manipulated variable. In addition, it also improves the numerical properties of the optimization process [85]. As so, the generic quadratic cost function is typically used:

$$J = \sum_{p=1}^{N} [\hat{y}(k+p|k) - r(k+p)]^2 + \sum_{p=1}^{N} [\Delta u(k+p-1|k)]^2 \tag{5.1}$$

where $\hat{y}(k+p|k)$ is a p-step ahead predictor of the system on instant k, $r(k+p)$ is the future reference trajectory and $\Delta u(k+p-1|k)$ is the control signal increment and N is the optimization horizon (for the predictor and control signal in this case).

It is important to note that the relevance of each performance metric to the final cost function can be adjusted according to several weighting factors. They are usually tuned to achieve a desired closed loop dynamic performance but they can also be dictated by economic objectives of the control system. The choice of a well posed performance index is also a fundamental condition when developing a MPC strategy capable of achieve offset free reference tracking [85], i.e. in steady state, the minimum of J must be consistent with zero tracking errors. Equation (5.1) satisfies this condition by considering Δu rather u in the cost function penalty factor. If the absolute value of u was used instead, the performance index would be biased, favoring operation points which require control signals with smaller absolute magnitude - for obvious reasons such constraint does not comply with the goals of a closed loop control system with a wide operation region.

Ultimately, the choices taken in the previous blocks sum up in an optimization problem which has to be solved online in between each sampling instant according to the new information inferred by the current state of the process. The reliance of MPC in linear models is motivated by the reduced computational complexity necessary to find the solution for the optimization problem and easiness in developing adaptive strategies to cope with time-varying conditions in specific application scenarios [74]. Although providing a sub-optimal representation of non-linear processes, linear models allow one to synthesize a simple linear algebra problem yielding an explicit solution of the problem whereas non-linear models invariably escalate the the complexity of synthesizing the control law to a non-linear optimization problem, which must be solved using heavy iterative methods such as the Levenberg-Marquardt [65, 66] or the Broyden–Fletcher–Goldfarb–Shanno [90] algorithms. Furthermore, such methods provide no guarantees to find an optimal solution in useful time due to the non-convex nature of the problem. As so, under certain circumstances it is an acceptable compromise to have a sub-optimal representation and an optimal controller based on it. Nevertheless, as will be further presented in this chapter, by using linear approximations of non-linear models in the vicinity of the current process operation point, one is capable to retain a significant modeling accuracy (ultimately defining the success in closed loop reference tracking) while simultaneously reducing the optimization problem complexity.

5.2 Generalized Predictive Control

One of the most used implementations of MPC in industry is the Generalized Predictive Control (GPC) [14] due to its simplicity, flexibility and robustness in controlling complex systems where self-tuning controller methods such as pole-placement and other minimum-variance methods [74] are less efficient due to their sensitivity to initial design assumptions. Similarly to many other MPC implementations, on its unconstrained form GPC synthesizes the control law based on the minimization of a multi-step cost function which weights the quadratic terms of the control error and the control increments on a finite time horizon into the future, as represented in equation (5.2)

$$J = \sum_{p=d+1}^{N_p} [\hat{y}(k+p|k) - r(k+p)]^2 + \sum_{p=d+1}^{Nu} [\lambda(z^{-1})\Delta u(k+p-1|k)]^2 \tag{5.2}$$

where $\hat{y}(k+p|k)$ is a p-step ahead predictor of the system on instant k, $r(k+p)$ is the future reference trajectory, $\Delta = 1 - z^{-1}$, $\lambda(z^{-1})$ is a weight polynomial introducing a penalty factor over the control signal activity and $d+1$ is the the first output value that can be controlled from the present iteration. The variables N_p and N_u are the prediction and control horizons, respectively. Figure (5.2) illustrates the main GPC concept, considering a dead-time $d = 1$.

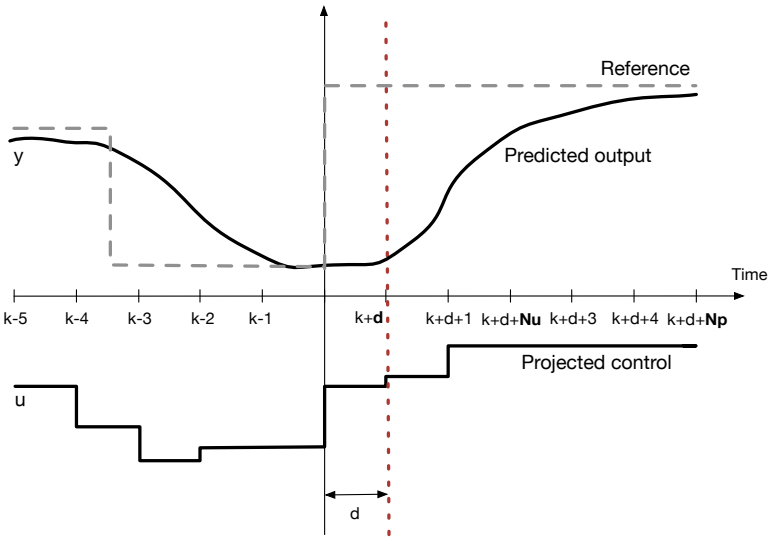

Figure 5.2: Reference, control and predicted output in a Generalized Predictive Control algorithm.

The choice of the parameter d is deeply related with the system dead-time. If a system

has a dead-time of 2 samples, for example, it would be superfluous to try to minimize the difference $y(k+1)-r(k+1)$ since this quantity although in the future, cannot be influenced by present or future control actions. When no *a priori* knowledge of the delay is present, it is usual to set this value to 0. Concerning the length of the prediction window (N_p), this value should be selected in order to ensure the predictor's validity over the chosen interval - if the process is of non-linear nature, its dynamics may change significantly during the prediction window. Regarding the parameter N_u, it is pointless to attribute a value higher than $(N_p - d - 1)$, since only control actions up to this point would have effect in the output within the horizon N_p. Nonetheless, as is suggested by [14] the value of N_u usually is substantially smaller than the prediction horizon. The concept of control horizon is in fact one of the novelty factors introduced by the GPC strategy, which considers the control signal increments null after the N_u window. This simplification significantly reduces the dimensionality of the matrix operations required to compute the control signal and improves the robustness of the control law when unknown future weighting factors, (λ), are required for the controller to be realizable.

When no other constraints are imposed to the process' variables, the attainment of the optimal control signal is a simple algebraic cost function minimization problem. Without entering at this stage in significant calculations, the GPC controller synthesis problem based on linear models starts by assuming that the predicted output of the model, $\hat{y}$ results form the contribution of the forced response of the system y_f and its free response y_0, as presented in figure (5.3). The forced response is determined by future increments of the manipulated variable while the free response depends only on the past values of the manipulated variable and the previous values of the system output.

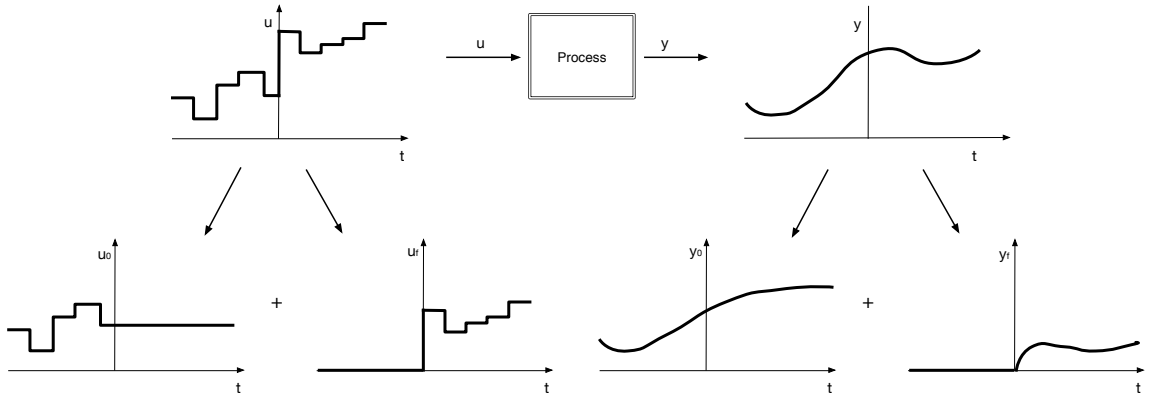

Figure 5.3: Free and forced response.

Based on this property, one can rewrite the model transfer function as presented in equation (5.3)

$$\hat{\mathbf{y}} = \mathbf{y}_f + \mathbf{y}_0 \tag{5.3}$$

which can be further rewritten as

$$\hat{\mathbf{y}} = \mathbf{G}\Delta\mathbf{u} + \mathbf{y}_0 \tag{5.4}$$

where G is a N_p by N_u lower triangular matrix representing the impulse response of the transfer function from u to y

$$\begin{bmatrix} g_{1,0} & 0 & 0 & \cdots & 0 \\ g_{2,1} & g_{2,0} & \cdots & \cdots & 0 \\ g_{3,2} & g_{3,1} & g_{3,0} & \cdots & 0 \\ \vdots & \vdots & \vdots & \ddots & \vdots \\ g_{N_p,N_p-1} & g_{N_p,N_p-2} & g_{N_p,N_p-3} & \cdots & g_{N_p,N_p-N_u} \end{bmatrix} \tag{5.5}$$

It worths noting that if the plant dead-time is $d > 0$ the first p rows of G will be null. Generally in self-tunned modeling scenarios d will not be known *a priory* but, despite that, GPC theory provides a stable solution for the minimization problem even if the leading rows of G are zero, as long as a reasonable estimate of the model order is used [14].

Assuming that the control activity weight factor λ is constant over the time, the cost function (5.2) can be represented using a vector/matrix form. Thus, it can be written as

$$\begin{aligned} J &= (\hat{\mathbf{y}} - \mathbf{r})^T(\hat{\mathbf{y}} - \mathbf{r}) + \lambda\Delta\mathbf{u}^T\Delta\mathbf{u} \\ &= (\mathbf{G}\Delta\mathbf{u} + \mathbf{y}_0 - \mathbf{r})^T(\mathbf{G}\Delta\mathbf{u} + \mathbf{y}_0 - \mathbf{r}) + \lambda\Delta\mathbf{u}^T\Delta\mathbf{u} \end{aligned} \tag{5.6}$$

By setting the partial derivatives of J with respect to Δu as zero, one obtains the control law for the unconstrained scenario as presented in equation (5.7).

$$\Delta\mathbf{u} = (\mathbf{G}^T\mathbf{G} + \lambda\mathbf{I})^{-1}\mathbf{G}^T(\mathbf{r} - \mathbf{y}_0) \tag{5.7}$$

As GPC is used in a receding horizon fashion, only the first optimal control increment of $\Delta\ \mathbf{u}$ is applied so, the effective control signal is obtained as $u(k) = u(k-1)+\Delta\mathbf{u}(1)$. At the next sampling event, the "optimal" control increment is calculated once again considering new N_p step-ahead predictions, effectively closing the control loop.

From equation (5.7), a very simple interpretation regarding the operation of the MPC

can be attained. If the expected future reference tracking error is zero, i.e. the free response of the system y_0 is sufficient to achieve the control set-point r, no further increments in the control signal are necessary. Otherwise, there will be an increment in the control action proportional to the future error independently from the current absolute value of the control variable. Moreover, it is evinced the importance of the prediction model accuracy: since the controller gain is solely proportional to the future error, if the model predictions become biased the controller will not achieve the sought zero error reference tracking.

Figure (5.4) summarizes the procedure of synthesizing a control law based on the Generalized Predictive Control theory.

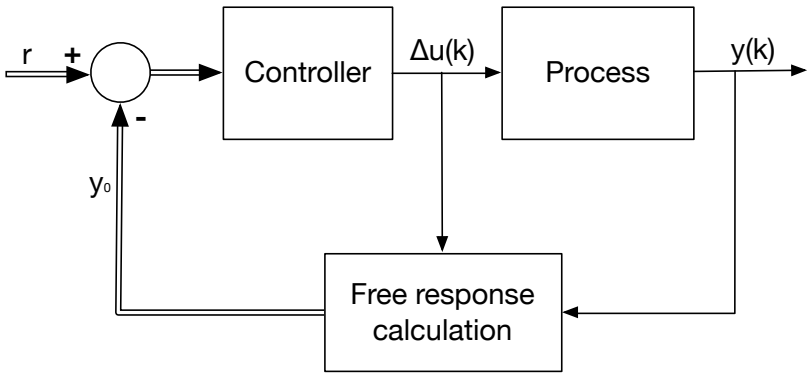

Figure 5.4: MPC algorithm control law.

5.3 Derivation of a n-step ahead predictor

To optimize the cost function presented in equation (5.2) one has to firstly obtain an optimal prediction $\hat{y}$ for every sample within the prediction horizon. Most SISO plants can be described around a particular set-point and after linearization by a Controlled Auto-Regressive Moving Average (CARMA) model, as presented in equation (5.8)

$$A(z^{-1})y(k) = B(z^{-1})z^{-d}u(k-1) + \frac{C(z^{-1})}{\Delta}v(k) \tag{5.8}$$

where $u(k)$ and $y(k)$ are the input and output sequences of the plant, d is the dead time of the system, $v(k)$ is an unknown disturbance and $\Delta = 1 - z^{-1}$. A, B, and C are

the following polynomials in the backward shift operator z^{-1}:

$$\begin{aligned} A(z^{-1}) &= 1 + a_1 z^{-1} + a_2 z^{-2} + \cdots + a_{na} z^{-na} \\ B(z^{-1}) &= b_1 z^{-1} + b_2 z^{-2} + \cdots + b_{nb} z^{-nb} \\ C(z^{-1}) &= 1 + c_1 z^{-1} + c_2 z^{-2} + \cdots + c_{nc} z^{-nc} \end{aligned} \tag{5.9}$$

When no specific disturbance model is used, polynomial C is chosen to be 1 which is sufficient to account with the influence of white noise or a random walk disturbance in the system [85]. By solely consider the disturbance part of equation (5.8), we can rewrite it as follows:

$$n(k) = \frac{1}{\Delta} v(k) \;\equiv n(k) = n(k-1) + v(k). \tag{5.10}$$

In fact, the integrator present in the disturbance model introduces the required integral action into the GPC control law so one estimates the system's steady-state output and get offset-free reference tracking. This feature is more clear if we represent the model in an incremental fashion. This model known as Controlled Auto-Regressive Incremental Moving Average (CARIMA) model, presented in equation (5.11), relates its output to control increments $\Delta u_k = u_k - u_{k-1}$.

$$\Delta A(z^{-1}) y(k) = B(z^{-1}) z^{-d} \Delta u(k-1) + C(z^{-1}) v(k); \tag{5.11}$$

This representation can be obtained by subtracting two consecutive estimations ($\hat{y}(k)$ and $\hat{y}(k-1)$), effectively eliminating the influence of non zero mean unknown disturbances due to the relation stated in equation (5.10) (assuming its average value remains constant - $n(k+1) = n(k)$). As so, the only perturbation remaining is $v(k)$ which is zero mean and its influence can be assumed null in the future time-steps.

Based on the CARIMA transfer function model previously presented, there exist several different ways of deriving the prediction equations necessary to minimize the cost function (5.2). A straightforward and transparent approach is to make use of the one-step ahead predictor, as presented in equation (5.12)

$$\hat{y}(k+1|k) = \underbrace{-\tilde{a}_1 y(k) - \cdots - \tilde{a}_{na} y(k-na-1) + b_2 \Delta u(k-1) + \cdots + b_{nb} \Delta u(k-nb)}_{\text{free response}} + \underbrace{b_1 \Delta u(k)}_{} \tag{5.12}$$

where the coefficients $\tilde{a}$ are obtained as follows:

$$\tilde{A}(z^{-1}) = \Delta A(z^{-1}) \tag{5.13}$$

By recursively deriving successive predictors, a compact matrix/vector form can be written explicitly in terms of the model coefficients as presented in equation (5.14).

$$\underset{k\rightarrow}{y} = \underbrace{G\underset{k\rightarrow}{\Delta u}}_{\text{forced response}} + \underbrace{F\underset{\leftarrow k}{y} + G'\underset{\leftarrow k-1}{\Delta u}}_{\text{free response}} \tag{5.14}$$

Details regarding the derivation of the G, F and G' matrices (the latter is obtained from G) based on the successive recursion of the predictor can be found in [85]. While the underlying principles of this approach are more tractable for the user, the method's notation may become cumbersome for large prediction horizons. Thus, a more efficient way of coding this process for an arbitrary prediction and control window advocates the Diophantine methods [13], as will be hereby presented.

In order to obtain an explicit expression for prediction model ($\hat{y}$) for any future sampling instant p, one has to consider the Diophantine equation (5.15) for the time instant p (assuming the disturbance polynomial C equal to 1)

$$1 = E_p(z^{-1})\tilde{A}(z^{-1}) + z^{-p}F_p(z^{-1}) \tag{5.15}$$

The polynomials $E_p(z^{-1})$ and $F_p(z^{-1})$, presented in equation (5.16), are of order $p-1$ (with $(d+1) \leq p \leq N_p$) and na respectively, and are obtained dividing 1 by $\tilde{A}(z^{-1})$ until the remainder can be factorized as $z^{-p}F_p(z^{-1})$.

$$E_p(z^{-1}) = e_{p,0} + e_{p,1}z^{-1} + \cdots + e_{p,p-1}z^{-(p-1)} \tag{5.16a}$$

$$F_p(z^{-1}) = f_{p,0} + f_{p,1}z^{-1} + \cdots + f_{p,na}z^{-na} \tag{5.16b}$$

Multiplying equation (5.11) by $E_p(z^{-1})z^p$, and considering that $v(k)$ is white noise, one obtain equation (5.17)

$$E_p(z^{-1})\tilde{A}(z^{-1})y(k+p) = E_p(z^{-1})B(z^{-1})\Delta u(k+p-d-1) + E_p(z^{-1})v(k+p) \tag{5.17}$$

which, by considering equation (5.15), can be rewritten as:

$$(1 - z^{-p}F_p(z^{-1}))y(k+p) = E_p(z^{-1})B(z^{-1})\Delta u(k+p-d-1) + E_p(z^{-1})v(k+p) \quad (5.18)$$

and subsequently, simplified as:

$$y(k+p) = F_p(z^{-p})y(k) + E_p(z^{-1})B(z^{-1})\Delta u(k+p-d-1) + E_p(z^{-1})v(k+p) \quad (5.19)$$

Since the degree of the polynomial $E_p(z^{-1}) = p-1$, the noise terms in equation (5.19) are all in the future. Therefore, the best prediction of $y(k+p|k)$ is given by equation (5.20):

$$\hat{y}(k+p|k) = G_p(z^{-1})\Delta u(k+p-d-1) + F_p(z^{-1})y(k) \quad (5.20)$$

where $G_p(z^{-1}) = E_p(z-1)B(z^{-1})$.

The polynomials E_{p+1} and F_{p+1} can be obtained by the same procedure previously presented and can ultimately be derived recursively as:

$$E_{p+1}(z^{-1}) = E_p(z^{-1}) + e_{p+1,j}z^{-j} \quad (5.21)$$

where $e_{p+1,j} = f_{p,0}$. The coefficients of the polynomial $F_{p+1}(z^{-1})$ can be recursively obtained as follows:

$$f_{p+1,i} = f_{p,i+1} - f_{p,0}\tilde{a}_{i+1} \qquad i = 0, \cdots, na-1 \quad (5.22)$$

where $f_{p,na} = 0$. The polynomial G_{p+1} can be obtained recursively as follows:

$$\begin{aligned} G_{p+1} &= E_{p+1}B = (E_p + f_{p,0}z^{-j})B \\ &= G_p + f_{p,0}z^{-j}B \end{aligned} \quad (5.23)$$

That is, the first j coefficients of G_{p+1} will be identical to those of G_p and the remaining ones will be given by equation (5.24).

$$g_{p+1,p+i} = g_{p,p+i-1} + f_{p,0}b_i \qquad i = 1, \cdots, nb \quad (5.24)$$

To initialize the recursion of equation (5.15) for $p = d+1, \cdots, N_p$ iterations, one

has to consider the following initial values for the polynomials $E_{d+1}(z^{-1})$, $F_{d+1}(z^{-1})$ and $G_{d+1}(z^{-1})$:

$$E_{d+1} = 1, \tag{5.25}$$

from equation (5.15) comes

$$F_{d+1} = z^{d+1}(1 - \tilde{A}(z^{-1})), \tag{5.26}$$

thus,

$$G_{d+1} = E_{d+1}(z^{-1})B(z^{-1}) = B(z^{-1}). \tag{5.27}$$

Considering now the following set of j ahead optimal predictions:

$$\begin{array}{rcl} \hat{y}(k+d+1|k) & = & G_{d+1}(z^{-1})\Delta u(k) + F_{d+1}(z^{-1})y(k) \\ \hat{y}(k+d+2|k) & = & G_{d+2}(z^{-1})\Delta u(k+1) + F_{d+2}(z^{-1})y(k) \\ & \vdots & \\ \hat{y}(k+d+N_p|k) & = & G_{d+N_p}(z^{-1})\Delta u(k+N_p-1) + F_{d+N_p}(z^{-1})y(k) \end{array} \tag{5.28}$$

they can be rewritten in a more compact form as in equation (5.29) (as previously presented in equation (5.14))

$$\mathbf{y} = \underbrace{\mathbf{G}(z^{-1})\mathbf{u}}_{\text{forced response}} + \underbrace{\mathbf{F}(z^{-1})y(k) + \mathbf{G'}(z^{-1})\Delta u(k-1)}_{\text{free response}} \tag{5.29}$$

where:

$$\mathbf{y} = \begin{bmatrix} \hat{y}(k+d+1) \\ \hat{y}(k+d+2) \\ \vdots \\ \hat{y}(k+d+N_p) \end{bmatrix}, \qquad \mathbf{u} = \begin{bmatrix} \Delta u(k) \\ \Delta u(k+1) \\ \vdots \\ \Delta u(k+N_u-1) \end{bmatrix}$$

$$\mathbf{G}(z^{-1}) = \begin{bmatrix} g_{1,0} & 0 & \cdots & 0 \\ g_{2,1} & g_{2,0} & \cdots & 0 \\ g_{3,2} & g_{3,1} & \ddots & \vdots \\ g_{N_p,N_p-1} & g_{N_p,N_p-2} & \cdots & g_{N_p,N_p-N_u} \end{bmatrix}, \qquad \mathbf{F}(z^{-1}) = \begin{bmatrix} F_{d+1}(z^{-1}) \\ F_{d+2}(z^{-1}) \\ \vdots \\ F_{d+N_p}(z^{-1}) \end{bmatrix}$$

$$\mathbf{G}'(z^{-1}) = \begin{bmatrix} (G_{d+1}(z^{-1}))z \\ (G_{d+2}(z^{-1}) - g_0 - g_1 z^{-1})z^2 \\ \vdots \\ (G_{d+N_p}(z^{-1}) - g_0 - g_1 z^{-1} - \cdots - g_{N_p-1} z^{-(N_p-1)})z^{N_p} \end{bmatrix},$$

Based on the cost minimization procedure generically presented in section 5.2, the optimal control increments are obtained by:

$$\mathbf{u} = (\mathbf{G}^T\mathbf{G} + \lambda\mathbf{I})^{-1}\mathbf{G}^T(\mathbf{R} - \mathbf{F}y(k) - \mathbf{G'}\Delta u(k-1)) \tag{5.30}$$

where $\mathbf{R} = [r(k+d+1), \cdots, r(k+N_p))]$ is the reference set-point in the N_p prediction horizon.

As MPC is implemented in a receding horizon fashion, the control signal sent to the process is incremented by the first value of $\mathbf{u}$, $\Delta u(k)$, which is given by:

$$\Delta u(k) = \mathbf{K}(\mathbf{R} - \mathbf{F}y(k) - \mathbf{G'}\Delta u(k-1)) \tag{5.31}$$

where $\mathbf{K}$ is the first row of matrix $(\mathbf{G}^T\mathbf{G} + \lambda\mathbf{I})^{-1}\mathbf{G}^T$,

$$K = [1\ 0\ 0\ \cdots 0]_{N_u}(\mathbf{G}^T\mathbf{G} + \lambda\mathbf{I})^{-1}\mathbf{G}^T \tag{5.32}$$

Following this approach, the accuracy problems that the prediction model may present when extrapolating the system's response in long time horizons are minimized due to the constant corrections of the optimal control trajectory performed according to the most recent system samples.

5.4 Extension of Model Predictive Control to Non-Linear Models

The predictor derived in the previous section assumes the existence of a linear plant model complete enough to fully capture the process dynamics. If the process non-linearity is not significant, the integral action of the linear GPC algorithm will compensate eventual inaccuracies and eliminate the steady-state error. However, since some physical processes possibly present complex non-linear relations, a simple linear model may prove itself insufficient for a successful application of the GPC algorithm. The mismatch between the model and the corresponding physical process is more significant in situations where operation point of the process changes fast and significantly, resulting in slow or unstable closed loop response in such operation regions [77]. For this reason, to apply the GPC principles in domains where its success has been hindered by the non-linear behavior of the process, several extensions to its original linear formulation have been proposed in recent years. Though, it is important that such enhancements, apart from improving the performance of the closed loop system, maintain the similar level of simplicity and effectiveness that traditional linear MPC accustomed its practitioners in industry.

The most straightforward way of dealing with MPC in non-linear processes is to directly use a single non-linear model describing every operational regime and directly solve an optimization problem that yields the control trajectory that minimizes a considered cost function. Models based on ANNs are particularly successful for such purpose due to their regular structure and universal approximation capabilities [77]. However, without any further simplifications of the model, a non-linear MPC optimization problem has to be solved on-line at each sampling instant. Apart from being computationally demanding, non-linear optimization algorithms do not guarantee that a global optimal solution is found due to the non-convex nature of the problem (which may result in unsatisfactory control quality), neither that convergence to a sub-optimal one is obtained in useful time (what may hinder their use in on-line MPC implementations requiring short sampling periods).

Despite the increasingly availability of powerful embedded systems in the market, practical implementations of MPC for non-linear processes circumvent this problem by relying on linear approximations of the non-linear model. This approach, known as instantaneous linearization [77], computes at each sampling instant a linear model of the process so one can obtain a estimation of the free and forced responses of the process over the prediction horizon. By using this procedure it is possible to derive an explicit control law using a sim-

ilar process as previously presented on section 5.3. The idea of such approach is presented on figure (5.5).

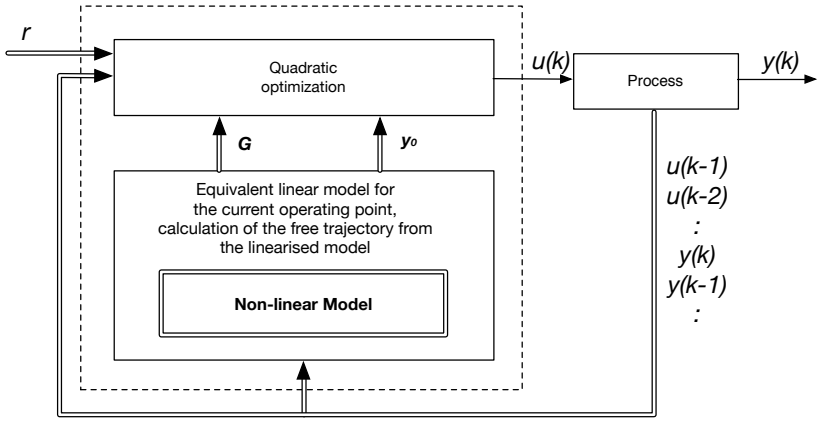

Figure 5.5: Structure of the MPC algorithm based on a linearization of a non-linear model.

As is clear from the difference in the amount of publications between both lines of work, "theoretical purists tend to stay away from linearization approaches" [77]. The main reason for such conduct is that linearization procedures make the stability and robustness analysis much more difficult than in the case of MPC based on pure non-linear models due to the possibility of existing discontinuities in the parameters of the models underlying the controller synthesis procedure [87].

There exist two main lines of work regarding the use of linearized models in MPC. In the first approach, one calculates a linear approximation of the non-linear model for the current operating point and consider its parameters constant for the whole prediction horizon. Yet, in some scenarios where changes in the operation region are significant, there may exist a larger discrepancy between the real process trajectory and the estimated one in the end of the prediction horizon, what may lead to suboptimal results. When such assumption is not sufficient, one can alternatively perform the linearization along a future input trajectory to account with the possible model variations. Since such trajectory is not known *a priori*, the optimization process requires a larger number of iterations within the prediction horizon to converge to the optimal control increments. Nevertheless, when the inherent limitations of MPC designs based on single linear approximation are accounted for, very little differences can be seen between the optimal trajectories obtained by both approaches [77].

As was presented in chapter 4, TS Fuzzy Systems proved their ability to accurately approximate any non-linear dependency between input and output variables. In the present application scenario, this modeling approach is particularly advantageous since its structure inherently considers a set of locally linearized models valid within a certain operation region defined by its non-linear fuzzy boundaries. By employing the available fuzzy inference mechanisms, one can also efficiently interpolate the output of the several local models to obtain an approximate linear model valid for the current operation regime. Performing this operation at each sampling instant, a TS Fuzzy Model can in fact be considered a linear time-varying model and, for that reason, be easily integrated with traditional model-based control methodologies such as GPC to overcome the majority of the limitations and difficulties imposed other approaches based on non-linear models. Successful applications resulting from the synergy between Fuzzy Models and Predictive Control can already be found in literature, spanning more theoretical analysis such as in [87] and [91], focused in the analysis of the robust stability conditions and supported with numerical simulations, to more practical ones evincing the robustness of the method to disturbances in industrial domains such as in the control of a non-linear heat-exchanger pilot plant [92], a continuous-stirred tank reactor [71] or a binary distillation column [93].

5.4.1 Generalized Predictive Control using Type-2 TS Fuzzy Models

The extension of the Model Predictive Control based on TS Fuzzy Systems to the Type-2 FL case is a straightforward procedure. As was presented in chapter 4, a Type-2 Fuzzy Model can ultimately be represented by two average sub-models (related with the upper and lower bounds of the output value uncertainty interval). Based on each sub-model, the GPC theory can be directly applied thus, two control increments will be obtained - $\Delta\overline{u}$ and $\Delta\underline{u}$. The effective control action performed by the controller is then given by averaging the control increments obtained, as presented in equation (5.33)

$$u(k) = u(k-1) + \frac{\Delta\overline{u} + \Delta\underline{u}(k)}{2}. \tag{5.33}$$

In figure (5.6), the functional diagram of the MPC based on Type-2 TS Fuzzy Models is presented.

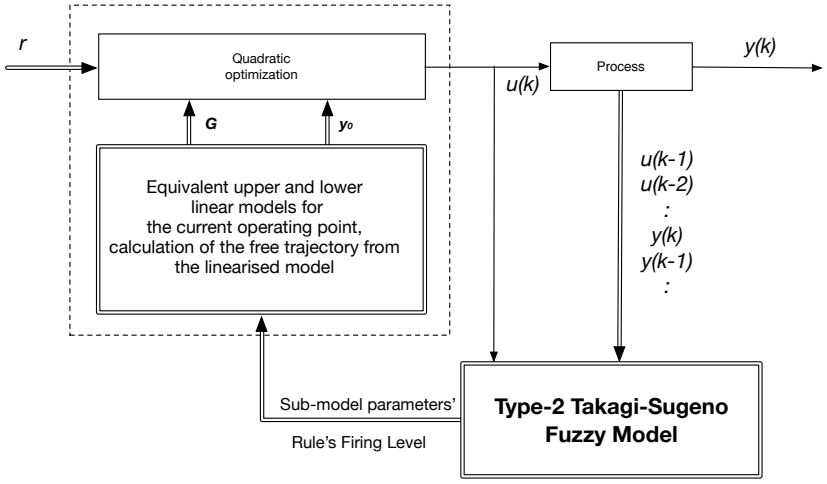

Figure 5.6: Structure of the MPC algorithm based on Type-2 Takagi-Sugeno Fuzzy Models.

5.5 Application scenarios

To evaluate the enhancements obtained by combining the modeling capabilities of IT2FLSs and the GPC theory, the Fermentation Reactor and Coupled Tanks Systems presented in the previous chapter will be used as benchmark for the proposed model based predictive controller. Additionally, its performance will be compared with two additional implementations based on an linear ARX and a Type-1 TS Fuzzy models. Figure (5.7) generically displays the evaluated closed loop system along with the considered disturbances affecting its operation.

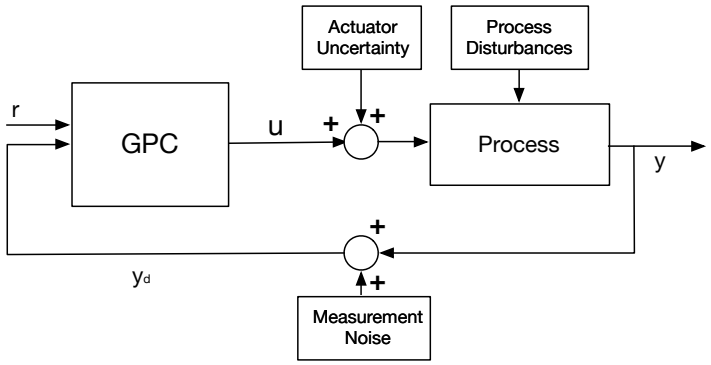

Figure 5.7: Diagram of the closed loop control system and the considered disturbances.

The models used as support for the GPC algorithm are considered fixed during closed loop operation. While model adaptability is a highly sought feature in control systems [74], it also presents several problems due to its unpredictable influence in the model parameters and consequently the controller behavior. Considering the particular scenarios where the closed loop control system must perform quick changes between different operation regimes, the use of adaptive models may eventually result in suboptimal or even unstable control as the model update rate may be insufficient to cope with the significant changes verified on some parameters. Nevertheless, by considering the compared models fixed, the advantages of the GPC control algorithm based on Type-2 TS Fuzzy models in coping with inherent modeling uncertainties will be better highlighted. In the evaluations performed, the dynamic equations of the benchmark systems were implemented in continuous time while the GPC is executed in discrete time.

5.5.1 Fermentation Reactor Temperature Control

As was previously presented, from the perspective of a control algorithm the fermentation reactor is a single-input single-output process, the coolant flow rate (F_{ag}) the manipulated variable and the reactor's temperature (T_r) the controlled one, as shown in figure (5.8).

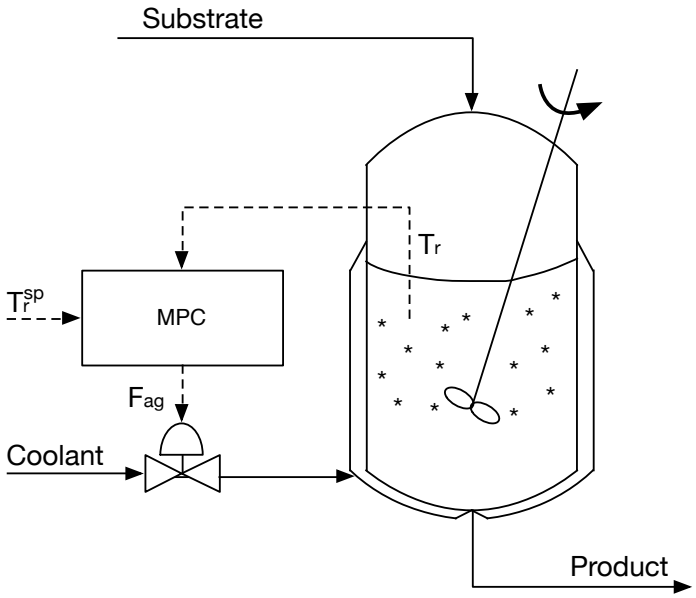

Figure 5.8: Diagram of the continuous fermentation reactor.

The maximum allowed cooling fluid's flow rate is $80l/h$ and the reactor's temperature is controlled within the [28-33]$^{\circ}C$ interval. The performance of the Generalized Predictive Controllers in the Fermentation Reactor's Temperature Control will be assessed considering the following operation scenarios:

- Different amplitude reference step signals are used by closed loop system as control goals. An unmeasured gaussian disturbance with zero mean and standard deviation of $0.1l/h$ is added to the control signal while the reactor's temperature measurements are corrupted by a gaussian disturbance with zero mean and $0.05^{\circ}C$ standard deviation. The system's model is trained under these conditions.

- Under similar operation conditions of the previous scenario, a step change in the substrate temperature from $25^{o}C$ to $27^{o}C$ was introduced. This type of disturbance can occur due to ambient temperature changes.

In every predictive control implementation tested, the considered prediction and control horizons were 10 and 3 samples respectively and the control signal updated once every hour. When employing TS fuzzy models the control activity penalty factor (λ_{GPC}) is set to 0.01. Its value changed to 0.1 when the ARX model is used. These parameters are chosen so a control signal with satisfactory transient response is attained while maintaining its robustness to noise. The difference in the control activity penalty factor between the ARX and the TS Fuzzy based implementations already anticipates the superiority of the latter approaches since they allow one to synthesize a faster control law for identical disturbance levels. As was presented in the previous chapter, the TS structures used to implement the respective controllers are composed by 5 rules. The Type-2 TS Model used considered 5% and 12% uncertainty factors over the antecedent and consequent part parameters, respectively. The obtained results were evaluated using four distinct metrics: the Mean Squared Error (MSE), the overshoot (O_S), the settling time (T_S) of the controlled variable and the Control Effort (CE) of the actuation variable. The latter one was estimated by the cost function as presented in equation (5.34).

$$CE = \sum_{k=t}^{t+N} \frac{\Delta u(k)^2}{N} \tag{5.34}$$

In figure (5.9), the closed loop response of the system is presented considering different set-points and operating conditions identical to the training stage.

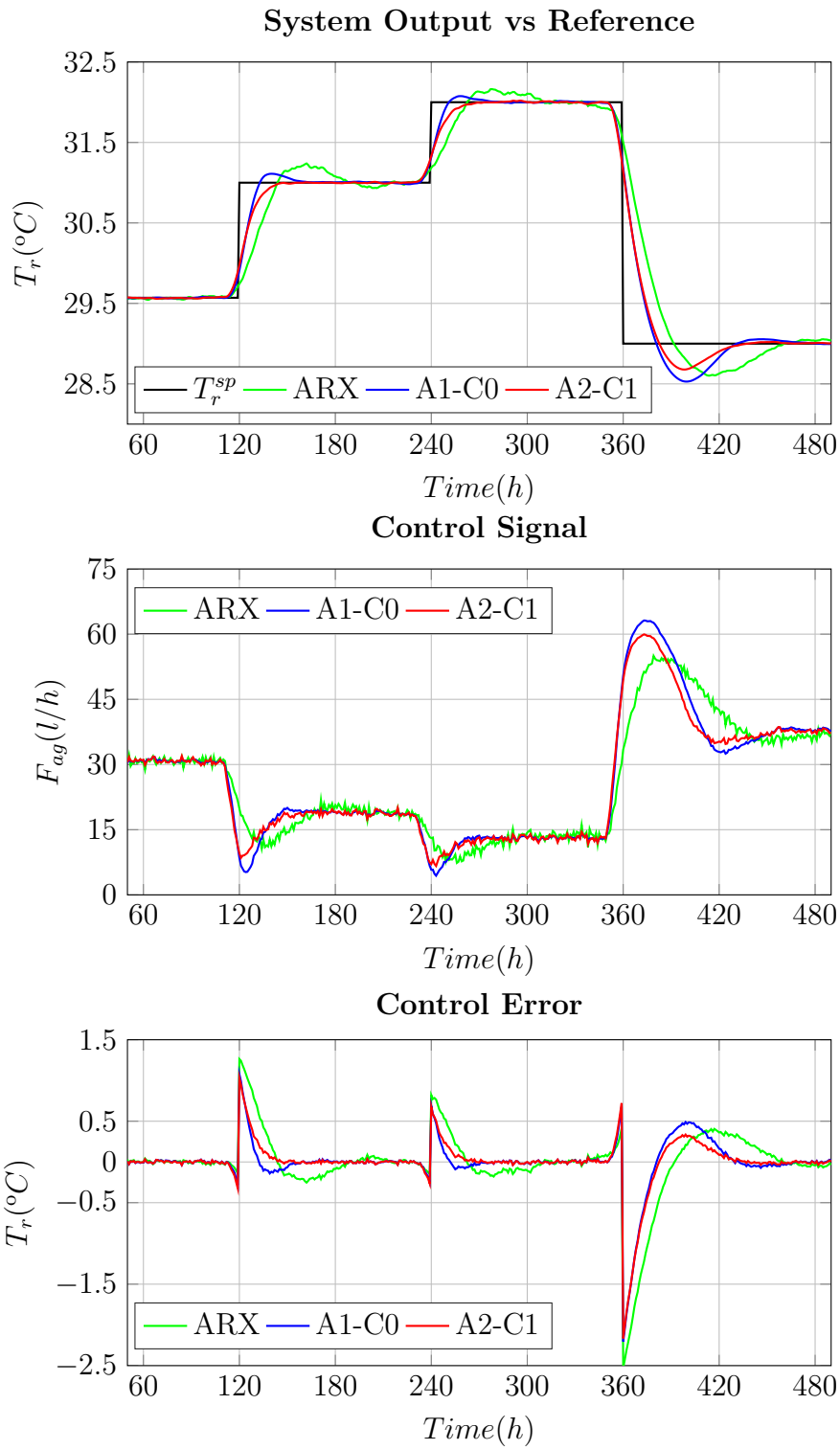

Figure 5.9: Closed loop behavior of the reactor's temperature during a yeast fermentation reaction using three different GPC algorithms based on locally linear models.

This evaluation scenario shows that the closed loop responses of the TS Fuzzy Model based controllers present a similar transient response, standing out a slight improvement when the Type-2 one is used. Despite the worse performance of the linear ARX based controller during the step transient stage, it is also capable of achieve zero steady-state error. This result attests the robustness of GPC even in the case of significant model mismatches (as long they are compensated with an adequate control activity penalty factor). A detailed view of the system's behavior when the set-point is changed from $29°C$ to $31.5°C$ is presented in figure (5.10), while the comparative metrics relative to the three control systems are presented in Table (5.1).

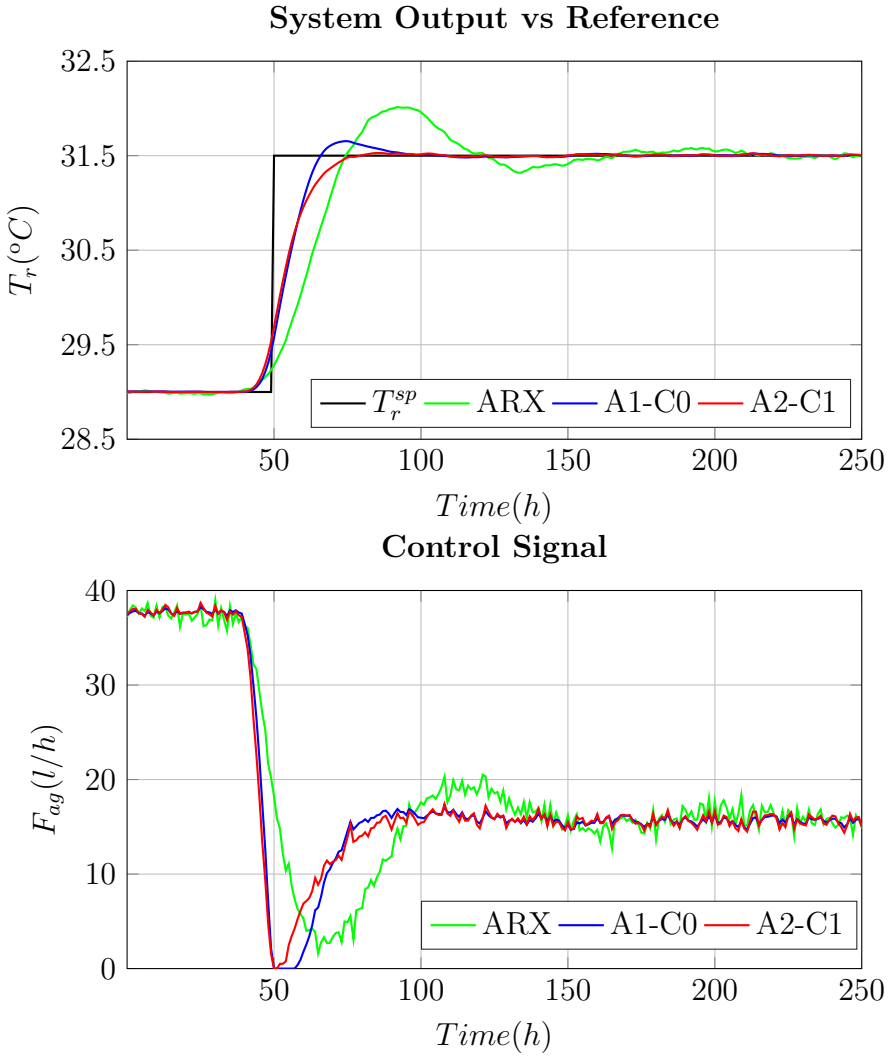

Figure 5.10: Detailed view of the process's response to a change in the controller's reference signal.

Table 5.1: Comparative metrics under nominal operation measured at reference step (29.0º to 31.5ºC) as presented in figure (5.10).

	MSE	Control Effort	O_s (ºC)	T_s (h)
ARX	$1.95 * 10^{-1}$	10.2	0.499	180
A1-C0	$7.54 * 10^{-2}$	14.6	0.153	53
A2-C1	$6.81 * 10^{-2}$	11.9	0.028	48

In this comparison scenario, the Type-2 TS based GPC achieves improved metrics relatively to the Type-1 and ARX based controllers, reducing the MSE over the evaluated interval by approximately 6% and 65% respectively. Additionally, there is a significant improvement in the step response overshoot and settling time which, in this specific application, leads to a reduction of the transient response length by several hours. As there is a large dependence of the reaction sub-products' parameters on the reactor's temperature, the use of a faster controller allows one to perform a quick change between different operation regimes as production requirements dictate.

To evaluate the disturbance rejection capabilities of each controller and its performance under model mismatches, several set-point changes were performed after the raw material's temperature at the reactor's intake is increased from 25°C to 27°C at instant $t = 50h$, as shown in figure 5.11. The obtained results reveal that the Type-2 TS GPC controller provides a faster transient response when external perturbations interfere with the reactor's temperature. Additionally, its advantages are more pronounced when the controller is operating in a different regime that the one it was trained for. Despite the significant change on the cooling fluid's flow rate required during the period [0h-50h], the Type-2 TS based controller provides a more "desirable" closed loop response. Table (5.2) briefly summarized the comparative metrics obtained for the three controllers.

Table 5.2: Comparative metrics measured at reference step (29°C to 31.5°C) after introduction of a disturbance, as presented in figure (5.11) in the interval [350h-550h].

	MSE	Control Effort	O_s (ºC)	T_s (h)
ARX	$4.15 * 10^{-1}$	14.6	0.350	130
A1-C0	$3.14 * 10^{-1}$	31.4	0.275	100
A2-C1	$2.56 * 10^{-1}$	30.4	0.051	68

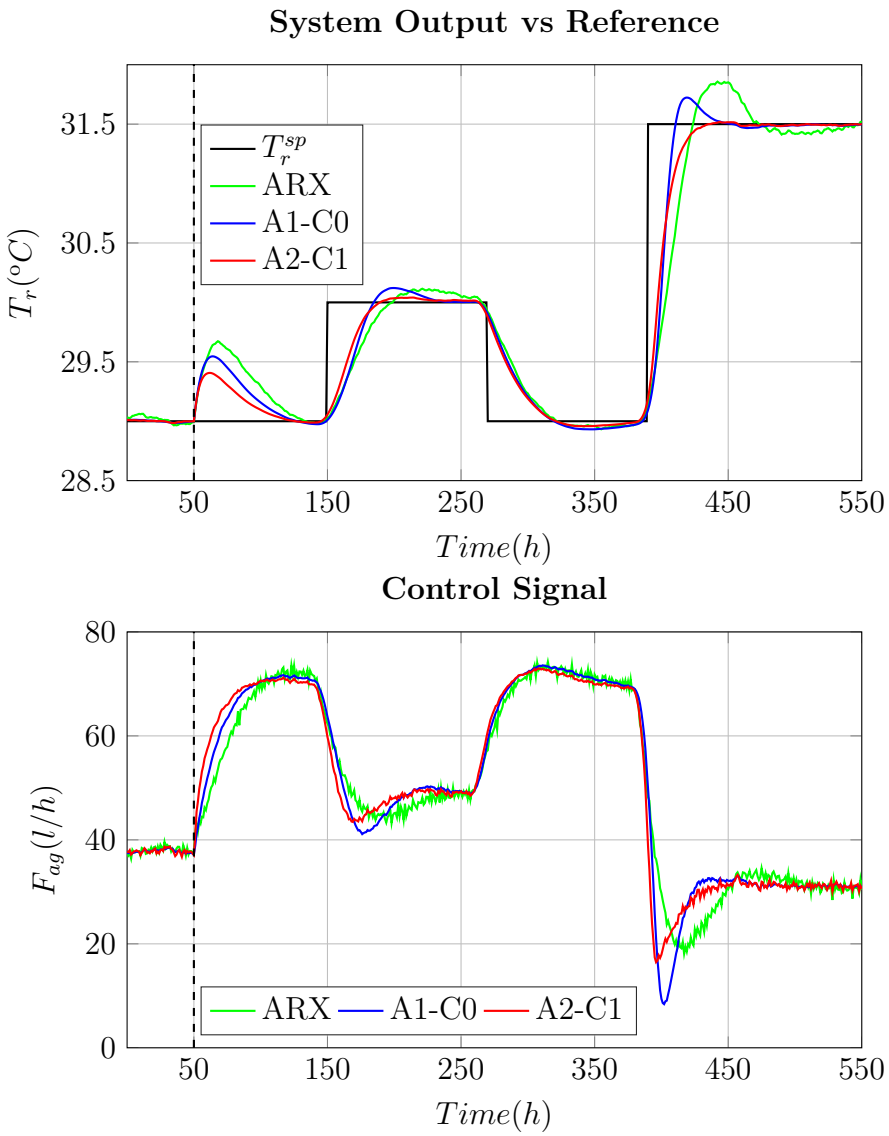

Figure 5.11: Evaluation of the closed loop performance after the process is disturbed by a change in the Substrate temperature.

Ultimately, to assess the model dimensionality reduction capabilities of Type-2 Fuzzy Models, the 5 Rule Type-2 TS Fuzzy model was compared with a 9 Rule Type-1 TS one. By increasing the number of rules of the latter model, one expects it to perform similarly to its Type-2 counterpart. Figure (5.12) displays their performance under nominal operating conditions.

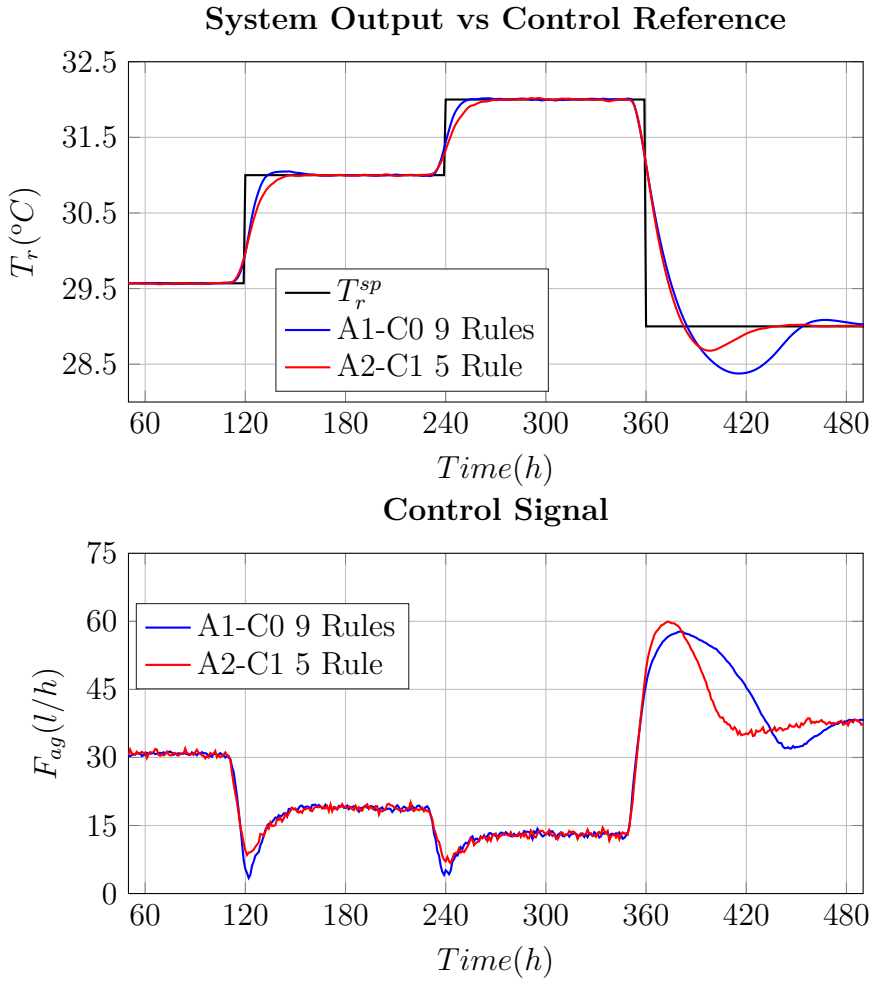

Figure 5.12: Comparison between two predictive controllers based on a 5 Rule Type-2 TS Fuzzy model and a 9 Rule Type-1 TS Fuzzy model (N_p=10; N_u=3, λ_{GPC} = 0.01).

Establishing a comparative standpoint with the previous evaluations, figure (5.13) provides a close-up depiction of the system's response when the reference signal is changed from 29°C to 31.5°C. The comparative metrics summarized in Table (5.3).

Table 5.3: Comparative metrics under nominal operation measured at reference step (29.0° to 31.5°C) presented in figure (5.13).

	MSE	Control Effort	O_s (°C)	T_s (h)
A1-C0 (5 Rules)	$7.54 * 10^{-2}$	14.6	0.153	53
A1-C0 (9 Rules)	$8.64 * 10^{-2}$	37.4	0.051	49
A2-C1 (5 Rules)	$6.81 * 10^{-2}$	11.9	0.028	48

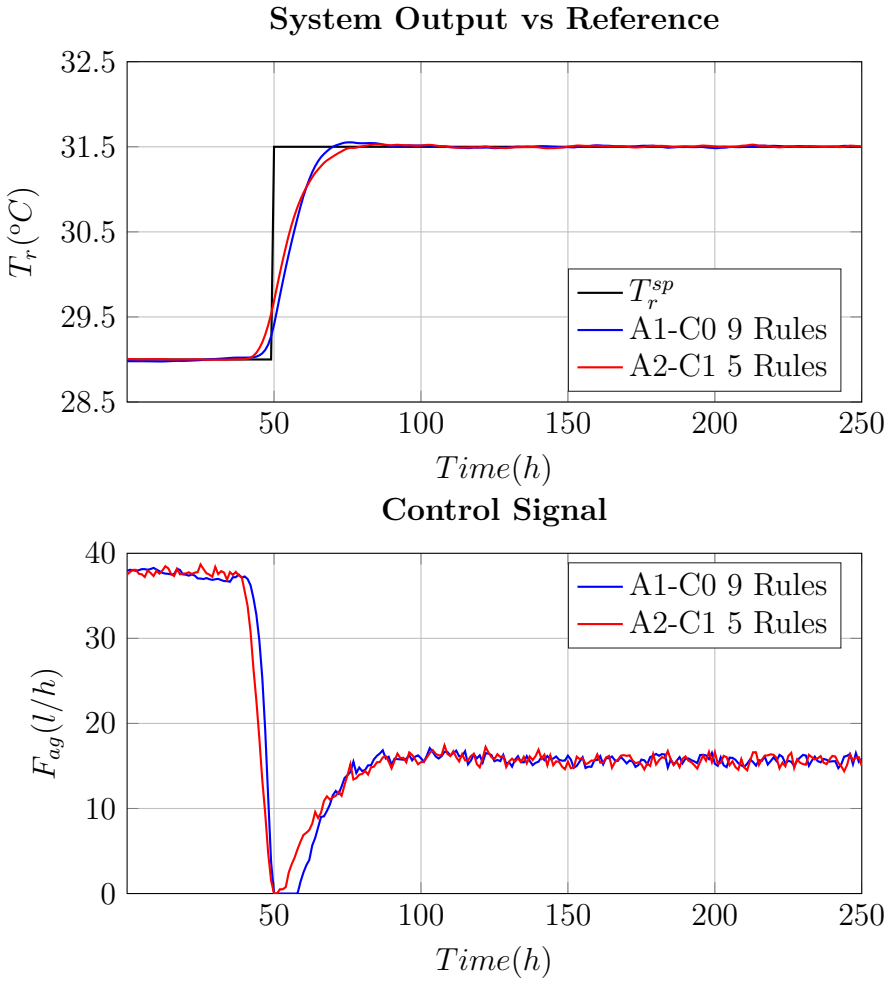

Figure 5.13: Detailed view of the process's closed loop response under identical conditions to the training procedure using a GPC based on a 9 Rule Type-1 and a 5 Rule Type-2 Fuzzy Model.

The results evince that the controller based on the Type-1 TS Fuzzy model achieves now a transient response closer to the one obtained with the Type-2 model in the ascending transitions. This improvement comes at the cost of an slight increase of control signal activity, what is not necessarily good as the system's noise robustness may be reduced. It is observed though that the descending transitions of the system's response is slightly degraded comparing to the controller based on the 5 Rule Type-1 TS Fuzzy model (presented in figure (5.9)). This behavior is due to the non-linear nature of the Reactor's temperature model in the warming-up /cooling-down stages.

Evaluating now the system's behavior after increasing the raw material's temperature from 25°C to 27°C, the differences between both modeling approaches become more prominent. Figure (5.14) displays the results of this test. The comparative metrics presented on Table (5.4).

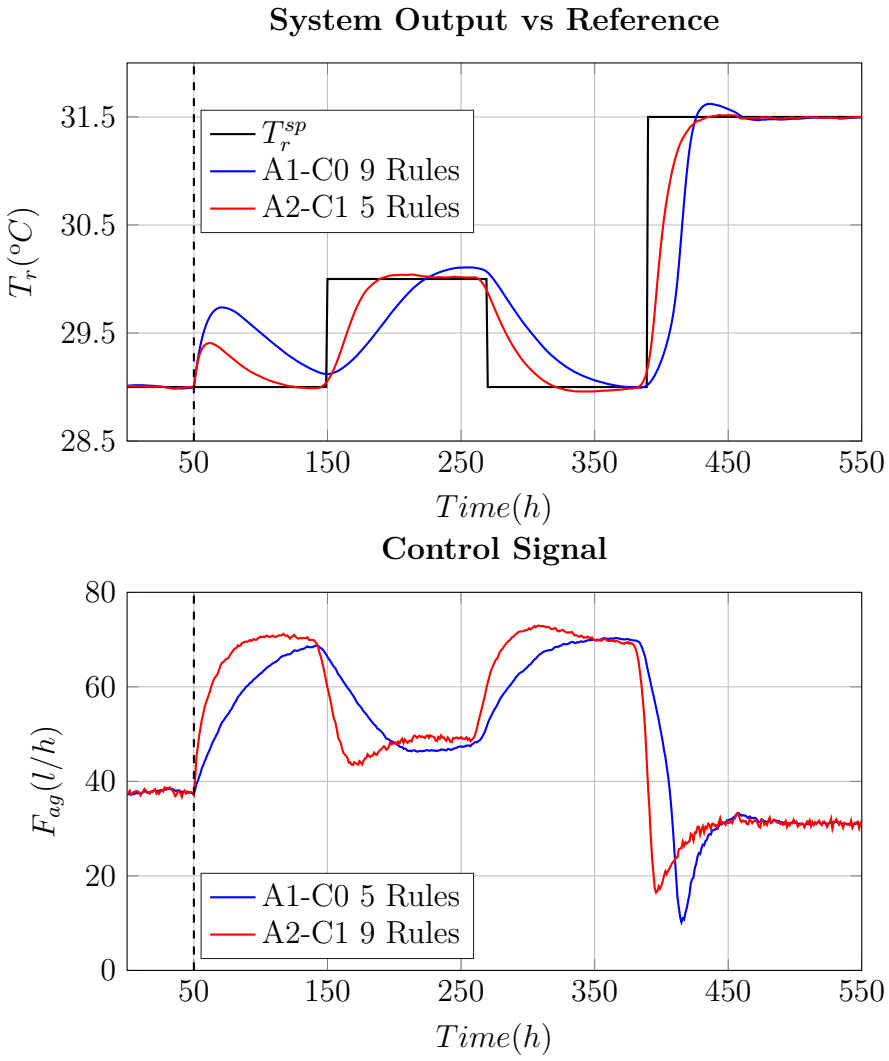

Figure 5.14: Comparison between two predictive controllers based on a 5 Rule Type-2 TS Fuzzy model and a 9 Rule Type-1 TS Fuzzy model (N_p=10; N_u=3, $\lambda_{GPC} = 0.01$) after the raw material's temperature (T_{in}) is changed from 25° to 27°C at instant $t = 50h$.

Table 5.4: Comparative metrics under constant disturbance: measured at reference step (29º to 31.5ºC) after introduction of a disturbance, as presented in figure (5.14) in the interval [350h-550h].

	MSE	Control Effort	O_s (ºC)	T_s (h)
A1-C0 (5 Rules)	$3.14 * 10^{-1}$	31.4	0.275	102
A1-C0 (9 Rules)	$6.73 * 10^{-1}$	10.10	0.122	112
A2-C1 (5 Rules)	$2.56 * 10^{-1}$	30.4	0.051	68

With these results, one may conclude that the Type-2 TS Fuzzy Model improvements are not solely related to its equivalence to a larger Type-1 one. The Type-Reduction mechanism establishes a dependency between the uncertainty degrees of the input space partition (defined by the upper and lower bounds of a rule's firing level) and the system's output that has additional degrees of freedom than the one obtained with a Type-1 TS Fuzzy Model, ultimately leading to systems which perform differently. Therefore, it is not expected to attain a proportional relationship between the number of rules and the performance metrics obtained of the two types of TS Fuzzy Models.

The manipulation of the additional degrees of freedom provided by Type-2 Fuzzy Logic naturally requires a superior computational complexity comparatively to its Type-1 counterpart. Therefore, Table (5.5) presents an overview of the mean control loop execution time and its standard deviation for the two modeling approaches. The obtained metrics refer to the execution of the one step-ahead predictor and the synthesis of the control law, resulting from the average of 56 set-point changes.

Table 5.5: Execution time of the GPC algorithm based on TS Fuzzy Models.

	5 Rule A1-C0 Model	5 Rule A2-C1 Model	9 Rule A1-C0 Model
Mean	$8.74 * 10^{-4}$s	$15.35 * 10^{-4}$s	$10.22 * 10^{-4}$s
Std. Deviation	$5.08 * 10^{-9}$s	$1.78 * 10^{-8}$s	$6.86 * 10^{-9}$s

The use of a GPC based on the 5 Rule Type-2 TS Fuzzy Models requires a larger computational effort, approximately 1.76 and 1.5 times larger than the 5 Rule and 9 Rule Type-1 TS Fuzzy models, respectively. Nevertheless, after the analysis performed in this chapter, one may conclude that the Type-2 TS Model based controller presents in this scenario an improved servo performance and disturbance rejection that, when no computational time constraints are present, makes it the preferred approach.

5.5.2 Coupled Tanks Liquid Level Control

The Coupled Tanks system is a setup widely used for benchmarking control algorithms [6, 78] due to the multitude of combinations of actuation and controlled variables that can be defined upon. As was presented in chapter 4, by choosing which pumps and rotary valves are directly manipulated, one can develop either a SISO or a MIMO control system to control the liquid level of one of the tanks. In the scenario presently evaluated, the Pump 1 will be the actuation variable and the liquid level of the Tank 2 the controlled variable. The maximum flow rate for the Pump 1 is $90cm^3/s$, while the Pump 2 (which will act as an unmeasured disturbance) is limited to $20cm^3/s$ and the liquid height in Tank 2 controllable in the [0,45]cm interval. By coupling solely two reservoirs, this setup can be seen as a non-linear second order SISO system, where the remaining actuators available are unmodeled disturbances which will be used to evaluate the robustness of the developed control algorithm. Figure (5.15) depicts the setup used in the present test.

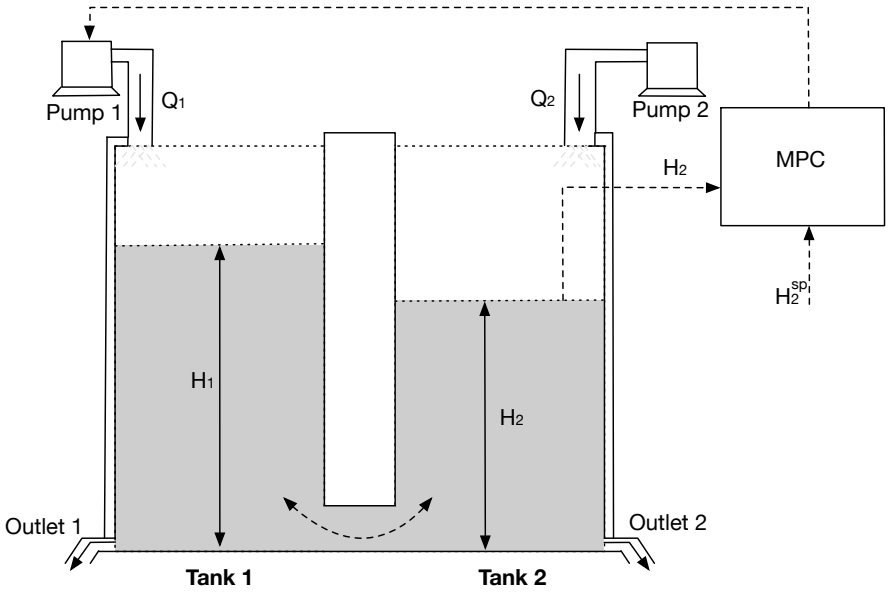

Figure 5.15: Diagram of the Coupled Tanks control system.

Similarly to the application scenario previously evaluated, three predictive controllers' implementations based on linear ARX, Type-1 TS and Type-2 TS Fuzzy Models will be compared. The results further presented were obtained according to the following test scenarios:

- Different amplitude reference step signals are used. An unmeasured gaussian disturbance is introduced in the control signal of Pump 1 with zero mean and variance of $0.5cm^3/s$ while the Tank 2 liquid level measurements are corrupted by a gaussian noise with zero mean and variance of $0.05cm$. The Pump 2 is turned off during this evaluation. The system's model is trained under these operation conditions.

- Under similar conditions of the previous test, the Pump 2 is used to introduce a gain change in the closed loop system by turning it on with a constant flow rate of $20cm^3/s$, directly disturbing the Tank 2 liquid level.

- Ultimately, maintaining the actuation and measurement disturbance levels of the initial test, the Pump 2 is used to introduce a low frequency disturbance in the closed loop system. To do so, Pump 2 is controlled so its flow rate varies sinusoidally in the interval $[0, 16]cm^3/s$ with a period of 800 seconds.

In the three GPC implementations, the prediction and control horizons were 10 and 3 samples and the control activity penalty factor $\lambda_{GPC} = 0.5$. The controller algorithm updates its output every 2 seconds (at the same rate of the sampling interval). According to the models developed in the previous chapter, a good compromise between modeling accuracy and dimensionality is achieved using TS Fuzzy Models with 4 rules. The Type-2 TS Model used considered 5% and 8% uncertainty factors over the antecedent and consequent part parameters, respectively.

Regarding the first evaluative scenario, the response of the plant to the several control systems is presented in figure (5.16). The advantages of the GPC controller based on the Type-2 TS Fuzzy Model comparing to the remaining ones are clear, providing a closed loop response with the fastest settling time and minimal overshoot (close to a critically damped behavior) without saturating the control signal. Table (5.6) overviews the evaluated metrics, obtained during the [1300-1900] seconds time interval. When comparing the controllers based on the linear ARX and the Type-1 TS models, at first instance the former approach seems more advantageous. However, such results come at a cost of a significantly higher control effort given the linear ARX model mismatches (evinced in the chapter 4). As so, to attain a more stable control signal, this penalty factor would have to be increased ultimately yielding a slower transient response.

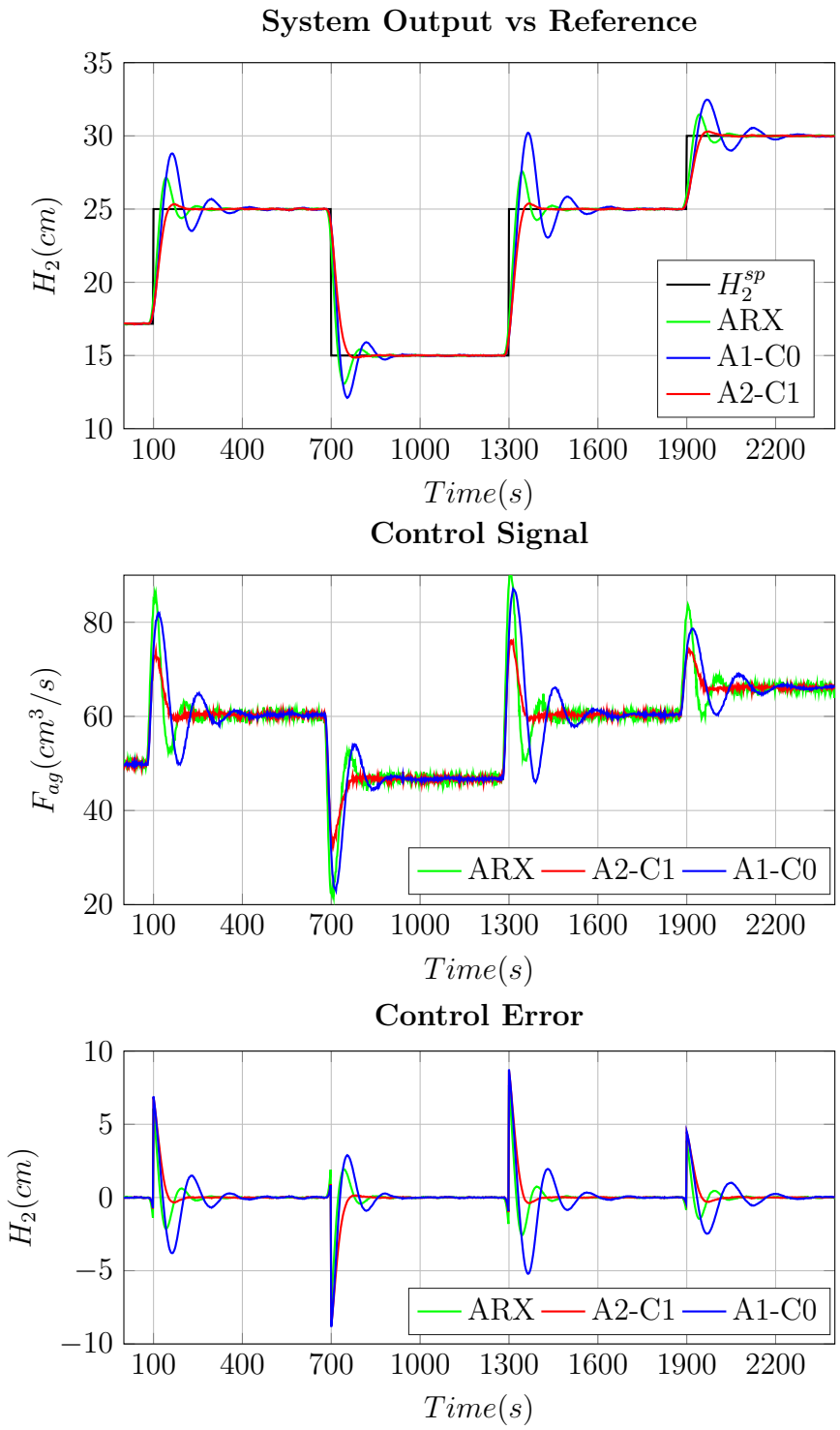

Figure 5.16: Closed loop behavior of the Couple Tanks system using three different GPC algorithms based on locally linear models.

Table 5.6: Comparative metrics under nominal operation measured during the reference step ($15cm$ to $25cm$) presented in figure (5.16).

	MSE	Control Effort	O_s (cm)	T_s (s)
ARX	3.20	32.7	2.5	180
A1-C0	4.55	6.53	5.1	302
A2-C1	2.48	4.96	0.4	102

To test the model based controllers when the plant deviates from the nominal operation conditions, the Pump 2 is manipulated to supply a constant flow rate of 20 cm^3/s. This disturbance is activated at the time instant $t = 200s$, introducing a change in the plant's steady state gain. This test is depicted in figure (5.17).

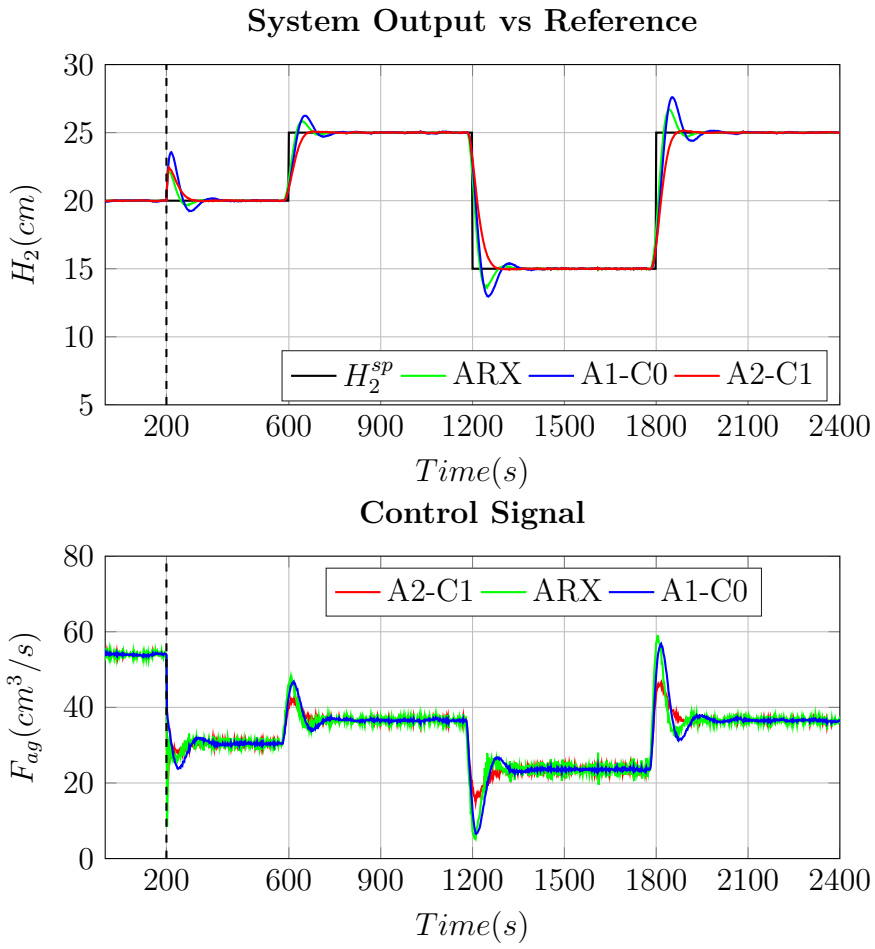

Figure 5.17: Evaluation of the closed loop performance after the process is disturbed by Pump 2 with a constant liquid flow rate ($Q_2 = 20cm^3/s$) after $t = 200s$.

Similarly to the previous evaluation, the GPC based on the Type-2 TS Fuzzy Model maintains a superior closed loop performance, presenting faster disturbance suppression and a critically damped behavior on the subsequent set-point transitions. Table (5.7) presents an overview of the obtained metrics.

Table 5.7: Comparative metrics under constant disturbance: measured at reference step ($15cm$ to $25cm$) presented in figure (5.17).

	MSE	Control Effort	O_s (cm)	T_s (s)
ARX	3.32	33.4	1.7	162
A1-C0	3.79	3.79	2.6	311
A2-C1	2.05	3.37	0.2	139

Finally, the process is subjected to an unmeasured sinusoidal disturbance introduced by the Pump 2. Its flow rate was manipulated sinusoidally, with an amplitude varying within the [0-16]cm^3/s interval and a period of 800 seconds. This low frequency disturbance was considered to be in the region of interest of the system, considering the settling time values during nominal operation conditions. As depicted in figure (5.18), the sinusoidal disturbance was significantly attenuated in every controller implementation, existing a maximum ripple of approximately $0.35cm$ around the reference signal. Yet, the TS Fuzzy Models based ones perform significantly better in terms of the required control effort. The comparative metrics presented in Table (5.8).

Table 5.8: Comparative metrics under sinusoidal disturbance: MSE, Control Effort, Overshoot (O_S) and Oscillation Amplitude at the output (O_a) measured after the reference step ($15cm$ to $25cm$) presented in figure (5.18).

	MSE	Control Effort	O_s (^oC)	O_a (^oC)
ARX	2.70	27.35	1.82	0.15
A1-C0	2.16	7.16	2.98	0.35
A2-C1	2.08	4.23	0.02	0.3

The evaluation scenarios hereby presented particularly evinced the importance of the control activity penalty factor on the control signal's robustness. While from a first instance observation of the closed loop system output behavior based on the linear ARX system is very close to the Type-1 TS based one, such result comes at the expense of an increased actuator's activity cost. A coarser model may provide sufficient information about the system's behavior trend so a well dampened control law is capable of control the system's

output. However, for a finer control quality and faster transient response a more accurate model is required. As so, the results attained justify the choice of the approach based on Type-2 TS Fuzzy models despite their increased computational cost.

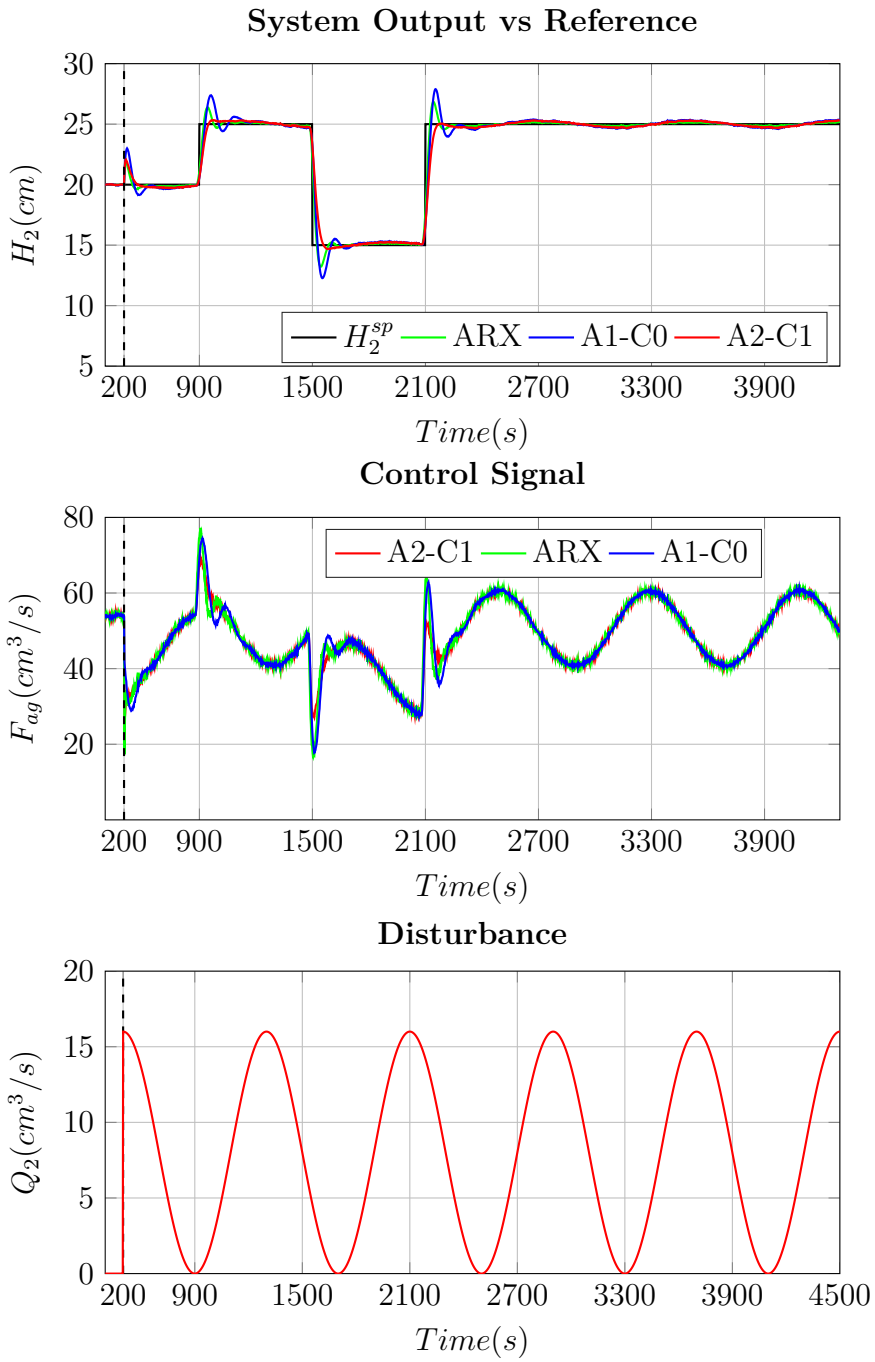

Figure 5.18: Evaluation of the closed loop performance after the process is disturbed by Pump 2 with a sinusoidal flow rate (Q_2).

5.6 Conclusions

The procedure hereby described to extend the use of a Type-2 Fuzzy Model to Model Predictive Controllers can be interpreted as an instantaneous linearization of the process dynamics on the current operating point. The process non-linearity is naturally embedded on the firing level that weights the contribution of each sub-model to the final one, and ultimately leads to the development of a simple linear structure with variable parameters. As the modeled plant is of non-linear nature, the validity of the global model predictions is restricted to a limited operation region. Hence, MPC algorithms based on linearized models are inherently sub-optimal because their predictions are likely to be different from those obtained by the original non-linear one. Thus, one must not rely too heavily on the linearized model (as when using long prediction horizons) and design a controller that does not violate the limitations of the approximation such as avoiding abrupt changes in the operation region by simply limiting the process's set-point slew-rate. When such limitations are considered, one has a computationally efficient non-linear MPC framework capable of achieve well performing closed loop control systems.

Chapter 6

Processor-In-the-Loop Simulation

6.1 Introduction

Empowered by the increasing computational power broadly available in current computer technology, the use of simulation software is an ubiquitous approach both in academia and industry during the development path of a large number of systems. Process's modeling and control is one particular domain that greatly benefited from the availability of such tool, overcoming two important constraints that dictate the course of actions taken during a new product's implementation - Time and Cost [94]. Such factors are typically related with the following problems:

- Availability of the plant.
- Cost and time of building a control system prior to testing.
- Difficulty in obtaining repeatable conditions during the development stage.
- Time consuming testing for system's validation.
- High cost due to failure.

Simulation tools are also an important asset during the initial stages of control systems' development because they allow the execution of several benchmark trial cases which can then be taken as reference for the subsequent validation stages of the algorithm implementation. However achieving optimal results under a simulated environment is solely a partial achievement towards its deployment under real operation conditions. While the computational power of a general purpose computer is of great advantage for the simulation stages, the very same systems are not adequate for the final implementation of application specific

control loops. For such purposes, embedded computer systems are better suited since their "simpler" hardware and software architectures often feature low-level access to peripheral devices interfacing with actuation and sensor systems and are better compliant with the strict timing requirements that control algorithms typically demand.

Ideally, an embedded control system is tested against the real plant but it is common to find scenarios where exist several limitations and risks in the scope of the testing (such as going beyond the range of the control system parameters or plant capabilities). Hence, the validation of complex algorithms implemented in such platforms presents additional engineering challenges: How can a meaningful set of test vectors that closely approximate the input/output behavior of a process under control be generated? How can the control algorithm behavior be analyzed in real-time under specific operation conditions? How will the algorithm's turnaround time affect the operation of the actual system? The advantages of physical process's simulation previously enunciated can be used as well to overcome such questions and, together with the algorithm's execution in an embedded platform, provide a superior test platform closer to the conditions experienced when a system is deployed in the real environment.

Hardware-In-the-Loop (HIL) simulation is a technique for performing system-level testing of embedded systems in a comprehensive, cost effective and repeatable manner using a combination of electronic hardware and custom software. Such approach is mostly used in the the validation of embedded systems when they cannot be tested easily, thoroughly, and repeatably in their operational environments [94]. To accomplish so, HIL replaces the plant under control with a powerful computer system capable of simulate several interconnected processes in Real-Time based on their dynamic models. In the tested system's point of view, there will be as little differences as possible comparatively to a real scenario. Figure (6.1) generically depicts this closed loop architecture.

The interconnection between the simulation model and the controller hardware can be implemented using A/D and D/A conversion stages based on analog signals that approximate the plant's sensors and the actuation systems response but also supported by common serial communication interfaces such as RS-232, CAN, RS-422 or Ethernet, as evinced in figure (6.2).

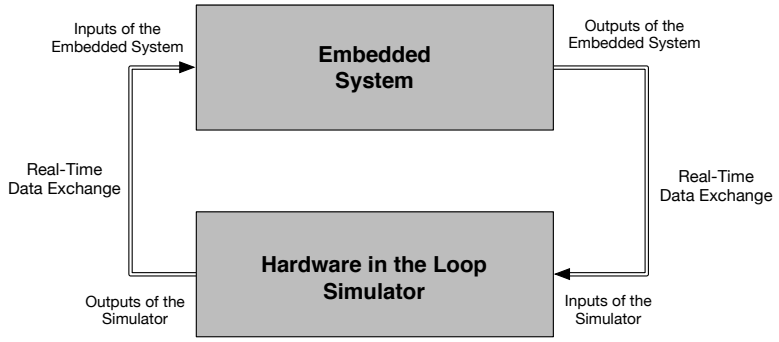

Figure 6.1: Block diagram of embedded system connected to a HIL simulator.

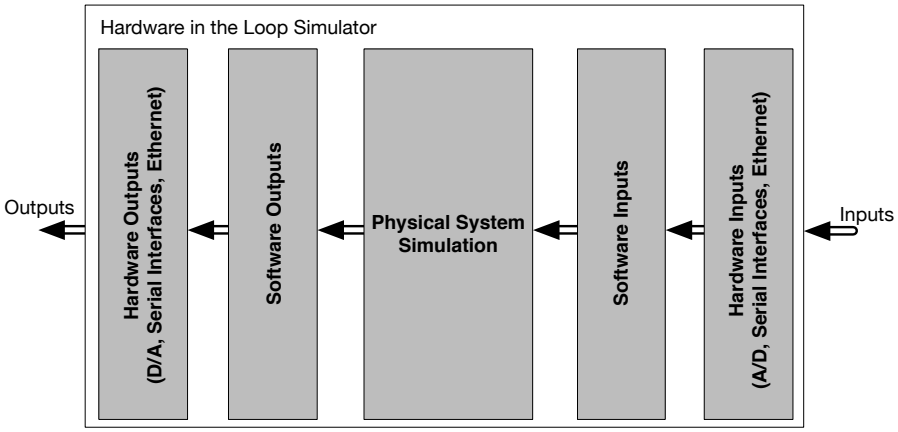

Figure 6.2: Components of a simple Hardware-in-the-Loop simulation.

Nowadays there exist several of-the-shelf platforms dedicated to HIL simulations, supported by powerful Digital Signal Processing architectures capable of conduct complex real-time simulations. A few examples are dSpace [95], National Instruments [96] and OPAL-RT [97], currently the world leaders in this market. Besides simulating the physical processes' nominal behavior, such systems often feature fault simulation tests which are particularly relevant for safety-critical systems in order to assess under repeatable conditions failure mode test scenarios which are difficult to conduct under real environment [95]. Complemented with simulation software such as Simulink [98] and analog and digital I/O Front-End software as NI's LabView [96], a HIL solution provides an efficient, reusable and safe environment where the product development can centered in the functionality of the controller without risks for either the engineer or the plant. The development of Electronic Control Units dedicated to vehicle's safety features [99] and engine control [100] in automotive industry or flight control systems in aerospace industry [101, 102] are some

examples of projects whose success heavily depends on HIL's testing reliability.

Despite all the advantages, HIL's architecture also poses some limitations that should be highlighted. Firstly, since such frameworks are intended for real-time design verification, the simulated systems must consider the throughput of the HIL's processor that iterates them. For that reason, it is necessary to deterministically bound the require execution time of each simulation iteration (by using fixed-step solvers for example [95]) so, as a consequence, highly complex process models are not adequate when a small iteration's turnaround time is required (as in high frequency control loops). Secondly, since the embedded system is decoupled from the HIL and is dependent on the simulator outputs, one cannot simple pause the simulator for in-circuit diagnosis. Hence, the full set of features provided by a HIL system are not necessarily the most adequate during earlier development stages which are more focused on the embedded system's firmware.

Processor-In-the-Loop (PIL) simulation can be considered as an intermediate stage between the traditional and HIL simulations. Similarly to the latter framework, a PIL simulation features a test environment where an embedded platform that runs the control algorithm is connected to a host computer that iterates a model of a physical process. Thus, an evaluation regarding the execution conditions of the developed algorithm in a computationally constrained system can be performed, enhancing the optimization procedures for important factors such as code size, memory footprint and algorithm execution turnaround time. However, in the PIL case the simulation process is not executed in real-time, but its the pace established by the code execution time and message exchange delays between both platforms. By doing so, the validation of the developed firmware can be performed step by step by comparison with the results obtained in the earlier computational simulations. The principles of PIL based development are depicted in figure (6.3).

Price-wise speaking, the costs of development based on a PIL framework are significantly smaller compared to the off-the-shelf HIL systems. Currently, some simulation software as Simulink [98] and PLECS [103] already support several development boards based on microcontrollers from the major brands in the market (STM and Microchip for example), providing code generation tools [104] that significantly ease the task of converting the developed algorithms for different execution platforms.

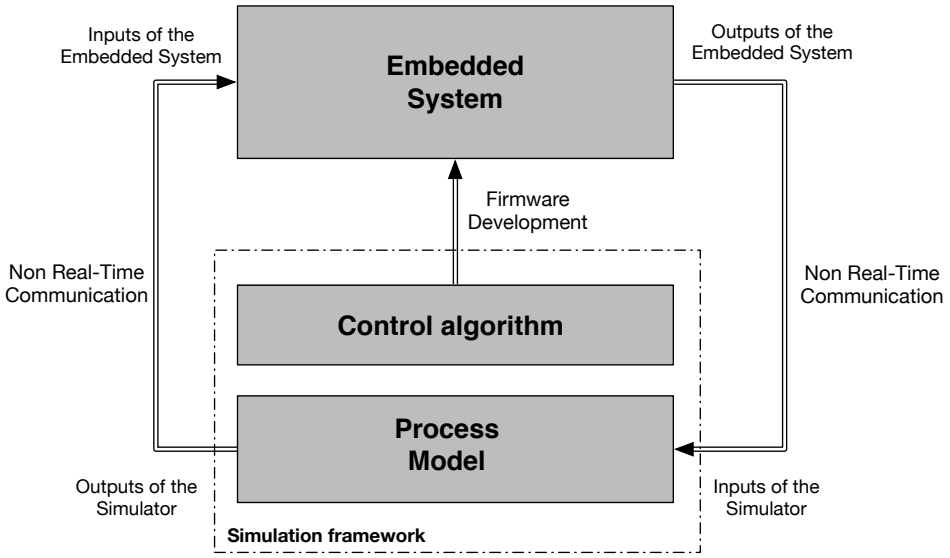

Figure 6.3: Block diagram of embedded system connected to a PIL simulator.

Yet, the use of such tools present some restrictions and drawbacks, namely:

- Support a limited set of commercially available embedded systems and development boards that may not be a perfect match for a final product.
- Due to the complexity of some algebras used in control algorithms, code generation tools most certainly will not produce the most efficient firmware for an embedded system.
- Are mostly based on closed-source code.

For those reasons and to ease the evaluation of the control algorithms implemented in this thesis in an embedded platform, a PIL architecture based on the MATLAB/Simulink environment (for model simulation) and a embedded control system supported by the FreeRTOS real-time kernel [105] was developed. The details of the referred framework will be following presented.

6.2 PIL architecture

According to the principles of a Processor-In-the-Loop testing framework previously presented, three main elements of its architectures must be specified, namely:

- The simulation software used by a host for the iteration of continuous time models.
- The embedded system software architecture.
- The communication interface.

The Simulink toolbox [98], as part of the MATLAB software provides an important framework for simulation of continuous time systems described by their transfer functions. Furthermore, its simulation capabilities can be significantly enhanced with the integration of additional toolboxes that already include models of complex processes and elements which can be interconnected in a block-based approach, spanning categories such as mechanical parts, hydraulics, thermodynamic features, or electronics components, which reduce the necessity of having a deep knowledge about the otherwise required mathematical models. Since Simulink features several methods of simulation (and among them a script based one), it is possible to implement discrete time control systems that take advantages of Simulink's continuous-time simulation - the control systems implemented in the previous chapter were simulated according to this approach. Consequently, the control algorithm can be decoupled from the model execution, easing the extension of the simulation software to include an embedded system in the loop for the implementation of the control algorithm. As so, in the MATLAB environment the code of control algorithm is exchanged by a communication link that transmits the plant data to the Micro-Controller Unit (MCU) and receives from it the output of the control algorithm. In the MCU side, the firmware is developed around two main tasks: receive and transmit the data over the communication link and implementation of the control algorithm. These main elements are sequentially interconnected as presented in figure 6.4.

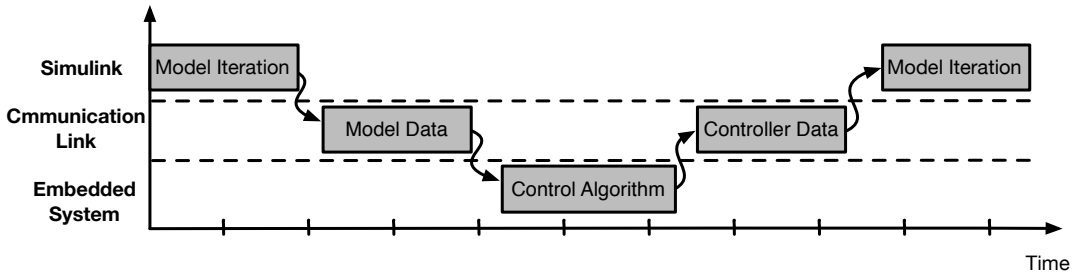

Figure 6.4: Sequence of events during one loop of the Processor-In-the-Loop simulation.

6.2.1 Development Board

The implementation of versatile digital feedback control loops based on embedded systems greatly improved the quality of many industrial processes. Still, the best performing control algorithms are based on computationally intensive procedures which, when executed in low-cost embedded systems, severely restrict their usability to applications with relatively slow dynamics to cope with the control loop calculations' turnaround time. Tackling the high performance algorithmic needs in low-cost embedded designs, ARM recently introduced in the market a System-on-a-Chip based on a new processor family - the ARM Cortex-M4. Complementing the available portfolio composed by the broadly used, general purpose, low-cost and low-power ARM Cortex-M3 and M0 families, systems based on the Cortex-M4 core stand out in the state-of-the-art of embedded systems by featuring an instruction set optimized for Digital Signal Processing operations, a single cycle Multiply and Accumulate (MAC) unit and a single-precision hardware Floating-Point Unit (FPU). The availability of a hardware FPU in such a small semiconductor die at relative low cost per unit is perhaps one of the most important enhancements of the referred architecture as it significantly simplifies the development of computationally heavy algorithms that otherwise would have to be developed through fixed-point representations. Depending on the complexity of the algebras employed in the implemented algorithms, such procedure can become an elaborate task, requiring a deep analysis of every intermediate calculation to ensure overflow and underflow conditions will not be met during normal execution.

In order to ease the prototyping of embedded control systems, it is important to have a reusable core system featuring a basic set of peripherals devices frequently used in such applications. In the past, MCUs were often encapsulated in easy to use Dual In-ine Packaging (DIP) MCUs but, currently the most powerful embedded systems are only available in high density pin-out packages which significantly increase the complexity of the earlier

prototyping stages. Hence, to overcome such constraint, during the present work a system-on-a-module based on a ARM Cortex-M4 MCU was designed following a DIP layout that can be easily integrated in prototype electronic systems. Figure (6.5) depicts the developed module.

Figure 6.5: Development board for embedded control based on ARM Cortex-M4 core.

The computing power of the ARM Cortex-M4 core covers the needs of several different applications in a broad range of domains, spanning from embedded control loops to multimedia applications. For the purpose of control system's development, the NXP LPC-4337 MCU was used [106] featuring a dual core architecture with a 204MHz ARM Cortex-M4 and a low power ARM Cortex-M0 co-processor (which can be used to handle less demanding tasks as communications with other devices and free up the main core for real-time processing), 1MB of flash and 136kB on-chip SRAM, along with several configurable peripherals as two High-speed USB controllers, Ethernet, Hardware controlled Pulse Width Modulated output ports, multiple communication buses and typical digital/analog ports. Hence, considering control and digital signal processing applications, the development board was designed to provide easy access to the following features:

- 16 hardware controlled PWM outputs using the Motor Control peripheral and State Configurable Timer (SCT) outputs.
- 8 channels for two 10-bit ADCs and one 10-bit DAC with data conversion rate 400 kSamples/s.
- Network communications based on 10/100 Ethernet link for high throughput data comunications.
- Two CAN, one SPI and one I2C interfaces for connecting additional devices.

- Integrated USB/UART converter.
- High Speed USB controller with Host and Device capabilities.
- One I2S for connectivity with digital audio systems.

To ease the interconnectivity of the board with the remaining systems, its pin-out was organized in functional groups as depicted in figure (6.6). It is important to note that the output ports of the board are not exclusive to the highlighted features and it is possible to remap some of them with several other functionalities (peripherals or general purpose I/O).

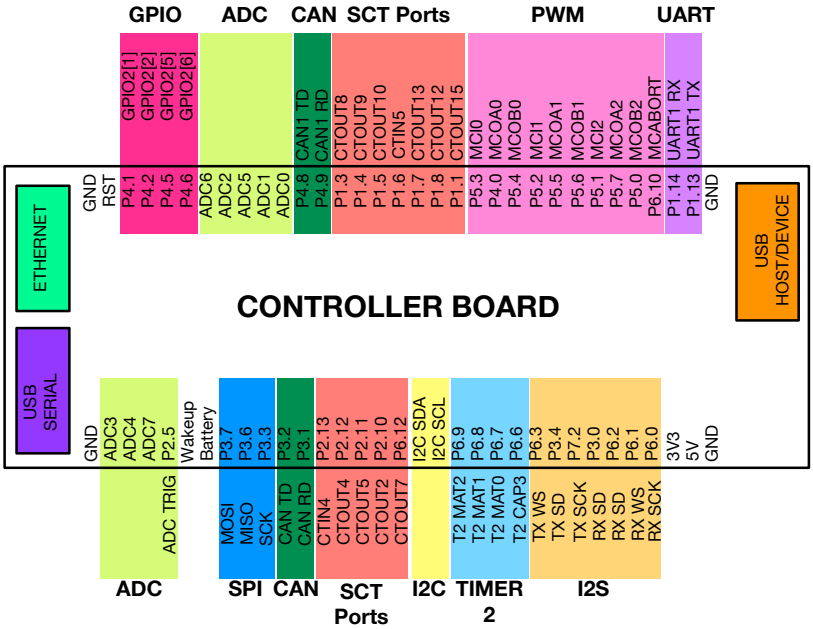

Figure 6.6: Peripherals available in the controller board.

6.2.2 Embedded System's Software Architecture

The increasingly computational power, memory resources and high peripheral integration available in the most recent embedded systems led to significant changes in the software architecture paradigm of such small devices. In the past, embedded systems were mostly developed focusing on a particular task but, nowadays it is not uncommon to integrate several control loops and additional functionalities such as network communications in the same system which compete for processor time for their execution. In such highly

integrated products, implementing software under a monolithic approach can easily become intractable for a developer. For that reason, following the longstanding practices of software development supported by an operative system, the development of an embedded system's firmware under a multi-task model with several abstraction layers has become crucial for the implementation of more complex projects. Complying with these requirements, the open-source FreeRTOS real-time kernel [105] provides an platform agnostic Application Programming Interface (API) that establishes an abstraction layer for creating of multi-task systems and managing their timings, execution priorities and inter-task communication requirements. The implemented tasks are scheduled by a tick-based fixed priority scheduler that supports preemption, which is particularly relevant for an easy development of time-triggered systems such as control loops.

Even though a program can be segmented in several tasks, in most cases there exist interdependencies among them such as execution precedences or concurrent access of shared resources as memory or peripherals. For that reason, FreeRTOS also provides on its API synchronization mechanisms such as semaphores, mutexes and message queues to avoid race conditions between tasks which would ultimately result in an inconsistent execution of the program. Since its API is written mostly in C and is open source, this kernel is highly portable and scalable. Hence, a large portion of a system's firmware easily ported to a diverse range of embedded platforms currently supported.

PIL Integration

Using the task-based organization provided by the FreeRTOS kernel, the embedded system's firmware can be segmented in three main objectives to be successfully integrated in the PIL framework: communication with the simulation host, update of the control system's variables and execution fo the control algorithm. Following this approach, the embedded system tested in the PIL framework will require very little changes to be interfaced with a real controlled plant.

As part of a PIL system, the three implemented tasks follow a producer/consumer paradigm, existing a precedence order for their execution. Since they cannot be executed concurrently, they are created with the same priority level. Figure (6.7) depicts the sequence of events that occur at each control algorithm iteration.

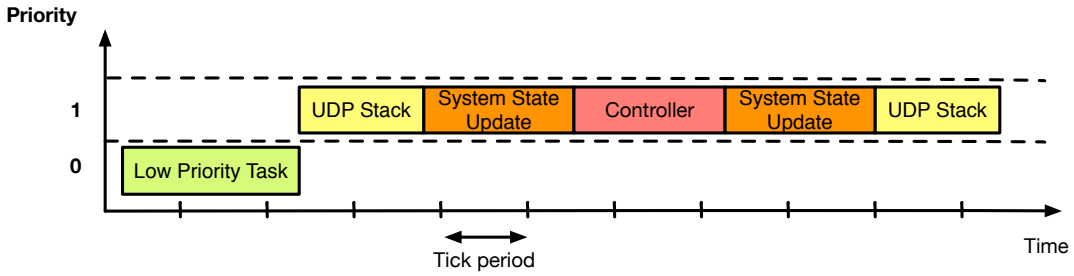

Figure 6.7: Event triggered RTOS tasks during the Processor-In-the-Loop simulation.

Taking advantage of the high transmission rates of the Ethernet interface available in the development board, the communications between the Simulator and the Embedded System are performed over an UDP socket. Such simple transmission model encompasses a minimum set of protocol mechanisms which avoid significant overhead at network level related with message delivery failures, which is particularly suited to time-sensitive applications. In such cases, as in real-time systems, dropping packets is preferable to waiting for delayed ones. Establishing a parallelism with a deployed control system, the UDP communication task assumes the role of the ADC and DAC systems, providing the communication endpoints with the controlled process (remotely executed in this case). The System State Update task is responsible for the management of the relevant data for the controlled algorithm, as updating its regression variables (previous plant's samples and controller's outputs). Finally, the controller task implements the evaluated control algorithm. The low priority task can be used for debug purposes, as to signal stack overflow conditions or any other relevant events during the firmware development.

Since the purpose of the PIL architecture is to provide an easy test framework for the validation of the final control system, the previously developed system can be easily extended to a time-triggered operation mode. In this scenario, the importance of the UDP stack execution is deprecated to a low priority level since its role is exchanged by a task responsible for managing the ADC readouts and control the process's actuators. Communications with a host computer can still be performed for data-logging and reconfiguration purposes which do not present any real-time requirements. As is depicted in the figure (6.8) the sampling task and controller tasks are now time-triggered according to the required sampling and actuation frequencies.

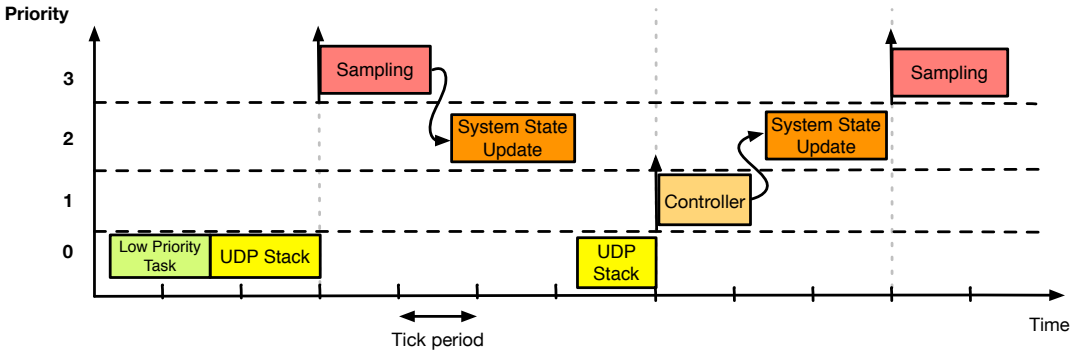

Figure 6.8: Time triggered RTOS tasks during the real process control.

6.3 System Evaluation

To evaluate the Processor-In-the-Loop framework and assess the capabilities of the developed system-on-a-module, the Fermentation Reactor Temperature Control simulator developed in this thesis will serve as benchmark for the following tests:

- Firstly, the GPC control algorithm based on the Type-2 TS FLS is executed in the embedded system and will be compared with the implementation previously evaluated on simulation.
- Secondly, the performance improvements obtained with the introduction of the FPU in the embedded system architecture will be assessed by comparing the algorithm's turnaround time when the calculations are performed using either the hardware or software floating-point implementations.
- Ultimately, the computational cost of the three Generalized Predictive Control implementations that were used as comparison standpoint in the previous chapter will be evaluated by measuring their execution turnaround time.

Similarly to the models used as support to the GPC implementations in the previous chapter, the linear approximations of the process were based on the typical second order systems's with no dead-time structure (yielding a 4 parameter linear model) and, in the cases where Type-1 and Type-2 Fuzzy Logic Models are used, a total of 5-Rules are employed to partition the model's input space.

The first evaluation scenario will highlight the PIL framework as a firmware development aiding tool. The MATLAB work environment allows one to inspect the simulation results and the state of every intermediate variable so it is possible to verify that the values computed in the ideal simulation and on embedded system mutually agree. In this test, the loop is closed by a GPC controller based on Type-2 TS Fuzzy Models which is executed in the MCU. As depicted in figure (6.9), it is seen that the control signal waveform for the MATLAB implementation and the MCU one overlap near perfectly. Consequently, the resulting process's closed loop response is similar to the results obtained in the Chapter 5.

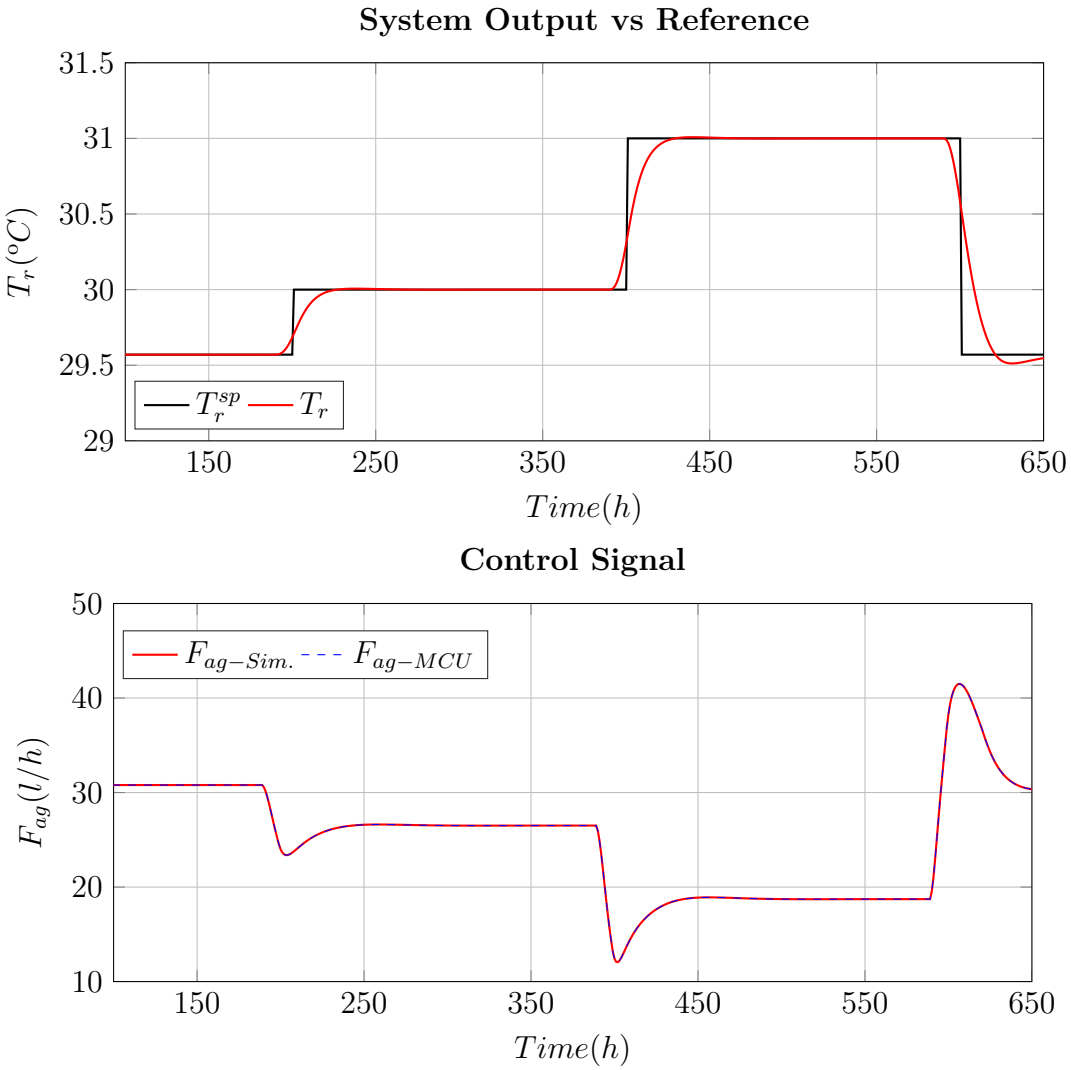

Figure 6.9: Closed loop behavior of the reactor's temperature during a yeast fermentation reaction using a PIL simulation.

Although not clear at a first instance, there is a negligible difference between both controller signals as presented in figure (6.10). Though, this mismatch is several orders of magnitude smaller than the signal of interest and is justifiable for accumulated errors due to the differences in the floating point representations between both architectures (MATLAB uses the double-precision representation while the MCU uses single-precision one).

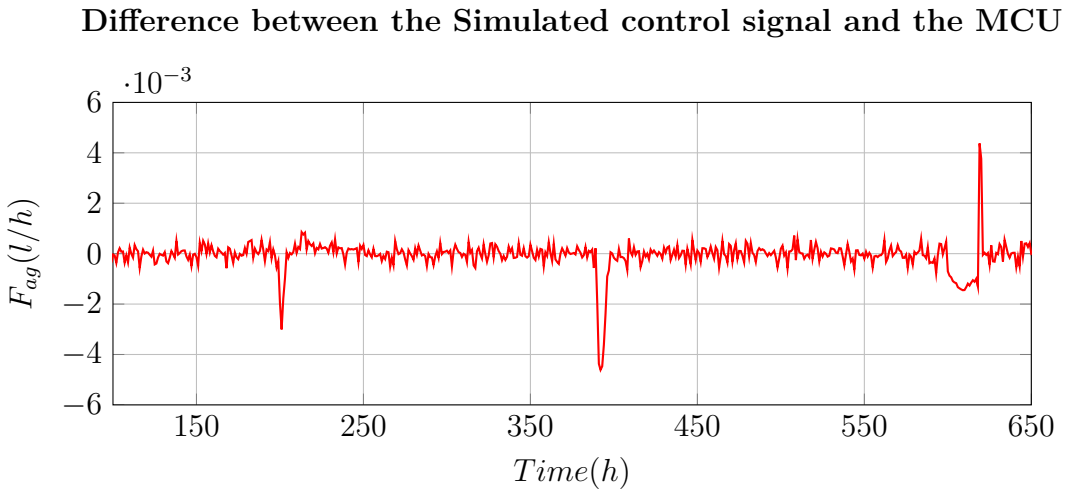

Figure 6.10: Difference between the control signal when executed in the embedded system and in the MATLAB.

Putting now into perspective the importance of the hardware Cortex-M4 FPU for solving computationally intensive mathematical algorithms, the execution turnaround time for the GPC control system implementation based on a Type-2 Fuzzy Model was measured. The obtained results are presented on table (6.1). In this test, the Cortex-M4 core was configured to run at its maximum operating frequency (204 MHz) and the measurements were taken considering the execution of the required floating-point computations either using the standard C floating-point emulation library or using the available hardware FPU.

Table 6.1: Turnaround time of the predictor and control algorithm based on Type-2 Fuzzy model.

	CM4 with Hardware FP	CM4 with Software FP
GPC	$59\mu s$	$513\mu s$
Type-2 Fuzzy Model	$110\mu s$	$924\mu s$
Total	$169\mu s$	$1.43ms$

Meeting our initial expectations, the introduction of the Cortex-M4 hardware FPU lead to a significant improvement of the algorithms' turnaround time, reducing it by a factor of approximately 8.5. Such achievement is of significant relevance as it enables one to develop control loops for a broader range of processes. The ones with faster dynamics are particularly challenging as they demand for high frequency control loops in order correctly track their response to disturbances and operation regime's variations [107].

Comparing now the computational burden of the three GPC algorithm's implementations (based on the linear ARX model, Type-1 Fuzzy model and Type-2 Fuzzy model) the turnaround time of the predictor and control algorithms was measured (when using the hardware FPU), as presented in table (6.2).

Table 6.2: Algorithms' turnaround time using based on different model based control implementations.

	ARX linear model	Type-1 Fuzzy Model	Type-2 Fuzzy Model
GPC	$25.4\mu s$	$29.2\mu s$	$59\mu s$
Model	N.A.	$15.7\mu s$	$110\mu s$
Total	$25.4\mu s$	$44.9\mu s$	$169\mu s$

Similarly to the results presented in chapter 5, the GPC implementation based on the Type-2 Fuzzy Model poses a higher turnaround time due to the greater number of model parameters and required calculations to obtain the control action. For the opposing reasons, the linear ARX based implementation presents the smaller computational time. Focusing firstly in the comparison between the linear ARX/ Type-1 Fuzzy model's metrics, the major difference in the measured execution time dues to the necessity of executing the Type-1 Fuzzy Model and perform its linearization to obtain a control law. Since in the GPC implementation based on the linear ARX structure the model is considered fixed, the metrics related with the model's execution time are not available (N.A.). Considering now the two Fuzzy Model based GPC implementations, the differences in execution time are a consequence of the superior complexity of the Type-2 Fuzzy Model. The observed difference is mainly due to the Type-Reduction algorithm which takes approximately 79 μs to complete (72% of the model's execution time). The GPC algorithm takes approximately the double amount of time to execute in the Type-2 Fuzzy Model case as it effectively executed twice in order to obtain the upper and lower bounds of the control signal.

Contextualizing the measured computational time in the deployment of process's of control loops, one verifies that the use of the hardware FPU in the Cortex-M4 core significantly reduces the MCU work load, leaving a large headroom to cope with systems with faster dynamics (thus requiring a control loop with higher execution frequency) or to perform additional non real-time tasks without compromising the schedulability of the overall system. Despite the higher turnaround time in the Type-2 Fuzzy Model based GPC, assuming that the MCU computational power is dedicated to the control task and a Direct Memory Access controller to transfer the ADC measurements to the control algorithm variables' memory region, one can expect to execute a control loop at approximately 6 KHz (for the model structure considered in this evaluation), what covers the control specification requirements of many "fast" processes.

6.4 Conclusions

The possibility of developing control algorithms in simulation frameworks and execute them in computationally constrained platforms such as general purpose embedded systems is of great importance for their deployment in real environments and achieve the sough performance improvements in process's manipulation. Processor-In-the Loop frameworks are undoubtedly a valuable tool supporting this transition. Yet, in many cases such step is ultimately not adopted since the complexity of the developed methods hinder their broad deployment given their superior costs of implementation. Type-2 Fuzzy Logic based systems have been several times pointed as computationally demanding but, as was assessed in this chapter, it is well under the capabilities of currently available embedded systems - the performance improvements achieved with the hardware FPU significantly contributed to the success of this analysis.

As a direct consequence of the observed results, one can say that such powerful microcontrollers will ease the development of quicker and better control loops coping with physical systems with faster dynamics. Additionally, the available performance head-room can certainly be used to deal with the overhead introduced by additional features such as a real-time kernel. Developing software in embedded systems under a monolithic approach can easily become intractable for a developer so software abstraction layers implemented by frameworks as FreeRTOS kernel become crucial to efficiently develop multi-task systems with real-time constraints.

Chapter 7

Conclusions

The knowledge embedded in Rule-Base systems, derived either from human experts or from clustering algorithms, is most of the times inconsistent due to interpersonal differences on the definition of the rule's membership functions or incomplete in some regions of the input/output space as a result from operation conditions not experienced during a model's training stage. Type-2 Fuzzy Logic Systems particularly focus on the mitigation of these problems and, with the development of simpler Interval Type-2 Fuzzy Sets and computationally efficient Type-Reduction algorithms, the range of its possible application scenarios has been broadly expanded in recent years. Despite the simplifications taken on its original theory, Type-2 Fuzzy Logic's main feature was not compromised - embed in a compact representation the multitude of small deviations that can be defined over a single membership function.

As an incremental step over the long-standing Fuzzy Logic theory, Type-2 Fuzzy Logic shares many of its principles and applications. Hence, the majority of its recent publications naturally focus on the comparative analysis with its Type-1 counterpart, assessing its robustness in modeling and control applications under time-variant and noisy operation conditions. However, despite all the successful implementations of model based control systems deployed both in industrial and in consumer level applications, Type-2 Fuzzy Logic and Model Predictive Control theories were up to the date two disjoint fields of expertise. Type-2 Fuzzy Control literature continues to put emphasis in traditional PID algorithms, becoming more recently significantly biased towards the use of computationally intensive Genetic and other Bio-Inspired optimization methods that, in a sense of control theory fundamentals, "blindly" seek the optimal controller parameters to achieve the best input/output behavior. While at first instance model based control algorithms (supported by representations such as the transfer functions) present the developer with

complex algebraic formulations to attain a control law, ultimately they become simpler to implement, are more predictable and provide well performing controllers which are better suited for real world applications. For that reason, this work proposed the development of a control system based on Generalized Predictive Control algorithms and Interval Type-2 Takagi-Sugeno Fuzzy Models.

In what regards to the model development procedures, as discussed in chapter 3, the ability of keeping a meaningful model representation after the training stage is important for its interpretability but at the same time for ensuring the robustness of the subsequent controller synthesis procedures. Comparatively to Type-1 Fuzzy Models, Type-2 TS ones inherently present a greater number of tunable parameters which grant them superior levels of adaptation but at the same time require greater care during the training stage. Since a Type-2 Fuzzy Set representation inherently establishes an interdependency between its tunable parameters (its uncertainty bounds are defined based on a spread factor over a nominal value), the training mechanisms must ensure that such parameters are not driven in significantly different directions, ultimately disrupting the concept of a Footprint of Uncertainty. Unfortunately, under long training procedures such scenario is not so uncommon. Therefore, in order to overcome such issue, the training methods used in this work focused on finding the approximate centers of such FOUs, introducing afterwards the uncertainty factors. Following such approach provides to the user a deeper insight about the influence of the uncertainty factors on the quality and accuracy of the developed model, makes the training algorithm less demanding in a computational sense given the smaller number of parameters that must be tuned, and improves its numerical robustness since a smaller number of degrees of freedom reduce the chances of the optimization problem to diverge to unwanted solutions or be trapped in a local minima. One open topic left by this thesis is how an "appropriate" FOU should be defined for each TS structure's parameter. Despite having an important role in Type-2 Fuzzy Logic, the definition of the FOU based on collected data is currently an open problem and an important line of work that should be given more attention in the following years - ideally not resorting solely in a *black-box* approach to obtain all the parameters related with the uncertainty factors. Nevertheless, in this work it was shown that a relatively small "fuzzily" defined FOU used in combination with a Type-Reduction algorithm already introduces significant changes in the input/output relationships of the model, yielding improved results without necessarily increase the model dimensionality. Surely such approach can be improved, giving some margin for obtaining even better results.

As was debated in the chapters 4 and 5, the efficiency of a GPC implementation is ultimately defined by the accuracy of the model used for approximating the expected future behavior of a physical process. Since in some applications the model mismatch is significant, the control law obtained is not capable to ensure the quality metrics sought for the closed loop system. To overcome such issue, non-linear GPC implementations received in recent year a crescent interest from researchers but still, methods based on linear approximations of the processes are of great value for industry due to the computational efficiency of the closed form algebraic methods required to solve them. Takagi-Sugeno Fuzzy Models stand as a particular type of structure that complies with both requirements and, by extending it with the Type-2 Fuzzy Logic formalisms, one aimed to improve the accuracy of its locally linearized models to extrapolate better n-step ahead predictors. Such improvements are particularly important during abrupt changes on the operation regimes - situations where the overall model results from the contribution of several locally linear sub-models with smaller validity and, consequently, the uncertainty over the obtained predictions is inherently higher. Based on results attained in this work, it was shown that, at the cost of a small increase of the computational effort, a predictive controller based on Type-2 FLSs presents an improved transient behavior comparatively to its Type-1 and linear ARX counterparts under similar operation conditions, presenting significant advantages when the controlled processes are subject to unmodeled disturbances. Although the computational time was not a limitation factor in the presented scenarios, the improvements achieved with the proposed method can be extended to non-linear systems with smaller time constants as well, proving itself as a valid alternative approach to non-linear model predictive control that require the use of heavy non-linear optimization algorithms at every control interval. The analysis performed only considered systems up to second order and without dead-time so the tests under different conditions remain for a future evaluation.

Even though the proposed control framework was developed and evaluated under simulated conditions, the data samples used during the model extraction procedures and the closed loop test scenarios were corrupted by gaussian noise, introducing disturbances with amplitudes similar to the ones possibly experienced in real operation conditions. Hence, together with the developed Processor-in-the-Loop framework, it is expected that the time of deployment of the proposed control system can be significantly reduced in future works inspired by this thesis, thus taking the state-of-the-art of Type-2 Fuzzy Logic one little step forward.

Bibliography

[1] Zadeh, L.: Fuzzy sets, Information and Control, vol. 8, pp. 338-353, (1965)

[2] Wu, D.; Tan, W.: Type-2 FLC Modeling Capability analysis, Proceeding of the 2005 IEEE International Conference on Fuzzy Systems, pp. 242-247, (2005)

[3] Wagner, C.; Miller, S.; Garibaldi, J.; Anderson, D.: From Interval-Valued Data to General Type-2 Fuzzy Sets, IEEE Transactions on Fuzzy Systems, vol. 23, issue 2, pp. 248-269, (2015)

[4] Wagner, C.; Hagras, H.: Towards General Type-2 Fuzzy Logic Systems based on zSlices, IEEE Transactions on Fuzzy Systems, vol. 18, issue 4, (2010)

[5] Liang, Q.; Mendel, J. Interval Type-2 Fuzzy Logic Systems: Theory and Design, IEEE Transactions on Fuzzy Systems, vol. 8, no. 5, pp. 535-550, (2000)

[6] Wu D.; Tan W.: A Simplified Type-2 Fuzzy Logic Controller for Real-Time Control, ISA Transactions, vol. 45, issue 4, pp. 503-516, (2006)

[7] Hagras, H.: Type-2 FLC: A New Generation of Fuzzy Controllers, IEEE Computational Intelligence Magazine, vol. 2, no. 1, pp. 30-43, (2007)

[8] Kumbasar, T; Hagras, H.: A Gradient Descent Based Online Tuning Mechanism for PI Type Single Input Interval Type-2 Fuzzy Logic Controllers, Proceedings of IEEE International Conference on Fuzzy Systems, (2015)

[9] Kumbasar, T.; Eksin, I.; Guzelkaya, M.; Yesil, E.: Type-2 Fuzzy Model Inverse Controller Design Based on BB-BC Optimization Method, 18th World Congress of the International Federation of Automatic Control (IFAC), (2011)

[10] Kumbasar, T.; Eksin, I.; Guzelkaya, M. ; Yesil, E.: Interval Type-2 Fuzzy Inverse Controller design in Non-linear IMC Structure: Engineering Applications of Artificial Intelligence, no. 24, pp. 996-1005, (2011)

[11] Zhao, L.: Direct-Inverse Modeling Control based on Interval Type-2 Fuzzy Neural Network, Proceedings of the 29th Chinese Control Conference, pp. 2630-2635, (2010)

[12] Ljung, L.: System Identification: Theory for the User, Prentice Hall (1987)

[13] Camacho, E.; Bordons, C.: Model Predictive Control, Advanced Textbooks in Control and Signal Processing, 2nd Edition, Springer-Verlag, (2007)

[14] Clarke, D.; Mohtadi, C.; Tuffs, P.: Generalized Predictive Control, Parts 1 and 2, Automatica, vol. 23, pp. 137-160, (1987)

[15] Mollov, S.; Babuška, R.; Abonyi, J.; Verbruggen, H.: Effective Optimization for Fuzzy Model Predictive Control, IEEE Transactions on Fuzzy Systems, vol. 12, issue 5, pp. 661-675, (2004)

[16] Mendes, J.: Computational Intelligence Methodologies for Control of Industrial Processes, Ph.D. Thesis, Department of Electrical and Computer Engineering, University of Coimbra, (2014)

[17] Huang, Y.; Lou, H.; Gong, J.; Edgar, T.: Fuzzy model predictive control, IEEE Transactions on Fuzzy Systems, vol. 8, issue 6, pp. 665-678, (2000)

[18] Albus, J.: A Therory of Cerebellar Function, Mathematical Biosciences, vol. 10, pp. 25-61, (1971)

[19] Newell, A.; Simon, H.: Human Problem Solving, Prentice-Hall, (1972)

[20] Mamdani, E.: Applications of Fuzzy Algorithms for Control of a Simple Dynamic Plant, Proceedings of IEEE, vol. 121, pp. 1585-1588, (1974)

[21] Verbruggen H.; Babuška, R.: Fuzzy Logic Control: Advances in Applications, World Scientific, (1999)

[22] Yasunobu, S; Miyamoto, S.; Ihara, S.: Train Automatic Operation System by Fuzzy Theory, Proceedings of 20th SICE, pp. 467-468, (1981)

[23] Yamakawa, T.; Stabilization of an Inverted Pendulum by a High-Speed Fuzzy Logic Controller Hardware System, Fuzzy Sets and Systems, vol. 32, no. 2, pp. 161-180, Elsevier, (1989)

[24] Rumerman, J.: NASA Launch Systems, Space Transportation/ Human Spaceflight, and Space Science 1989–1998, NASA Historical Data Book, vol. VII, The NASA History Series, Volume VII, (2009)

[25] Mamdani, E.; Applications of Fuzzy Logic to Approximate Reasoning using Linguistic Systems, IEEE Transactions on Transactions on Systems, Man and Cybernetics, vol. 26, issue 12, pp. 1182-1191, (1977)

[26] Takagi, T; Sugeno, M.: Fuzzy Identification of Systems and its Applications to Modeling and Control, IEEE Transactions on Systems Man and Cybernetics, vol. 15, issue 1, pp. 116-132, (1985)

[27] Kosko, B: Fuzzy Systems as Universal Approximators, IEEE Transactions on Computers, vol. 43, issue 11, pp. 1329-1333, (1994)

[28] Arima, T. Senday Subway 1000 Series, in `www.toonpool.com/cartoons/Sendai%20Subway%201000%20Series_126560`

[29] Delgado, M.; Duarte, O.; Requena, I.: Arithmetic Approach for the Computing With Words Paradigm, International Journal of Intelligent Systems, vol. 21, pp. 121-142, Wiley, (2006)

[30] Mendel, J.: Uncertain Rule-Based Fuzzy Logic Systems: Introduction and new directions, Prentice-Hall, (2001)

[31] Passino, K.; Yurkovich, S.: Fuzzy Control, Addison-Wesley, (1998)

[32] Mendel, J.; Zadeh, L.: Trillas, E.; Yager, R.; Lawry, J.; Hagras, H.; Guadarrama, S.: What Computing With Words Means to Me., IEEE Computational Intelligence Magazine, February, (2010)

[33] Zadeh, L.: The concept of linguistic variable and its applications to approximate reasoning, Information Sciences, Part I-III, pp. 199-249, pp. 301-357, pp. 43-80, (1975)

[34] Karnik, N.; Mendel, J.; Liang, Q.: Type-2 Fuzzy Logic Systems, IEEE Transactions on Fuzzy Systems, vol. 7, issue 6, pp. 643-658, (1999)

[35] John, R.; Coupland, S.; Type 2 Fuzzy Logic: a Historical View, IEEE Computational Intelligence Magazine, (2007)

[36] Mizumoto, M.; Tanaka, K.: Fuzzy Sets of Type-2 under algebraic product and algebraic sum, Fuzzy Sets and Systems, vol. 5, pp. 277-290, (1981)

[37] Dubois, D.; Prade, H.: Fuzzy Sets and Systems: Theory and Applications, Academic Press, (1982)

[38] Turksen, I.; Norwich, A.: Measurement of Fuzziness, Measurement of Fuzziness, Proceedings of the International Conference on Policy Analysis and Information Systems, pp. 745-754, (1981)

[39] Wagner, C.; Hagras, H.: Novel Methods for the Design of General Type-2 Fuzzy Sets based on Device Characteristics and Linguistic Labels Surveys, Proceedings of the 2009 International

Fuzzy Systems Association World Congress and the 2009 European Society for Fuzzy Logic and Technology Conference, pp. 537-543, (2009)

[40] Coupland, S.; John, R.; Geometric Type-1 and Type-2 Fuzzy Logic, IEEE Transactions on Fuzzy Systems, vol. 15, pp. 3-15, (2007)

[41] Karnik, N.; Mendel, J.: Centroid of a Type-2 Fuzzy Set, Information Sciences, vol. 132, pp. 195-220, (2001)

[42] Wu, D.: Approaches for Reducing the Computational Cost of Interval Type-2 Fuzzy Logic Systems: Overview and Comparisons, IEEE Transactions of Fuzzy Systems, vol. 21, issue 1, (2013)

[43] Hu, H.; Wang, Y.; Cai, Y.: Advantages of Enhanced Opposite Direction Searching Algorithms for Computing the Centroid of an Interval Type-2 Fuzzy Set, Asian Journal of Control, vol. 14, no. 6 pp. 1-9, (2012)

[44] Wu, D.; Tan, W.: Computationally Efficient Type-Reduction strategies for a Type-2 Fuzzy Logic Controller, Proceedings of IEEE International Conference in Fuzzy Systems, pp. 353–358, (2005)

[45] Wu, D.; Mendel, J.: Uncertainty Bounds and their Use in the Design of Interval Type-2 Fuzzy Logic Systems, IEEE Transactions on Fuzzy Systems, vol. 10, no. 5, pp. 622-639, (2002)

[46] Kayacan, E.: Interval Type-2 Fuzzy Logic Systems: Theory and Design, PhD Thesis, Bogaziçi University, Istanbul, Turkey, (2011)

[47] Nie, M.; Tan, W.: Towards an Efficient Type-Reduction method for Interval Type-2 Fuzzy Logic Systems, Proceedings of IEEE International Conference on Fuzzy Systems, pp. 1425-1432, (2008)

[48] Jang, J.; Sun, C.; Mizutani, E.: Neuro-Fuzzy and Soft Computing - A Computational Approach to Learning and Machine Intelligence, Prentice-Hall, (1999)

[49] Lin, T.; Lee, C.: Neural Network Based Fuzzy Logic Control and Decision System, IEEE Transactions on Computers, vol. 40, issue 12, pp. 1320-1336, (1991)

[50] Berenji, H.; Khedkar, P.: Learning and Tuning Fuzzy Logic Controllers through Reinforcements, IEEE Transactions on Neural Networks, 1992, vol. 3, pp. 724-740, (1992)

[51] Nauck, D.; Kurse, R.: Neuro-Fuzzy Systems for Function Approximation, 4th International Workshop Fuzzy-Neuro Systems, (1997)

[52] Juang, F.; Chin Lin, T.: An On-Line Self Constructing Neural Fuzzy Inference Network and its Applications, IEEE Transactions on Fuzzy Systems, 1998, vol. 6, pp. 12-32, (1998)

[53] Jang, R: Neuro-Fuzzy Modeling: Architecture, Analyses and Applications, PhD Thesis, Department of Electrical Engineering and Computer Science, University of California, Berkley, (1992)

[54] Abraham, A.; Nath, B.: Hybrid Intelligent Systems: A Review of a decade of Research, School of Computing and Information Technology, Faculty of Information Technology, Monash University, Australia, Technical Report Series, 5/2000, pp. 1-55, (2000)

[55] Benzaouia, A.; El Hajjaji, A.: Advanced Takagi–Sugeno Fuzzy Systems, Studies in Systems, Decision and Control 8, Springer, (2014)

[56] Boumella, N.; Djouani, K.; Boulemden, M.: On an Interval type-2 TSK FLS A1-C1 Consequent Parameters Tuning, IEEE Symposium on Advances in Type-2 Fuzzy Logic Systems, pp. 150-156, (2011)

[57] Nørgaard, M.; Ravn, O.; Poulsen, K.; Hansen, L.: Neural Networks for Modeling and Control of Dynamic Systems, Springler-Verlag, (2000)

[58] Martínez-Sotoa, R.; Castillo, O.; Aguilar, L.: Type-1 and Type-2 Fuzzy Logic controller design using a Hybrid PSO–GA optimization method, Information Sciences - Processing and Mining Complex Data Streams, vol. 285, pp. 35–49, Elsevier, (2014)

[59] Chia-Feng, J.; Yu-Wei, T.: A Self-Evolving Interval Type-2 Fuzzy Neural Network with Online Structure and Parameter Learning, IEEE Transactions on Fuzzy Systems, vol. 16, issue 6, pp. 1411-1423, (2008)

[60] Interval Singleton Type-2 TSK Fuzzy Logic Systems using Orthogonal Least-Squares and Back-Propagation methods as Hybrid Learning Mechanism, 2011 11th International Conference on Hybrid Intelligent Systems, pp. 417-423, (2011)

[61] Bezdek, J; Hathaway, R; Sabin, M.; Tucker, W.: Convergence theory for Fuzzy C-Means: Counterexamples and repairs, IEEE Transactions on Systems, Man and Cybernetics, vol. 17, issue 5, pp. 873-877, (1987)

[62] Yager, R.; Filev, D.: Approximate clustering via the Mountain Method, IEEE Transactions on Systems, Man and Cybernetics, vol. 24, issue 8, pp. 1279-1284, (1994)

[63] Chiu, S.: Fuzzy Model Identification Based on Cluster Estimation, Journal of Intelligent and Fuzzy Systems, vol. 2, no. 3, (1994)

[64] Su, M.; Rhinehart, R.: A Generalized TSK Model with a Novel Rule Antecedent Structure: Structure Identification and Parameter Estimation, Computers and Chemical Engineering, vol. 34, no. 8, pp. 1199–1219, (2010)

[65] Levenberg, K.: A Method for the Solution of Certain Problems in Least Squares, Quarterly of Applied Mathematics, vol. 2, pp. 164-168, (1944)

[66] Marquardt, D.: An Algorithm for Least-Squares Estimation of Non-Linear Parameters, Journal of the Society for Industrial Applied Mathematics, vol. 11, no. 2, pp. 431-441, (1963)

[67] Yen, J.; Wang, L.; Gillespie, C.: Improving the Interpretability of TSK Fuzzy Models by Combining Global Learning and Local Learning, IEEE Transactions on Fuzzy Systems, vol. 6, issue 4, (1998)

[68] Babuška, R; Verbruggen, H: Neuro-Fuzzy methods for Nonlinear System Identification, Annual Reviews in Control, vol. 27, pp. 73-85, Pergamon, (2003)

[69] Hägglund, T.: New Estimation Techniques for Adaptive Control, PhD Thesis, Department of Automatic Control, Lund Institute of Technology, Sweden, (1983)

[70] Kulhavý, R.: Restricted Exponential Forgetting in Real-Time Identification. IFAC Symp. on Identification and System Parameter Estimation, pp. 1143-1148, (1985)

[71] Mendes, J.; Araujo, R.; Souza, F.: Adaptive Fuzzy Identification and Predictive Control for Industrial Processes, Expert Systems with Applications, vol. 40, pp. 6964–6975, Elsevier, (2013)

[72] Bouillon, M; Anquetil, E.; Almaksour, A.: Decremental Learning of Evolving Fuzzy Inference Systems: Application to Handwritten Gesture Recognition, Machine Learning and Data Mining in Pattern Recognition, Lecture Notes in Computer Science, vol. 7988, pp. 115-129, (2013)

[73] Iserman, M.; Münchhof, M.: Identification of Dynamic Systems, Springer-Verlag, (2011)

[74] Åström, K.; Wittenmark, B.: Adaptive Control. Dover (2008)

[75] Herceg, M.; Kvasnica, M; Fikar, M.: Transformation of Fuzzy Takagi-Sugeno Models into Piecewise Affine Models, Rough Sets and Intelligent Systems Paradigms, Lecture Notes in Computer Science, vol. 4585, pp. 211-220, (2007)

[76] Bishop, C.: Pattern recognition and Machine Learning, Information Sciences and Statistics, 1st Edition, Springer-Verlag, (2006)

[77] Ławryńczuk, M.: Computationally Efficient Model Predictive Control Algorithms - A Neural Network Approach, Studies in Systems, Decision and Control, vol. 3, Springer-Verlag, (2014)

[78] Ogata, K.: Modern Control Engineering, 5th Edition, Prentice Hall, (2009)

[79] Nagy, Z.: Model Based Control of a Yeast Fermentation Bioreactor Using Optimally Designed Artificial Neural Networks, Chemical Engineering Journal, no. 127, pp. 95–109, Elsevier, (2007)

[80] Luyben, W: Chemical Reactor Design and Control, Wiley, (2007)

[81] Maciejowski, J.: Predictive Control with Constraints, Prentice Hall, (2001)

[82] Quin, S.; Badgwell, T.: A Survey of Industrial Model Predictive Control Technology, Control Engineering Practice, vol. 11, no. 7, pp. 733-764, (2003)

[83] Del Re, L.; et. al. : Automotive Model Predictive Control - Models, Methods and Applications, Lecture Notes in Control and Information Sciences, Springer Verlag, (2010)

[84] Hafez, A.: Design and Implementation of Modern Control Algorithms for Unmanned Aerial Vehicles, Ph.D. Thesis, Queen's University, Ontario, Canada, (2014)

[85] Rossiter, J.: Model-Based Predictive Control: A Practical Approach, Control Series, CRC Press, (2004)

[86] Sousa, J., Kaymak, U.: Model Prediction Control using Fuzzy Decision Functions, IEEE Transactions on System, Man, and Cybernetics, vol. 31, issue 1, pp. 54-65, (2001)

[87] Mollov, S.; et al.: Robust Stability Constraints for Fuzzy Model Predictive Control, IEEE Transactions on Fuzzy Systems, vol. 10, issue 1, pp. 50-64, (2002)

[88] Rouhani, R.; Mehra, K.: Model Algorithmic Control (MAC): Basic Theoretical Properties. Automatica no. 18, pp. 401-441, (1982)

[89] Cutler, C.; Ramaker, L.: Dynamic Matrix Control - A Computer Control Algorithm, Proceedings of the AIChE National Meeting, (1979)

[90] Nocedal, J.; Wright, S.: Numerical Optimization, 2nd Edition, Springer-Verlag, Berlin, New York, (2006)

[91] Lu, C.: Wavelet Fuzzy Neural Network for Identification and Predictive Control of Dynamic Systems; IEEE Transaction on Industrial Electronics, vol. 58, no. 7, pp. 3046-3058, (2011)

[92] Skrjanc, I.; Matko, D.: Predictive Functional Control based on Fuzzy Model Predictive Control, IEEE Transactions on Fuzzy Systems, vol. 10, issue 1, pp. 50-64, (2002)

[93] Mahfouf, M.; Linkens, D.; Abbo, M.: Adaptive Fuzzy TSK Model-Based Predictive Control Using a CARIMA Model Structure, Chemical Engineering Research and Design - Process Control, vol. 78, no. 4, pp. 590-596, Elsevier, (2000)

[94] Schlager, M.; Hardware-in-the-Loop Simulation: A Scalable, Component-based, Time-triggered Hardware-in-the-loop Simulation Framework, VDM Verlag, (2008)

[95] dSpace HIL Simulation Systems, Information retrieved from `www.dspace.com`, (2016)

[96] National Instruments HIL Simulation Systems, Information retrieved from `www.ni.com`, (2016)

[97] OPAL-RT HIL Simulation Systems, Information retrieved from `www.opal-rt.com`, (2016)

[98] Simulink - Simulation and Model-Based Design, Information retrieved from `www.mathworks.com`, (2016)

[99] Heidrich, L.; et. al.: Hardware-in-the-Loop Test Rig for Integrated Vehicle Control Systems, Advances in Automotice Control, vol. 7, part 1, 7th IFAC Symposium on Advances in Automotive Control, (2013)

[100] Poon, J.; et. al.: Hardware-in-the-Loop Testing for Electric Vehicle Drive Applications, IEEE Applied Power Electronics Conference and Exposition (APEC), pp. 2576-2582, (2012)

[101] Badaruddin, K.; Hernandez, J.; Brown, J.: The Importance of Hardware-In-The-Loop Testing to the Cassini Mission to Saturn, IEEE Aerospace Conference, pp. 1-9, (2007)

[102] Guowei, G.; Chen, et. al.: Design and Implementation of a Hardware-in-the-Loop Simulation System for Small-Scale UAV Helicopters, Mechatronics, vol. 19, issue 7, pp. 1057-1066, Elsevier, (2009)

[103] PLECS Simulation Software for Power Electronics, Information retrieved from `www.plexim.com`, (2016)

[104] Embedded-Coder MATLAB Toolbox, Information retrieved from `www.mathworks.com`, (2016)

[105] FreeRTOS Cross Platform Real Time Operating System, Information retrieved from `www.freertos.org`, (2016)

[106] LPC 433x Product Datasheet, Information retrieved from www.nxp.com/documents/data_sheet/LPC435X_3X_2X_1X.pdf, (2016)

[107] Antão, R., Mota, A., Martins, R., Adaptive Control of a Buck Converter with an ARM Cortex-M4, 16th International Power Electronics and Motion Control Conference and Exposition (PEMC), Antalya, Turkey, IEEE Conference Publications, (2014)